Tether-Supported Biomembranes with Alpha-Helical Peptide-Based Anchoring Constructs

by

LINA ZHONG

A Dissertation Submitted to the Graduate Faculty in Engineering in Partial Fulfillment of the Requirements for the Degree of Doctor of Philosophy, The City University of New York

2011

This manuscript has been read and accepted for the Graduate Faculty in Engineering in satisfaction of the dissertation requirement for the degree of Doctor of Philosophy.

_____ _____

Date Prof. M. Lane Gilchrist

Chairman of Examining Committee

_____ _____

Date Prof. Mumtaz Kassir

Executive Officer

Prof. M. Lane Gilchrist (Mentor)

_____

Prof. Raymond. S. Tu (Co-Mentor)

_____

Prof. Alexander Couzis

_____

Prof. Charles Maldarelli

_____

Prof. Steven B. Nicoll

_____

Supervisory Committee

THE CITY UNIVERSITY OF NEW YORK

Abstract

by

Lina Zhong

Co-Advisers: M. Lane Gilchrist, Raymond S. Tu

The strict requirement of constructing a native lipid environment to preserve the structure and functionality of membrane proteins is the starting constraint when building biomaterials and sensor systems from these biomolecules. In order to enhance the viability of supported biomembranes anchored via polymer tethers, we have applied rationally designed peptide anchor technology to the lipid bilayer interface. For the investigation of the interactions between membrane proteins and lipid bilayers and the improvement of biomembrane-based materials, supported biomembrane systems are widely established and mimicked. Our aim is to design alpha-helical peptide complexes to tether the membranes and enhance their stability and biological compatibility. We employ ($K_3A_4L_2A_7L_2A_3K_3$) as anchoring molecules, where incorporation of a protected lysine at the in terminus (via Fmoc-Lys(Dde)-OH) allows us to access a variety of chemistries (such as introducing fluorescent dye as probes, etc.) for orthogonal modification.

These peptides are designed to crosslink to amino-terminated surfaces and incorporated into DOPC lipid bilayers supported by microbeads. Here the silica bead (5µm diameter) surface is biofunctionalized with NHS-PEG_{3000}-NHS as “polymer cushion” spacers. This is achieved by fusion of liposomes containing fluorescently labeled peptide and DOPC on silica microsphere surfaces. We aim to ultimately control

the receptor site densities on lipobeads by varying the mole fraction of different lipids and ligands, determine the biomembrane distributions of fluorophore-labled lipid, ligand and receptors using flow cytometry and confocal microscopy. Moreover, hydrophobic peptide spanning within lipid bilayers is considered to mimic cytoskeletal stuctures in cellular biomembranes, and the helical structure of peptides within biomembranes is characterized with circular dichroism.

In the current study, we have designed peptide-based anchoring lipid bilayers that attach to a solid microparticle interface through integral tethering molecules (NHS-PEG_{3000}-NHS). In earlier designs of tether-supported membranes, a wide variety of tethering molecules have been employed ranging from polymers to peptides. Thus far, primarily single lipid moieties connected at the end of tethers have been used to anchor membranes to solid supports. Our approach is to use an alpha-helical peptide as a tethering molecule. Compared to a lipid tether and protein tether, which inserts into one leaflet of the lipid bilayer, peptide anchor is expected to impart more stability to the tethered bilayer. The control of variations in the peptide sequence and orthogonal modification of the fabricated supported biomembrane systems enables us to rationally investigate the influence of peptide structure in supported lipid bilayers.

Confocal microscopy was used to analyze the lipobead surface at different stages of surface modification by employing fluorophore staining techniques. Tether supported lipid bilayer membranes were constructed successfully on cushion tethered silica particles (5μm) using self-assembly method. The fluidity of the peptides within supported membranes was quantified using fluorescence recovery after photobleaching (FRAP)

technique.

Tether supported lipid bilayer membranes were constructed successfully on 5μm silica particles. The data on these systems show that the peptide exhibits a high alpha helical content when the peptide spans the lipid bilayers. Additionally, the diffusion coefficient of peptide anchors within polymer-cushioned and tethered biomembranes enhances peptide mobility compared with untethered systems. The results define a novel platform where the application of rationally designed peptide based anchors can be used to tether lipid bilayer, creating a more native lipid environment on spherical particles.

Preface

This thesis describes an experimental study on the fabrication of tether-supported lipid bilayer membranes on silica microparticles using peptide anchors. We have used peptide based conjugates to anchor the lipid bilayer to the supporting silica particles. Our work can be divided into four major parts: synthesis and characterization of peptide conjugates, modification of silica surface with diverse polymers to make it optimal for use as a supporting surface, fabrication of lipid bilayers on silica surface using peptide conjugates as integrated anchors, and characterization of supported lipid bilayers.

In Chapter 1, we have introduced the basic motivation for our work. Our strategy to stabilize these proteoliposome assemblies based on the biomimetic approach has been described. The overall objectives of our project have been discussed. And background information on the lipids and the lipid bilayer assemblies has been provided. These include the concepts of proteoliposomes, supported bilayers, tethers, spacers, polymer cushioned lipid bilayers, various issues related to membrane proteins application and biomembrane stability questions, which are directly related to the functionality of native-like environment. Also, the basic information on solid-phase peptide synthesis, alpha-helical structural evaluation via Circular Dichroism, and confocal microscopy has been discussed. Fluorescence recovery after photobleaching (FRAP) and the flow cytometry technique has also been introduced.

Chapter 2 describes the synthesis of the alpha-helical peptides and characterization of the resulting bioconjugates. The aims of rational design of the peptides as related to their stable spanning within lipid bilayers are discussed. Also, the protocols of

construction of NHS-ester-α-helical peptide conjugates, Fmoc cleavage and labeling of the peptide with fluorescein isothiocyanate (FITC) are introduced. The diverse methods of characterization are described, including reverse phase HPLC purification, molecular weight determination via Mass Spectrometry, and analysis of alpha helical content via Circular Dichroism. We've successively synthesized peptide conjugates for use as anchoring contructs in supported membranes.

Chapter 3 discusses the details of surface modification of silica microspheres. This chapter describes different modification of beads for more stability and feasibility in following application of supported surface. We have discussed the requirements to modify the silica surface. A brief literature review for silica surface modification using silanization technique has been provided. We have used amine-based coupling to conjugate NHS-PEG_{3000}-NHS to silica surface. The modified beads were further incubated with proteoliposomes tagged with FITC to facilitate localization via fluorescence imaging. And also, the SATP modification and available Fmoc assays for estimation of available amino groups on microbeads were introduced. The protocols to characterize these conjugates using Fluorescence-activated cell sorting (FACS) and quantification of peptide on the substrates, circular dichroism (CD) investigation and confocal laser scanning microscopy (CLSM) have been described. Also, the analysis of the modified beads by various reagents using confocal microscopy and discussion of the tests for non-specific adsorption of proteoliposomes on the modified surface has been included.

Fabrication of the NHS- PEG_{3000}-NHS tether supported lipid bilayer assemblies on

silica bead surface has been described in chapter 4. Various experiments describing the development of our methodology are introduced, including some experiments that did not yield successful tethered systems. Characterization of the lipid assemblies on the bead surface using confocal microscopy, investigation for second structure of peptide tethers using Circular Dichoism and estimation of surface density of peptide tethers using FACS technique are also discussed. The lateral fluidity of the fluorescently tagged peptides was analyzed using the FRAP technique, and these results are compared with the case of untethered lipid bilayer on plain silica bead surface.

Finally, chapter 5 gives an overview of the results achieved in the current thesis and relates them to the future work. Some critical issues that remain are discussed. In order to establish optimal conditions for the formation of these structures and for the stability comparison with conventional case of existed membranes, future work is described in two categories: (i) different methods for investigation (ii) different systems for study, focusing on NMR characterization and formation of other supported functional systems.

Acknowledgments

The completion of my dissertation and subsequent Ph.D. has been a long journey, which is the most important decision to change the pathway of my life. Yes, the writing of a dissertation can be a lonely and persistent experience, yet it is obviously not possible without the personal and practical support of numerous people. Thus my sincere gratitude goes to my parents, all my friends, and my companions for their love, support, and patience over the last few years.

I'd like to give a heartfelt, special thanks to Profs. M. Lane Gilchrist, Raymond S.Tu at City College of New York, for inspiring and encouraging me to pursue a career in chemical and biochemical studies, and to Prof. Ilona Kretzschmar, for aiding me in support and student affairs consulting comprehensively, and to Profs. Alexander Couzis, Charles Maldarelli, Steven B. Nicoll for participating in my examination committee and giving me suggestions to make more progress.

I am also grateful for the hospitality and support of Dr. Bin He, from Chemical Engineering Department of CCNY. I deeply appreciate the welcome and encouragement I have received this past year from Mr. Andrew Eng, Mr. Zhengrong Xu, and from the faculty, staff, and administration of CUNY, and my wonderful new colleagues in the Department of Chemical Engineering Studies at City College of New York. My research for this dissertation was made more efficient but also much more extensive through the use of several electronic resources. Thus I gladly express my gratitude to Dr. Lijia Yang from Chemistry Department at City College of New York, Dr. Cliff Soll and the staff at

Hunter College of City University of New York, especially for performing a special analysis for me, and to Vikas Jain, Lorraine Leon for aiding me with the operation of “Olis system programs” and “Biomates 35”, which I have used so frequently.

Many people on the faculty and staff of Grove School at City college of New York assisted and encouraged me in various ways during my course of studies. I am especially grateful to Profs. Charles Maldarelli, Alexander Couzis, Ilona Kretzschmar, David Rumschitzki, Leslie Isaacs, Morton Denn, Jeff Morris, Reuel Shinnar, for all that they have taught me. I was also greatly inspired by Profs. Charles Maldarelli and Carol Steiner, for whom I was a Teaching Assistant for one year, and I thank the students whom I was privileged to teach and from whom I also learned much.

My graduate studies would not have been the same without the academic challenges and diversions provided by all my student-colleagues of City College of New York. I am particularly thankful to my friends, Jingqin Cui for welcoming me so warmly to the New York City, and to Xiaoxiao Chen, Yan Xue, for giving me frequent respite and much love. We not only studied, relaxed, and traveled well together, but they were even willing to provide very useful ideas for me.

Finally, this dissertation would not have been possible without the expert guidance of my esteemed advisors: Profs. M. Lane Gilchrist, Raymond S. Tu. My enormous debt of gratitude can hardly be repaid to them, who not only proof-read multiple versions of all the chapters of this dissertation, but also provided many stylistic suggestions and substantive challenges to help me improve my presentation and clarify my arguments.

Their oral and written comments are always extremely perceptive, helpful, and appropriate. Of course, despite all the assistance provided by Profs. M. Lane Gilchrist, Raymond S.Tu, I alone remain responsible for the content of the following, including any errors or omissions which may unwittingly remain.

Last but not least, a big thank you to my parents. Without their support and love, I was not here to pursue my dream, and it would have been certainly much harder to finish a PhD. Still today, learning how to show filial obedience to them makes me a better person. Special thanks to them also for helping me with persisting in completing this dissertation.

I finish with a final silence of gratitude for my life.

Table of Contents

List of Tables

List of Figures

Chapter 1
Introduction and Background

Motivation

Biomembranes accurately perform some of the most complicated tasks in nature down at the molecular level and are extremely sophisticated biological systems. Provided that the lipid composition is similar to the native environment, the activity of membrane proteins can be rejuvenated after they are reconstituted into synthetic lipid bilayers. More and more researchers focus on mimicking biological self-assembly with peptides or protein-based biomaterials. Recently, significant advances have been made in the field of membrane protein folding, namely, the determination of membrane protein structures, which enable us to examine their function and their mechanisms. [1]

Studies show that membrane proteins with large extramembrane domains are often immobile or exhibit severely restricted motion in simple supported bilayers [2]. It is generally presumed that interactions between the membrane protein and the solid support interactions will reduce or eliminate protein function and mobility. The phenomenon led to the desire to ‘soften’ the surface by coating it with a polymer and applying more elaborate strategies, such as tethering the membrane to the surface, thereby creating a greater space between the solid support and more fragile protein components in the membrane [3]. Nowadays biomembranes supported on solid substrates are widely used as cell-surface models that connect biological and artificial materials. They can be placed either directly on solids or on ultra-thin polymer supports mimicking the generic role of the extracellular matrix. These tools make it possible to couple many types of biomolecules to supported membranes and embed membrane proteins of interest, resulting in sophisticated interfaces that can be used to control, organize and study the properties and function of membranes

and membrane-associated proteins [2].

Our aim is to redesign these supramolecular complexes to enhance the stability, which is to be accomplished by designing supported membranes on the solid interface of a microparticle or a nanoparticle. The motivation of our research is to extend biomimetic approach to reintroduce the supporting structures of biomembranes, with transmembrane helices as custom-synthesized peptide-based anchors (peptide sequence $K_3A_4L_2A_7L_2A_3K_3$ conjugated with fluorescein isothiocyanate) for constructing tether-supported membranes on microparticle surfaces, meanwhile, preserving the biological properties and activity of functional molecules in supported biomembranes as in their native microenvironments.

Our recent work has realized the reconstitution of peptide-anchor tether supported lipid bilayers, developing methods for investigating the properties of constituents in target systems. The novelty in this approach is rational design and incorporation of α-helical peptides into the lipid bilayers at the aqueous/lipid interface, allowing us to have precise control over peptide concentration and orientation. Nonetheless, it is also possible to design longer affinity spacer molecules to expand the submembraneous space. Our results demonstrate that peptides that span the hydrophobic region of the lipid bilayer and anchoring the lipid bilayers to the solid support are suited for long-term investigations of native bilayer environments and the construction of *in vitro* biomembane systems on surfaces of various toplogies.

Supported lipid membranes play an important role due to their potential applicability in various areas. Most fundamentally, serving as a model of biological cell membranes and hence a very attractive architecture for the design of biomimetic interfaces [4]. *In vivo*,

lipid membranes house a variety of transmembrane proteins and this makes the supported membrane an ideal candidate for the *ex vivo* for reconstitution of these biomolecules upon isolation from the native cell. Potential applications for such organic systems range from understanding the functional role of a membrane protein to constituting biosensing devices. The basic block of these supported membranes being a lipid molecule makes these a natural method of biofunctionalization of surfaces. What's more, supported lipid bilayers have recently been used as a passivating background for attaching intact liposomes to an interface [5][6].

Many academic groups are making efforts in the direction of forming tether-supported lipid membranes. From the point of view of our research objectives, there are two main reasons to tackle this project: (1) to be able to space the bilayer farther from the substrate surface, the (2) stabilize the presentation of membrane proteins partitioned into these systems. Our supposition is that the tethering molecule can bring more stability to the bilayer if it is spanning the entire membrane instead of being inserted into one of the leaflets.

1.1 Background

In biochemical and bio-pharmaceutics industries, there is an intense attempt to learn from biological systems by using biomolecules, especially membrane proteins for designing novel materials. Why utilized membrane proteins? They perform some of the most intricate molecular tasks such as single molecule transport. [7]

Because biological molecules possess the ability to interact in a highly specific fashion, and they do this on extremely small length scales, it is difficult to emulate their behavior with synthetic systems. Various studies show that proteins play important roles in controlling the self-assembly of biological materials [8-12]. Reconstitution of membrane proteins into the bilayer of lipid vesicles (liposomes) is a standard approach to preserve their structure and functionality. These membrane protein-based biomaterials have a variety of applications in various areas, such as biosensors, biocatalysts, receptor-targeted drug delivery systems and novel biomaterials for tissue engineering and pharmaceutical preparations.

1.1.1 Lipids, Lipid bilayers, Liposomes and Proteoliposomes

Lipids are composed of a polar head group and a hydrophobic part that typically includes two fatty acid chains [13]. Lipid bilayers are self-assembled colloidal structures composed of lipid molecules. Integral membrane proteins are embedded in a water-solvated lipid bilayer that presents different features in a chemically heterogeneous environment. A transmembrane protein interacts with a variety of molecules, such as the aqueous solvent, an interfacial membrane region that contains abundant polar, zwitterionic, or charged lipid headgroups, and a hydrophobic membrane core (~25 Å thick region composed primarily of hydrocarbon tails). [14] Conceptually, the chemical complexity of native membranes makes it difficult to identify the factors that determine the folding and stability of membrane proteins [13].

Chemical Structure of Lipids

Lipid molecules are the major components of biological membranes. The most abundant membrane lipids are the glycerophospholipids (also called phosphoglycerides), whose structure can be divided into two parts, a polar head group and two hydrocarbon hydrophobic chains. The structure determines the amphipathic nature of lipid molecules. Usually, the tails are fatty acids containing 16 to 18 carbon atoms. There are two hydrocarbon chains, one is generally saturated while the other is often unsaturated. The unsaturation affects the packing efficiency of the lipids and hence the phase transition temperature (Tg) of the assembled lipid bilayers. Self-assembly of the lipid molecules in aqueous environments are caused by their amphipathic nature with the hydrophobic tails packed together and thus hidden from water. The fact that lipid monomers self assemble in a bilayer structure with the hydrophobic tails sandwiched between the polar head groups is attributed to their “cylindrical” shape. The exposure of lipid tails edges to water leads to spontaneous closure of phospholipids bilayer to form sealed compartments. These structures are called lipid vesicles or liposomes [3].

Phase Transition Temperature

The degree of fluidity of lipid bilayer depends on the lipid composition and the temperature. At temperatures below the phase transition temperature (Tg), the lipid molecules are closely packed against each other in a crystalline structure, and hence the bilayer presents in the ordered gel phase with minimal mobility (lower value of lateral diffusion coefficient D). Above the phase transition temperature (Tg), the lipid molecules are randomly packed in the bilayer and hence the bilayer presents the liquid crystalline phase with a significantly increased lateral diffusion coefficient *D*. Furthermore, the phase

transition temperature (Tg) depends on varieties of factors, such as the chain length, head group species and presence of unsaturation in the hydrophobic tails, etc. Tg increases with the chain length as interaction energy of the hydrocarbon tails increases with the chain length while decreases with the presence of a double bond as the kink in the hydrophobic tail interferes with efficient packing of the hydrophobic tails [3].

Lipid bilayers and Liposomes

At room temperature, most of the bilayer forming lipids are above their phase transformation temperature Tg. That is to say, in most cases the bilayer is in liquid crystalline phase. Hence the liposomes are sensitive to a variety of destabilization mechanisms, e.g. coagulation, shear stress, dissolution by surfactants/organic solvents, disruption by divalent cations e.g. Ca^{2+} or sucrose solution, etc. [15] The lipid bilayer in the context of the cell membrane is shown schematically as the “fluid mosaic” model of a cell membrane first postulated by Singer and Nicholson in 1972.

Lipid vesicles (liposomes), whose walls are composed of a single layer of phospholipids are colloidal particles with the capability of encapsulating within an aqueous space. Here the phospholipids are often isolated from cell membranes, this structure enables the liposome to encapsulate water-soluble compounds and help in the delivery of certain enzymes, nucleotides or drugs [19]. There are three categories in which closed liposomal structures have been divided based on size [25] as follows: multilamellar vesicles (MLV ~ 10,000 nm), large unilamellar vesicles (LUV, size 50-10000 nm) and small unilamellar vesicles (SUV 20-50 nm)

It is well known that liposomes are the best membrane models for the study of

molecular mechanisms in living systems, as well as the drug carriers presented in it. Bangham and Horne [15] first visualized phospholipid dispersions in water using electron microscopy technique and found the ‘bag-like’ structures consisted of self-assembling vesicles, which were named liposomes. Since then the field of liposomes has become a major area of research and significant progress has been made [15-18].

Generally, the preparation method consists in evaporation the organic solvent in which the lipids are dissolved and stored. There are two major steps for liposomes preparation from dried lipids, sonication and extrusion [20]. The dried lipids are dispersed in an aqueous buffer solution via sonication, which obtain vesicles of different size and structures, including multilamellar vesicles, oligolamellar vesicles and unilamellar vesicles. Sonication of the suspension above Tg gives rise to small unilamellar vesicles (SUVs) in the range of 20nm –50nm depending on the lipid composition and time of sonication [26]. Followed by extrusion, in the process multilamellar vesicles are structurally modified and ranged to large unilamellar vesicles. Lipid vesicles are physically extruded through polycarbonate filters containing pores of known pore sizes (20~100 nm) under pressure.

Alternatively, detergent molecules can be used to create liposomes, applying the higher solubility of detergent molecules over lipid molecules of similar size. Ollivon [27] describes the method, where lipid films are hydrated with detergent containing buffers, and, subsequently, the detergen is removed (e.g. dialysis, gel chromatography, bio-beads, successive dilution, enzymatic reactions, temperature and pressure jumps etc.). This results in a transformation from micelles to unilamellar lipid vesicles. Here we call the

resulting lipid dispersion as a homogenous formulation consisting of unilamellar vesicles liposomes [21].

Proteoliposomes

Proteoliposomes are lipid vesicles containing membrane proteins inserted in the lipid bilayer. Later, we also call the liposomes where peptide anchors have been inserted proteoliposomes. The aim of our research is reconstituting more proteins into lipid bilayers in a form suitable for functional studies and structural analysis at the molecular level [22]. Membrane protein reconstitution into liposomes has played an important role to identify and characterize the mechanisms of action of membrane proteins. In other words, proteoliposomes are powerful tools to provide important information about lipid-protein and protein-protein interactions as well as topological and topographic features [23, 24]. The structure of liposomes and proteoliposomes on supported surface is showed in Figure 1-2.

Liposome stability issues

Lasic [28] and Ringsdorf [29] discussed liposome stability issues: liposomes are prone to all kinds of destabilization mechanisms, including coagulation, shear stress, dissolution by surfactants/organic solvents, disruption by divalent cations (e.g. Ca^{2+}) or sucrose solution. What's more, the difference in the ionic concentration between encapsulated phase and bulk media leads to osmotic pressure differences causing the vesicles to become unstable.

In our work, the stability of liposomes is one of the key properties we desire to obtain from biomimetic systems. Polymerization of lipid chains inserted into the bilayers [30]

can give robust vesicles but destroys the lateral mobility of the lipids; a crucial dynamic property of the biological membranes [31]. In terms of liposome solution, it is widely known that one can sterically stabilize liposomes by using a hydrophilic polymer polyethylene glycol (PEG) on the surface [32], here long polymer chains on the surface of liposomes present a steric barrier to any objects and avoid liposome aggregation. Since PEG is a biocompatible polymer, PEGylated liposomes are suitable for *in vivo* applications. PEG linked to phosphatidylethanolamine (PE) can be linked to the surface of lipids used in formulations [33]. Upon self-assembly, PE gets inserted into the bilayers along with other lipids, and PEG portion is displayed on the surface of liposomes. Allen [34] found that optimum stabilization in vivo can be achieved with 5-10 mol % of PEG-PE with PEG chains of molecular mass ranging from 1000 – 2000.

1.1.2 Membrane Proteins

Unlike soluble proteins, membranes proteins require a bilayer membrane environment for correct folding. The biomembrane is essentially a two dimensional fluid, with membrane proteins that diffuse within the plane of the membrane, however, sometimes the lateral diffusion is bounded into phase-segregated lipid subdomains known as “rafts”. These organized structures and lipid-based structures such as lipid rafts within membrane domains [35] are a focus of significant research efforts. In most cases, the membrane protein is embedded in the lipid bilayer, which provides it with the native membrane-like environment. Undoubtedly, protein activity is directly related to the stability of the lipid bilayer. It is well known that reconstitution of membrane proteins into the bilayer of lipid

vesicles (liposomes) is a general approach to preserve their structure and functionality. Research on membrane proteins depends largely on the availability of the protein in its functional form for biophysical investigations.

It is of widespread interest in the pharmaceutical industry for high-throughput screening of membrane protein drug targets. The industrial goal is based on the development of robust biomembrane assemblies with proper substrate-to-membrane spacing. Then functional membrane proteins such as ion channels and hormone receptors could be displayed in arrays for high-throughput screening-based drug discovery [36].

The Membrane Interfacial Region: Hydrophobicity and Diffusion

The key role of the hydrophobic effect in the organization and stability of biological material [37] suggests that the folding of membrane proteins will differ significantly from that of soluble proteins. Transferring from a soluble state to a transmembrane configuration, a protein will pass through the membrane interfaces, and will adopt different conformations, e g. transient intermediates along the folding pathway. Transmembrane components can be isolated through specific operations, e g. ion-exchange chromatography, gel filtration chromatography, sodium dodecyl sulfate polyacrylamide gel electrophoresis (SDS-PAGE) and affinity chromatography [38].

Lateral diffusion plays a critical role to this pathway because folding and function depend on the lateral association or clustering of various components. Most functions associated with biological membranes involve proteins, including integral membrane proteins that span the membrane and membrane-anchored proteins. Examples of the

former include ion channels and numerous proteins participated in energy transduction such as the photosynthetic proteins and cytochrome oxidase. Membrane-anchored proteins are attached to membranes either permanently or transiently by the addition of a lipid-like structure such as a fatty acid or glycosylphosphatidylinositol (GPI) tether [39].

This relationship between the concept of hydrophobicity and membrane stability directs our design for the peptide anchors. The hydrophobic sequences in the peptide dictate the energy scales for partitioning. The biological hydrophobicity scale derived from measurements with the eukaryotic translocon [1] indicates that the physicochemical behaviors of membrane proteins can inform both membrane biophysicists and membrane biologists.

The Two-Stage Model: A Useful Simplification for Alpha Helical Membrane Proteins

In 1990, Popot and Engelman presented a “two stage model” [40] for the folding of the most abundant class of membrane proteins, those that span the bilayers as α-helices, based on the atomic structures of two bacterial reaction centers [41], the near-atomic resolution structure of bacteriorhodopsin [44] and diffraction based structures for the gel phase [42][43]. The two-stage model is focused on how protein sequence and lipid composition modulate the lateral interactions between transmembrane α-helices. Conceptually, the stability of a helical transmembrane protein can be understood by separating its folding into a two-stage model: (i) the formation of stable transmembrane helices independently and (ii) the lateral association of these helices into bundles. It is the best case to explain the association of single membrane spans into oligomers [40].

Taking the two-stage model into considerations of the stability of membrane proteins, we could recast the question “How do membrane proteins fold?” and the separate questions “What are the sequence determinants and lipid requirements for the formation of stable transbilayer helices?” and “What aspects of protein sequence and lipid composition drive or inhibit interactions between transmembrane helices?” [1]

The Key Direction of Studying Membrane Protein

From the perspective of membrane protein folding and stability, there are some questions we must keep in mind: What are the sequence and structural determinants of the stability of membrane proteins? What are the folding pathways and kinetic barriers for the insertion of polypeptides into membranes? How does the hydrophobicity and diffusion capacity affect protein folding? The answers to these questions may be as complicated, diverse, and all-inclusive as the chemical and biological characteristics of membrane proteins themselves.

However, vast sets of conditions destabilize these assemblies, including hydrophobic activities, shear stress, osmotic shocks, dissolution by surfactants or organic solvents, and disruption by divalent cations such as calcium [45]. The investigations of membrane protein folding and stability have been carried out extensively. White [46] and Booth [47] developed some more general principles and broad themes. However, there are severe bottlenecks that hampered expression and purification of membrane proteins, including their instability when subjected to detergent solubilization, the dependence on specific amphiphilic environments, and the conditionality of membrane protein stability and

function. Furthermore, instability restricts progress in biophysical and biochemical studies of membrane proteins and limits the development of membrane protein-based materials. How to maintain the stability and fluidity is the key direction of studying membrane proteins and an important aim of our research.

1.1.3 Why Study Supported membranes

On a solid surface membrane proteins can be reconstituted in a two-dimensional array of lipid molecules called the supported membrane. Supported membranes are generally fabricated by unrolling lipid vesicles onto a suitable surface, which could be modified or unmodified silica, quartz, or glass. These surfaces can either be planar or spherical. Moreover, the lipid bilayers can be simply adsorbed onto the surface or tethered through intermediate molecules, including polymers or peptides. In the case of a lipid bilayer supported on a solid surface without any tethers, the membrane is separated from the interface by an ultra thin, lubricating layer of water (~1-3 nm). [48][49].

However, due to the proximity of the layer to the surface, the membrane does not have sufficient lateral mobility on the supported surface, membrane proteins with domains that protrude from the bilayer will experience “pinning” or restricted mobility due to unfavorable interactions with the substrate. Studies have shown that the characteristics of supported membranes are determined by the underlying support. For example, in the case of a planar glass or silica surface, the supported bilayer will be continuous and have long-range order, while in the case of modified surface composed of hydrophilic and hydrophobic regions, there will be domains of lipid monolayer and lipid bilayer

respectively [3].

Solid Support of Membrane Proteins

Researchers have long been interested in studying membrane-protein interactions for understanding cellular surface processes, , especially on the use of liposomes as model for biological cell membranes. Two decades ago, researchers started to explore the use of planar supported membranes for such studies. Lipid bilayers supported by solid substrates are more robust and stable than black lipid membranes. In solid supported systems, a 10–20 Å layer of trapped water between the substrate and the bilayer maintains the membrane fluidity. A schematic diagram of a supported lipid bilayer is shown in figure 1-2 [50]. Initial design of planar membranes included the formation of lipid monolayers on hydrophobic alkylated surfaces using a Langmuir-Blodgett transfer mechanism [51]. The shortcomings of this approach led to the design of supported lipid bilayer membrane systems [52].

On the other hand, fabrication of supported membranes on spherical particles has some favorable properties over flat geometry, including increases in the surface to volume ratio, and the resulting membranes are easier to purifiy and process in general, leading to more versatility with regards to applications. It has been shown that lipid membranes spontaneously form on spherical silica beads when these are exposed to lipid vesicles. Supported membranes are separated from the supporting hydrophilic surface (planar or spherical) by a thin water layer (10-30 Å) [3]. Spherical supporting surfaces are also beneficial for the study of cell-biomembrane interactions using supported lipids as models

for cell membranes as the effect of finite radius of curvature (focusing effect) of vesicles could be examined. Furthermore, as the spherically-supported membranes are stable structures, it is straightforward to constructa static, sealed aqueous space between the lipid bilayer and the supporting surface.

Model Membrane Systems

There are several important properties/characteristics of these assemblies, which result in the increased development of biomaterials based on membrane proteins. Namely, [3] supported membranes present stable, native-like microenvironments for membrane proteins. *In vivo*, membrane proteins are found in cellular membranes that are a hydrophobic and a fluid environment is necessary for maintaining the structure and preserving their functionality.

Firstly, supported lipid membranes can preserve the lateral diffusivity of membrane proteins. Some membrane proteins form multimeric complexes in their functionally active form. For example, Epidermal Growth Factor Receptors require the lateral movement that enables interactions with other molecules. Secondly, supported lipid membranes can preserve the biological properties of the reconstituted protein, hence retaining its activity. Thirdly, supported lipid membranes present a mechanism for stability enhancement under flow and processing conditions. Membrane proteins can be reconstituted in functionally active form in proteoliposomes.

However, liposomes are not expected to be stable under various process conditions (e.g., shear stress, temperature etc.), which limits the applications of membrane protein-based

biomaterials. Due to an inherent supported structure, supported membranes can have higher stability compared to black liposomes without supporting surface. Hence, they can be a better choice for reconstitution of membrane proteins for the development of novel materials.

In our strategy, lipid bilayer will be anchored to the solid surface through polymer tethers. We chose to fabricate supported bilayer on spherical geometry instead of a flat interface, as there are certain advantages to this approach. Firstly, the geometry allows much more surface area to work with compared with flat geometry. Second, in spherical geometry, there is a possibility of achieving the compartmentalization of an aqueous space between the bilayer and the supporting surface. Third, these systems can be easily washed for removal of impurities such as excess liposomes. This is a crucial aspect as it can allow us to precisely encapsulate a number of molecules, varying from simple tracer molecules to the highly complicated signaling proteins in the enveloped volume.

Potential Applications of supported membranes

There are many potential applications of supported lipid membranes. We classify these into four groups. (1) A system consisting of arrays of microparticles (individual particles could have supramolecular assemblies of membrane proteins in tether supported lipid bilayer) on a functionalized surface can have an applicability as a sensing and or screening device for molecules of interest in the flow, e.g. biohazardous chemicals, potential drug molecules etc. (2) Supported membranes can be used to biofunctionalize a given surface for making novel biomaterials. (3) Supported membranes are a model for

biological membranes; so we can use them to study various processes occurring at cell surface, e.g. receptor-ligand interactions, cell adhesion etc. (4) As lipid bilayers provide the membrane proteins with a stable, native-like microenvironment, these can be used to design new biocatalysts based on membrane protein enzymes [3].

Prominent membrane protein systems in the biological and biomedical sciences involve receptors at membrane surfaces such as the neurotransmitter and cytokine receptors, the tyrosine kinase receptors, ligand-and voltage-gated ion channels, G protein-coupled receptors (GPCRs), and antibody receptors [53]. Since almost half of the 100 best-selling drugs on the market are targeted to a membrane receptors (Terstappen and Angelo, 2001) [53], the interactions with these receptors are not only of special importance in academic research settings, but also to the pharmaceutical industry.

In most cases, the simplest method for the immobilization of membranes on a sensor surface is to adsorb the lipid onto a hydrophobic surface (Plant, 1993; Terrettaz et al., 1993) [38][55]. The supported bilayer membranes (readily formed by self assembly), are stable and can be probed by quartz crystal resonant sensor (QCRS), surface plasmon resonance (SPR) and surface plasmon fluorescence spectroscopy (SPFS), as well as be analyzed with electrical measurements if the surface is conducting (e.g. metals, indium–tin oxide and conducting polymers) [54][55].

Vogel and coworkers employed a thiophospholipid possessing a triethyleneglycol spacer unit to capture membranes and membrane protein; they have carried out a large amount of pioneering work in these areas [56]. (Lang et al., 1994). This approach has enabled the functional reconsitutions of G protein-coupled Receptors (GPCRs), such as

rhodopsin [57] (Bieri et al., 1999; Heyse et al., 1998), ion channels such as OmpF [58] (Stora et al.,1999), and the nicotinic acetylcholine receptor [59] (Schmidt et al., 1998). Cornell and coworkers [60] used a similar strategy to deal with the addition of a membrane-spanning thiophospholipid in order to improve the stability of the tBLM. Boden and coworkers [61] formed mixed self-assembled monolayers of hydroxyland cholesterol-terminating thiols to capture lipid bilayers. Two years later, Jenkins and coworkers [62] used micro-contact printing techniques to obtain the micro-arrayed structure.

1.1.4 “Soft” cushion supported membrane with anchoring

With almost half of the drugs on the market today targeting membrane receptors (Terstappen and Angelo, 2001 [53], it is a trend to develop more and more methods to create spatially addressable arrays of lipid. Several methods have been developed to space a lipid bilayer at some distance away from the surface. Why space a lipid bilayer at some distance away from the surface? A lipid layer directly adsorbed onto the surface has a drawback that it cannot modulate transmembrane proteins with sizeable cytosolic or extracellular domains. Preliminary studies demonstrate the fact that when integral membrane proteins are reconstituted into the supported membrane, the extraneous portions of the proteins tend to interact with the surface, resulting in the immobilization of these molecules and their inability to diffuse laterally in the membrane. To solve the problem, many researches with an overall goal of separating the membrane from the surface with a polymeric cushion have been carried out recently [4].

In order to overcome the limitations above, the groups of Sackmann, Ringsdorf and Knoll [63][64] used a flexible polymer to tether lipid bilayers but structurally decoupled from the solid support. The soft polymer cushions offer a lubricating layer between the supported surface and the membrane, encapsulate more molecules in the enveloped volume, as well as enable the 'self-healing' of surface defects (decrease the degree of non-specific binding to the surface).

Preassembled supported bilayers can be incubated with simple polymers, which can be coated well with solid support [65]. More complex polymers [66] and lipopolymers [67] have been attached to glass and provide a softer cushion for supported membrane assembly. Wagner and Tamm's [66] indicated lateral mobility of cytochrome b5 and annexin on these polymer-supported membranes would be improved greatly as compared with glass-supported membranes.

Hereby, three basic principles have been employed: (1) tethering to the solid surface of an ultra thin film of a water-soluble natural polymer such as dextran or hyaluronic acid, which has been derivatized with long alkyl chains anchored to membranes [68-70], (2) Coupling to the lipid polymers that possess functionalized head groups [4], and (3) depositing hydrophilic multilayers of cylindrical molecules with alkyl side chains that insert into and anchor membranes [71, 72]. According to the ideas, fabricated lipid bilayers can be either supported on the polymer layer or are tethered directly to the polymer through various approaches The "soft" cushion ranging from simple tracer molecules to the highly complicated signaling proteins, here we adopt α-helical peptide as anchors.

Peptide anchors

The methodologies of constructing supported membranes for the immobilization of membrane proteins has progressed rapidly from physical adsorption of lipid bilayers to more elaborate approaches involving polymer tethering. In the cases of tether-supported membranes, versatile tethering molecules have been used, ranging from simple polymers to complex multi-functional polymer and peptides [73, 74].

In our view, an ideal membrane tethering molecule should have the following characteristics: (i) a hydrophobic part that will insert into the lipid bilayer; (ii) a hydrophilic polymer that can act like a spacer molecule; (iii) fluorophore labeling to characterize the anchoring; and (iv) a terminal functionality that will be useful in terms of anchoring the tether onto a suitable supporting surface [3]. Obviously, the capacity to form secondary structure might strongly influence the association of hydrophobic peptides within membranes [1]. Figure 1-3 shows the conceptual structure of an ideal peptide anchor for supported membrane. It is composed of membrane-spanning part, a polymer spacer and a terminal functional molecule. In most cases, we link biological dyes onto the tether molecule as detection probes. They enable us to study the localization and distribution of tethered and untethered peptides within the biomembranes. Figure 1-4 showed the assumed schematic structure of solid supported lipid bilayers that integrate custom peptide conjugates as tethering anchors, a functional alpha-helical peptide reconstituted into the bilayers and labeled with fluorescent dye. PEG acts as polymer spacer, and the PEG is anchored via terminal functionality connecting to the modified

solid surface.

Popot and Engelman [40] considered three possible fates for such a peptide arranged as a transbilayer helix that stretches 20 amino acids with predominantly hydrophobic side chains. (see Figures 1-4 and 1-5): (a) the α-helix solvated in lipids might leave the membrane to become an α-helix solvated in water, (b) the α-helix might unfold within the bilayer to a random coil solvated in lipids, (c) the transbilayer α-helix might associate with other α-helices. The whole-residue interfacial hydrophobicity scale of Wimley and White (WW interfacial scale) [75], can be applied to predict the partitioning of unfolded peptides into the membrane interface based exclusively on their sequences and amino acid compositions. It is expected that sequence will be a critical aspect to explain the thermodynamics of transmembrane helix insertion. At the angle of energy level, other estimates of the per-residue free energy for helical hydrogen bond formation range from -0.14 kcal· mol^{-1} to -0.25 kcal· mol^{-1}, which is considered to be a favorable hydrophobic transfer free energy. The free energy can predict partitioning behavior of charged peptides at interfaces and can be used as a basis for estimating nonadditivity.

Popot and Engelman [40] reasoned that most hydrophobic spans could probably be thought of as α-helices, or associations when they were inserted into a membrane. To examine the dependence of the membrane-anchoring properties of the hydrophobic sequences on their environments, many investigations have been carried out on different types of peptides, including amphipathic antimicrobial peptides [76], designed membrane-active peptides [77, 78], and viral fusion peptides. [79] Popot and Engelman [40] and White provide a conceptual framework, stable transmembrane helix formation by

presenting biophysical, biochemical, and biological experiments that test the roles of peptide hydrophobicity, peptide length, lipid composition, lipid acyl chain length, and the presence of polar, helixbreaking, or charged residues on incorporation of peptides, across bilayers.

A key issue remains open in the rational design process: What minimum and maximum lengths of hydrophobic sequences will function as transmembrane domains in biological systems? General researches showed that the composition and length of peptides needed to span bilayers is roughly related with the hydrophobicity and thickness of the lipid bilayers. Studies have shown that short sequences can form transmembrane domains if they are very hydrophobic: nine leucines can suffice in microsomes [80], while 11 leucines are needed in E. coli [81], a single proline in the middle of hydrophobic spans can enable the sequence to form a helical hairpin and cross the membrane twice [82]. Similar research in the Escherichia coli inner membrane showed that hydrophobic residues (four repeats of Leu-Ala-Leu-Val) are sufficient to anchor a protein or a segment of protein [83], that is to say, hydrophobicity should be the predominant characteristic of the “stop-transfer” sequence. The previous research showed that stretches of about 20-24 amino acids with predominantly hydrophobic side chains are suitable for the membrane-spanning regions of integral membrane peptides [115]. Similar studies in the *Escherichia coli* inner membrane showed that 16 hydrophobic residues (four repeats of Leu-Ala-Leu-Val) are sufficient to anchor a functional protein.

Here we adopt a hydrophobic stretch of 24 residues ($K_3A_4L_2A_7L_2A_3K_3$) flanked by lysine at the both end of the peptide, that is is able to incorporate into a series of lipid

membranes. Why choose lysine as the flanked amino residue? A role of charged peptide as flanking charges in inducing or preventing association of transbilayer helices is important in peptide spanning in lipid bilayers. Factors such as orientation of helix formation, ionic interactions between flanking charges of transmembrane peptides can induce helix-helix association [40].

Starting Point of peptide-based tethers

Sodrosky and coworkers carried out a study related with the bilayers fabricated on paramagnetic particles by detergent dialysis of biotin-DOPE doped lipid formulations. In their work, paramagnetic beads were coated with 1D4 antibody and streptavidin. Streptavidin allowed for the membrane reconstitution around beads while the 1D4 antibody allowed for the immobilization of CCR5 heptahelical protein in supported membranes [84]. Sharma and Gilchrist have eliminated the spontaneous formation of bilayers on bare silica surface by completely passivating it with a layer of polyethyleneglycol (PEG) of molecular weight 2000. In order to attach tethering molecules to the silica surface, they have functionalized it with streptavidin, synthesized Biotin-PEG_{3400}-bR conjugates and employed them as the tethering molecules [84][85][137].

In contrast to the research methods mentioned above, our work proposes to use versatile, custom-synthesized peptide molecules as the anchoring moiety. From our experience with construction of alpha helical peptides with covalent linkers, we can begin to build in molecules that could allow is to manipulate the biomembrane with external perturbations

(such as photoisomeration tags that we could use to control or tweak the conformation of the anchoring peptides with light) [86]. We can control the peptide sequence within the biomembrane that could allow for us bind (or repel) other membrane proteins of interest within the membrane [87]. Furthermore, we can control the length of the alpha helix to allow us to position anchors at specific places within complex biomembranes (for instance preferentially at the border of a "raft" domain within the lipid bilayers). The embedded fluorescent peptides can also be used as sites for functionalization of the supported bilayer surface for the attachment of molecules in ligand displays.

1.2 Research Outline Introduction

Overall objectives of our work in light of above discussion are following: Firstly, we need to design and synthesize optimal peptides for tethering the lipid bilayers and conjugate them with appropriate reporter groups, enabling us to investigate the peptide anchors in subsequent processes. Secondly, we need to identify suitable microparticles with desired properties, including surface smoothness, amenability for surface modification, solution stability, available amino group around the beads and minimal background UV/Vis or fluorescence properties for quantification. Thirdly, we have to identify a suitable molecule to be used as tether. Desired properties of the tether include suitable terminal functionality to be used to link it to the surface, a long chain spacer, which will keep the bilayer at a distance from the surface, and a molecule at the far end, which will interact and integrate itself with the bilayer. Figure 1-4 shows a schematic representation of such a tethering molecule. This required synthesis of the tethering

molecule of desired properties by bioconjugation techniques as will be discussed in detail in further chapters. Silica surface is highly hydrophilic and is expected to be somewhat resistant to non-specific adsorption by a variety of hydrophobic molecules ranging from fluorescent tracers to membrane proteins that we need to use in the project. In order to modify the silica surface, silane chemistry is used to functionalize the surface for attaching the tether. Subsequently, we attempt to evaluate the optimal method to fabricate supported bilayers around the tether-linked micro-particles.

1.3 Techniques

1.3.1 Solid phase peptide synthesis

Solid phase peptide synthesis (SPPS), developed by R. B. Merrifield [90], was a major breakthrough the chemical synthesis of peptides and small proteins. SPPS is a quick approach to synthesizing peptides and small proteins where the C-terminal amino acid is attached to a cross-linked polystyrene resin via an acid labile bond with a linker molecule. The N-terminus is protected with the Fmoc group, which is stable in acid, but removable by base. What must been kept in mind is that all the side chain functional groups are protected with base stable, acid labile groups. To begin a general coupling, the Fmoc group on the resin bound amino acid/peptide is removed with N, N-dimethyl formamide (DMF) with piperidine at appropriate concentration. It is then rinsed and a protected amino acid is added after being activated at its 'alpha' carboxyl group by creating the N-hydroxybenzotriazole (HOBt) ester in situ. In the presence of base, the activated amino acid and the resin-bound amino acid are allowed to react to form a new amide bond.

After the peptide is complete, it is ready to be cleaved from the resin by a mixture of trifluoroacetic acid (TFA) and scavengers, the latter serve to neutralize cations generated during the removal of the side chain protecting groups. Generally speaking, the solution is at least 80% TFA, and the rest a mixture of water, phenol, thioanisol, ethanedithiol (EDT), and triisopropylsilane (TIS). The peptide on the resin is allowed to react with the cleavage mixture for several hours at room temperature. It can then be precipitated and washed in tert-butyl methyl ether, and analyzed or purified as desired. This process is repeated until the desired peptide is assembled at the resin [88, 90, 91]. Figure 1-6 shows a schematic representation of SPPS using Fmoc-Chemistry flowchart [88].

1.3.2 HPLC-MS characterization and purification

Mass spectrometry has become a popular experimental method for identifying and characterising proteins and peptides. Because of this simplicity in fragmentation, it is possible to use the observed fragment masses to match with a database of predicted masses for one of many given peptide sequences. Reversed phase HPLC (RP-HPLC) consists of a non-polar stationary phase (generally made up of hydrophobic alkyl chains, C18) and an aqueous, moderately polar mobile phase. The retention time is therefore longer for molecules that are more non-polar in nature, allowing polar molecules to elute more readily. Less polar (more hydrophobic) analytes are more attracted to the stationary phase, hence longer retention time and are eluted at longer times. The samples are fractionated and analyzed on a C_{18} column at appropriate temperatures, using a binary gradient elution (usually methanol/H_2O or acetonitrile/H_2O) with a fluorescent detector.

The peaks area of the amino acids linearly correlated with their concentrations [92].

Since Fenn and coworkers first introduced electrospray ionization (ESI) coupled with mass spectrometry (MS) as an analytical technique, bioanalytical mass spectrometry has become a common tool. Mass spectrometry has emerged as an important contributor to biotechnological field, particularly because the mass of many peptides can be determined directly from a single mass spectrum of a mixture [92]. ESI-MS is now one of the most widely utilized and fastest growing mass spectrometric techniques for the analysis of bimolecular species. [93]

We apply electrospray ionization (ESI) to characterize our rationally designed peptides. The ESI tool has been the standard ionization method for liquid chromatography (LC)-MS and LC-tandem MS (MS/MS), ESI is usually employed for single and triple quadrupoles and quadrupole ion traps that typically give modest resolution [94]. Since ESI is a technique used in mass spectrometry to produce ions, it is especially useful in producing ions from macromolecules because it overcomes the propensity of these molecules to fragment when ionized. In electrospray processes, the ions observed may be quasimolecular ions created by the addition of a proton (a hydrogen ion) and denoted, or of another cation such as sodium ion, or the removal of a proton. Electrospray ion sources are soft ionization sources, that is, they produce mostly protonated molecular ions, MH^+. The proton transfer can occur in sample solution or in the droplets produced by the electrospray source.

$$M + H^+ \longrightarrow MH^+$$

The mass of the MH^+ ion is one greater than the molecular weight, M+1, because of

the extra hydrogen ion that gives the ion its charge [95]. In an ESI-MS spectrum, the Y axis is labeled as relative intensity, this is the intensity relative to the tallest peak in the spectrum with the tallest peak set to 100%, the X axis is mass divided by charge, m/z. The peptide conjugates are analyzed by reverse-phase high-performance liquid chromatography (RP-HPLC), and the eluent deriving from the chromatography separation is directly introduced into an ion-trap mass spectrometer through electrospray ionization (ESI-IT MS). Here samples are analyzed using liquid chromatography/electrospray ionization-mass spectrometry (HPLC-ESI-MS) with a C18 reversed-phase (RP) column and a solvent system containing acetonitrile/H_2O (or MeOH/H_2O) at an appropriate flow rate. Operating in the positive-ion mode, the sodium and/or proton adduct ions are generated in the ESI interface for alcohol, alkylphenol and amide ethoxylates, etc. Usually, coupled with MS analysis of each peak, a relatively simple RP-HPLC separation is sufficient to characterize many mixtures of peptides [96].

A spectrum will have a certain number of counts associated with the tallest peak in the spectrum. This number can be used to gauge the relative intensity or concentration of the analyte. Counts will also be affected by spray needle and over all source maintenance.

When using this technique, we note that:

1. Molecular ions are not generally observed in the electospray ionization process. A molecular ion is formed by the loss of an electron. In the electrospray process, ionization is accomplished by the loss or gain of a proton (or other adduct), some refer to this ion as the "pseudo molecular ion."

2. The electrospray process usually produces a population of multiply charged molecules

and this population is accurately reflected in the intensity of the peaks in the spectrum.

3. In positive ion mode the number of charged species normally observed in an electospray spectrum is reflected in the number of basic sites on a molecule that can be protonated at low pH.

1.3.3 Alpha-helical structural evaluation via Circular Dichroism (CD)

Circular dichroism (CD), a widely used technique for measuring the secondary structure, tertiary structure of complex molecules has an important role in the structural determinants of proteins. It is widely used to examine the structural periodicity of folding of proteins, peptides, nucleic acids, carbohydrates, biopolymers, and small chiral molecules. Additionally, it is an important tool to study the interactions of these molecules generating macromolecular and drug complexes [97, 98].

Circular dichroism (CD) spectroscopy measures differences in the absorption of left-handed polarized light versus right-handed polarized light, which is attributed to structural asymmetry. The absence of regular structure results in zero CD intensity, while an ordered structure results in a spectrum that can contain both positive and negative signals. Secondary structure of proteins and peptides can be determined by CD spectroscopy in the "far-UV" spectral region (190-250 nm) [98]. Within these wavelengths, the chromophore is the peptide bond, and CD signals give rise to distinct patterns in the spectra. Therefore, alpha-helix, beta-sheet, and random coil structures each give rise to a characteristic shape and magnitude within CD spectra. CD signal reflects only an average of the entire molecular population, and thus arises from mixtures of specific peptides

comprising the sample. Far-UV CD spectra require 20 to 200 µl of solution containing 1 mg/ml to 50 µg/ml protein [98] in a buffer that does not absorb strongly in this region of the spectrum.

The CD spectra are calculated for individual structures, based on peptide-group dipole transition moments obtained from semi-empirical molecular orbital theory and using the so-called matrix method. The secondary structure of peptides composed of amino acids can be calculated using ensembles of configurations that can be obtained by molecular dynamics simulation.

Applications

The comprehensive applications of CD are involved in the areas as following: (1) monitoring how proteins fold, misfold, and are correctly folded, how they fold within biomembranes (2) detecting the mutual changes in secondary and tertiary structure that occur when peptides and proteins interact with each other (3) identifying protein and peptide conformation (4) determing whether protein-protein interactions alter the conformation of protein and (5) investigating environmental effects on peptide and protein structure, thermal stability, pH stability, and stability to denaturants.

1.3.4 Basics of Confocal Laser Scanning Microscopy (CLSM)

Fluorescence Phenomenon and Fluorophores

Fluorescence is the phenomenon of emission of photons of visible light by certain molecules when they are excited by absorption of incident radiation of suitable wavelength. Emitted light is generally of longer wavelength compared to the absorbed

light. As well know that a fluorescent molecule has a characteristic excitation and emission spectrum instead of unique spectral lines, which depict the probability distribution for the wavelength dependent excitation or emission of light by the molecule. Figure 1-5 shows a simplified representation of the phenomena of fluorescence [3].

The first step in the fluorescence is the absorption of incident radiation, taking the molecule to an excited electronic energy state; a transition governed by the overlap between the probability distribution functions of the ground and excited state vibrational levels. In the second step, the molecule relaxes down to lower vibrational energy level from the first excited electronic energy state, which is called Internal Conversion. Finally, the loss of electronic energy stored in the molecule can occur in a two ways: radiative and nonradiative, taking the molecule to ground electronic energy state. Lifetimes associated with fluorescence phenomenon are on the order of nanoseconds. Other radiative process (Phosphorescence) which leads to delayed emission of light is through crossing of the molecule to the triplet state and subsequent relaxation to ground electronic state.

Each fluorescent probe has a characteristic excitation and emission spectrum, which is affect by a number of parameters including solvent composition, pH, solvent polarity, etc. A fluorescent dye can be tagged to a larger macromolecule (e.g., a protein, peptide, lipid or nucleic acid) in order to trace these molecules in a structural assembly, such a macromolecule is called a fluorescent bioconjugate. Fluorophores can be divided into two categories, intrinsic and extrinsic. Intrinsic fluorophores occur naturally, including aromatic amino acids (Tyr, Trp, Phe), porphyrins, and green-fluorescent proteins. Extrinsic fluorophores are synthetic molecules tagged on to a macromolecule to impart it with

specific spectral properties.

Our project requires us to build tethering molecular self-assembled structures around microspheres, and we apply fluorophores to characterize the localization of the peptides to the membranes. Using fluorescent markers that stain the modified silica surface at different stages, we facilitate the analysis of surface homogeneity and investigate the added functionality, as well as assist in establishing if the tether is successfully immobilized on the bead surface and aid in visualizing the lipid bilayer assembly on the supported surface.

Confocal Microscopy

Fluorescence based techniques have become important in different disciplines of optical imaging, including biological systems, medical sciences, and various engineering applications. Laser scanning confocal microscopy is the most revolutionary advancement in the field of fluorescence based microscopy techniques. Confocal microscopy has become a primary method of choice for obtaining clear three-dimensional images of microparticles, such as cells and microspheres, where ‘Confocal’ is defined as ‘having the same focuses’. A number of slices can be taken for a thick sample and can be combined to render a three-dimensional reconstruction of the sample. Confocal microscopy enables us to control the exact depth of field for imaging thick specimens and screen out of focus light to get sharply defined images as z-sections in the focal plane. Three dimensional reconstruction of fluorescent structures is obtained by collecting stacks of in focus z-sections and recombining them to form structures based on the fluorescence emission

intensity in each (X,Y,Z) pixel volume element or “voxel”. The crucial features are the use of point-by-point scanning of the sample with an attenuated laser beam and the rejection of out of focus light through spatial filtering of the emitted light beam [104].

The confocal laser-scanning microscope consists of four parts: the light source, the scanning unit, the photomultiplier and the multichannel detection. Schematic representation of the beam path for a confocal microscope has been shown in figure 1-7. Incident light beam from the laser source is first attenuated through a narrow aperture called the source pinhole, which reduces the beam size to few microns. The beam is subsequently reflected through a dichromatic mirror, passes through the objective and illuminates a point on the focal plane on the sample. A fraction of the fluorescence generated from this illuminated spot travels backward through the objective, passing through the dichroic mirror and subsequently focused onto the detector pinhole [104]. (See Figure 1-5)

Confocal microscopy possesses several prominent advantages, such as the controllable depth of field, the elimination of out-of-focus image and hence high-resolution and contrast, inherent improvement in the speed of the image acquisition, the ability to collect serial sections from thick specimens. Furthermore, another advantage is the ability to excite and detect multiple fluorescent probes in separate imaging channels simultaneously. This opens the opportunity for dynamic studies the structures based on distribution of specific labeling of a complex structure and co-localization of the fluorescent probes [100].

1.3.5 Fluorescence recovery after photobleaching (FRAP)

Analysis of the fluorophores conjugated to the anchoring peptide molecules, will reveal information about localization of the tether with lipid bilayers. Another important criterion that can be used to establish the structure of a supported lipid bilayer is the essential fluidity of the bilayer. This can be analyzed by a technique called fluorescence recovery after photobleaching (FRAP), a method for characterization of the molecular mobility of fluorescent molecules in a sample, which will be discussed in details in later section. In order to study the diffusive characteristics of biological molecules in living cells, Axelrod and coworkers developed the technique of FRAP, which relies on the ability to incorporate a fluorescent label into specific protein or lipid components [101, 102]. The analysis of FRAP data enables the calculation of diffusion coefficient of the fluorescent molecules because of diffusion of the unbleached molecules into the illuminated region [103]. This type of study provides a quantitative method for determining if a native-like lipid bilayer has been indeed formed based on the directly measuring the diffusion coefficient of fluorecent lipids within supported biomembranes.

FRAP was originally developed for quantifying two dimensional diffusion characteristics of cell membrane bound fluorescent probes [101], working on the basis of two physical phenomena: (1) photobleaching and (2) diffusion of fluorescent probes. In this process, photobleaching is permanent loss of fluorescent properties of a probe due to light induced irreversible changes in the molecule. The fluorescent molecule can interact with other molecules such as O_2 to result in a non-fluorescent entity. Photobleaching rate of the fluorescent molecules is linearly dependent on the illuminating laser intensity for

one-photon excitation [105-107]. In every excitation-emission cycle a fraction of the population is rendered inactive, and the average number of cycles that a molecule is fluorescent depends on the molecular structure and local microenvironment.

In a typical FRAP experiment, a selected region of a fluorescent sample (~1μm) is subjected to an intense laser beam, leading to photobleaching of the molecules in that region. If the molecules are mobile, fluorescent molecules from other regions will gradually replenish the bleached molecules in the selected region. Analysis of the average florescence intensity of the selected region before and after the bleach can provide the detailed information about the mobility characteristics, e.g. diffusion coefficient, mobile fraction, recovery fraction etc. [107]

The advantages of FRAP technique offered by CSLM are the following: (1) ability to rapidly switch laser power (on microsecond timescales) using acousto-optical tuneable filter (AOTF) between bleach and acquisition sequence; (2) high speed acquisition for fast diffusing components; (3) ability to bleach a wide variety of geometries; (4) ability to individually monitor the fluorescence changes in different regions of interest (ROIs). [103, 104, 108]

1.3.6 Fluorescence-activated cell sorting (FACS) and Quantification of peptide on the substrates

In terms of the feasibility and advantages of flow cytometer, there has been great progress in analysis capabilities, sorting, sample handling and sensitivity in the past decade. These advances contribute to its application in biological and chemical diversity,

sample throughput, high content, and complex systems biology [110]. Detection of fluorescence or other optical properties of cells in flow cytometer can distinguish a range of cell characteristics including surface markers, protein expression, intracellular ions and other biochemical species, DNA content, and cell functions such as apoptosis, cell cycle, and phosphorylation status. The applications of fluorescence-activated cell sorters (FACS) for biotechnology are involved in diagnostics and vaccine development, genomics, proteomics and protein engineering, drug discovery, reproductive biology, plant and marine biology, toxicology, and single molecule detection [109]. Microspheres of varying composition (latex, glass, and dextran) are used as solid supports for immunoassays of proteins, peptides, sequence analysis of nucleotides, phospholipids with incorporated receptors, and molecular assemblies involving receptors, signaling partners, toxins, and libraries of chemical compounds. Flow cytometer measures multiple parameters (fluorescence intensity and light scatter) for each particle and discriminates particle populations based on size, morphology, and other properties. It is a powerful tool to combine the potential for high-content analysis, the ability to measure multiple parameters on a single particle, and the ability to measure multiple classes of particles simultaneously [110].

The process begins by placing the particles of interest into a flask and forcing them to enter a small nozzle one at a time (Figure 1-7). The micro-particles travel down the nozzle which is vibrated at an optimal frequency to produce drops at determined distance from the nozzle. As the particles flow down the stream of liquid, a laser beam scans them. Some laser is scattered (green) by the particles, and this is used to count the amount and

measure the size of the particles. By collecting the information from the light (scatter and fluorescence) a computer can determine which cells are to be separated and collected.

The process begins by placing the particles of interest into a flask and forcing them to enter a small nozzle one at a time (Figure 1-7). The micro-particles travel down the nozzle which is vibrated at an optimal frequency to produce drops at determined distance from the nozzle. As the particles flow down the stream of liquid, they are scanned by a laser beam. Some laser is scattered (green one) by the particles and this is used to count the amount and also measure the size of the particles. By collecting the information from the light (scatter and fluorescence) a computer can determine which cells are to be separated and collected.

Particles suspended in a liquid are passed through a focused laser beam and the optical signals are processed in real time. Commercial flow cytometer analyzes and sorts cells or particles at rates up to 50,000 per second, can detect thosands of fluorescing molecules per particle depending upon the fluorescence properties of the molecule. The particles sizes detected range from submicron to tens of microns [110].

Detection of fluorescence or other optical properties of cells in flow cytometer can distinguish a range of cell characteristics including surface markers, protein expression, intracellular ions and other biochemical species, DNA content, apoptosis, cell cycle, and phosphorylation status [110][111]. Generally, the amount of surface peptide on a microsphere is not measured directly; rather, it is often calculated using a fluorescent ligand in combination with fluorescence intensity standard microspheres [112][113].

In order to calibrate the FACS apparatus, a bead-based standardization method can be

applied [114]. In our research, we use QuantumTM FITC-5 MESF Premix as the standard beads. The use of FACS and our standardization experiments will be discussed in detail in Chapter 3 and 4.

Figures and Tables

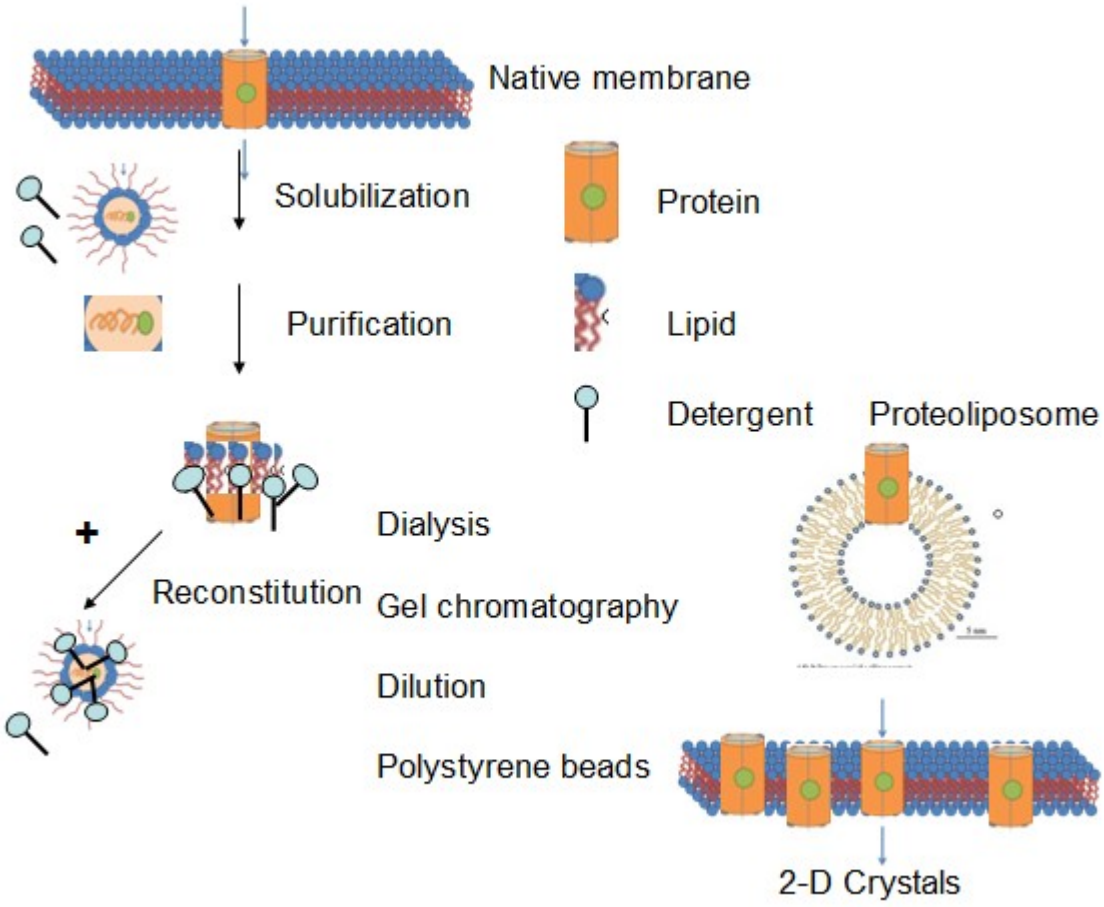

Figure 1-1 Detergent-mediated reconstitutions. Most membrane proteins are extracted from native membranes with solubilizing detergent concentrations. After purification, the solubilized protein is supplemented with an excess of lipids and detergents, leading to a solution of mixed lipid-protein-detergent and lipid-detergent micelles. For proteoliposome or 2-D crystal reconstitution, detergent is removed from these micellar solutions using different strategies [22].

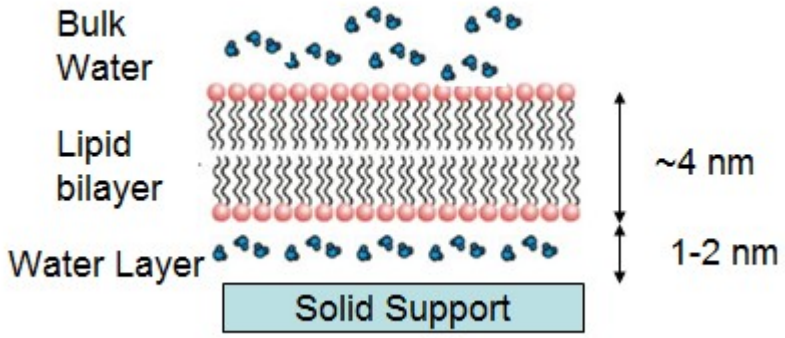

Figure 1-2 Schematic diagram of a solid supported phospholipid bilayer. The membrane is separated from the substrate by a 1-2 nm thick layer of water [104].

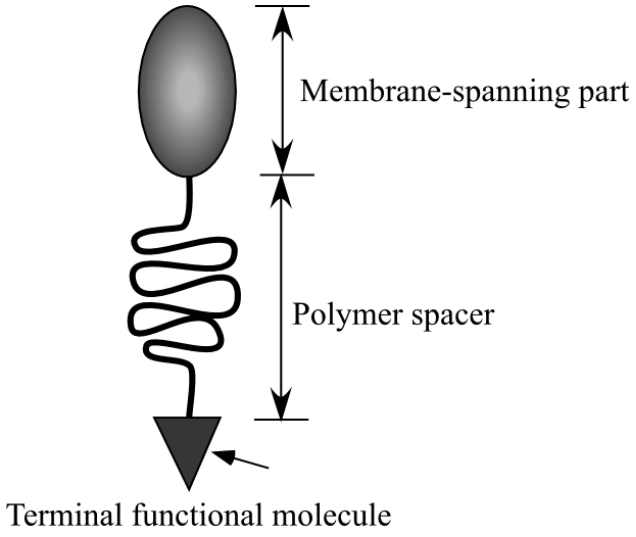

Figure 1-3 Schematic representation of a molecule suitable for use as a membrane tether.

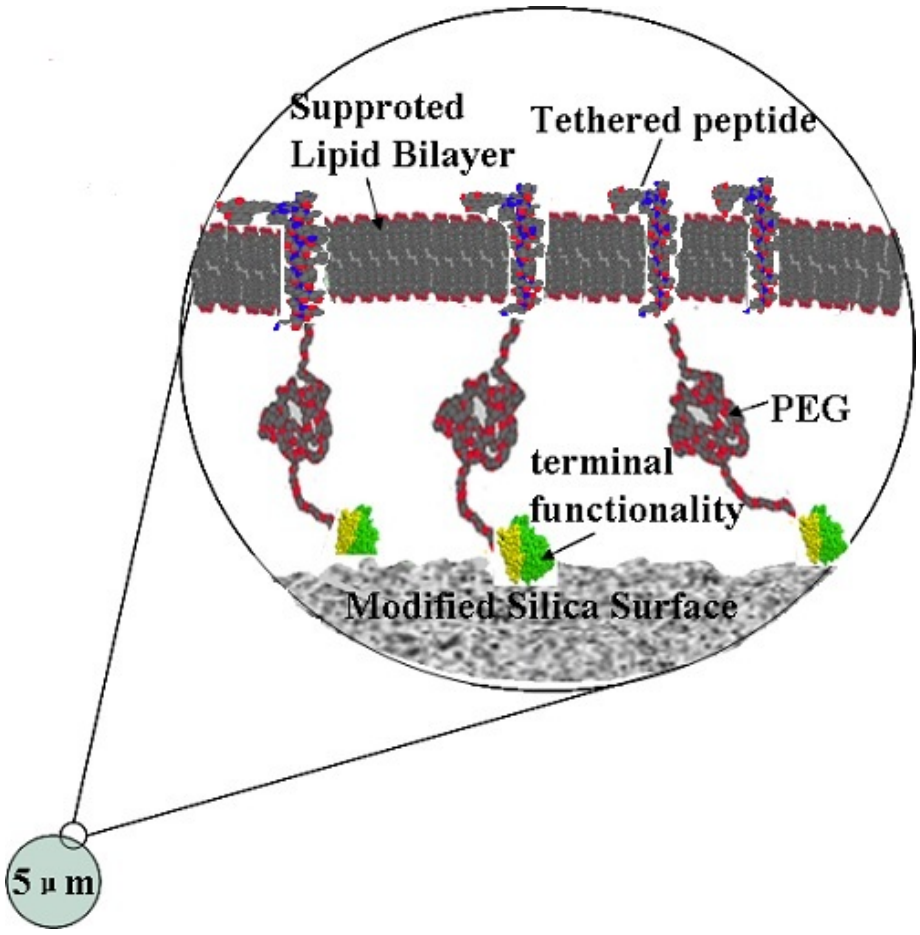

Figure 1-4 Schematic diagram of solid supported lipid bilayers that integrate custom peptide conjugates as tethering anchors

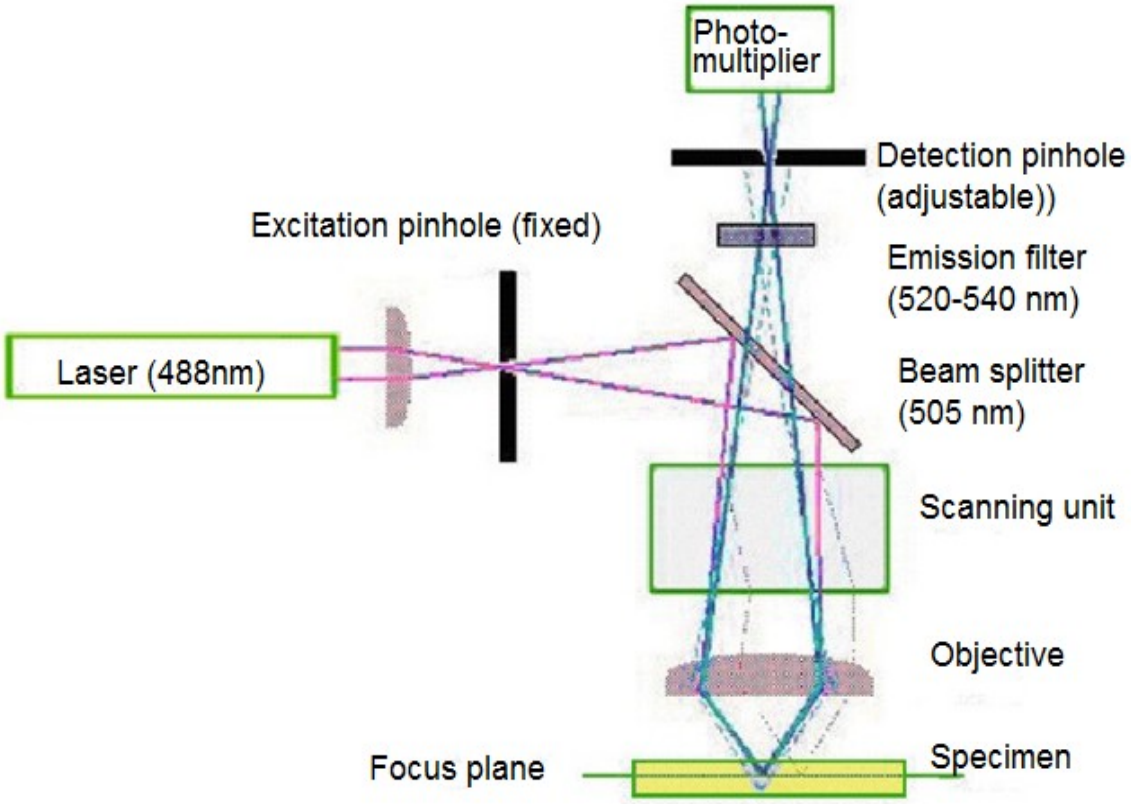

Figure 1-5 Schematic representation of the beam path in a confocal scanning laser microscope.

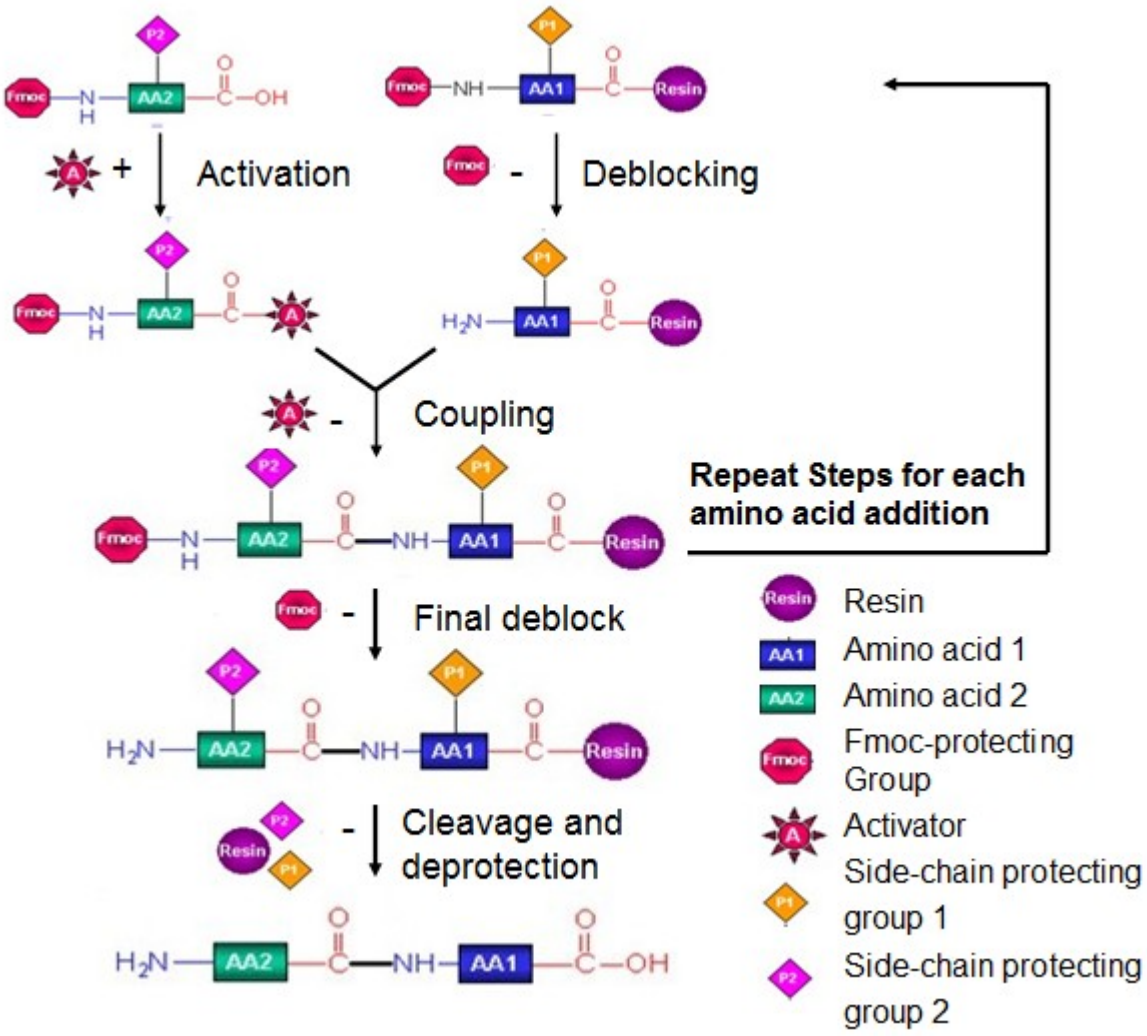

Figure 1-6 Basic Steps in Solid Phase Peptide Synthesis Using Fmoc-Chemistry (Developed by http://www.sigmaaldrich.com/)

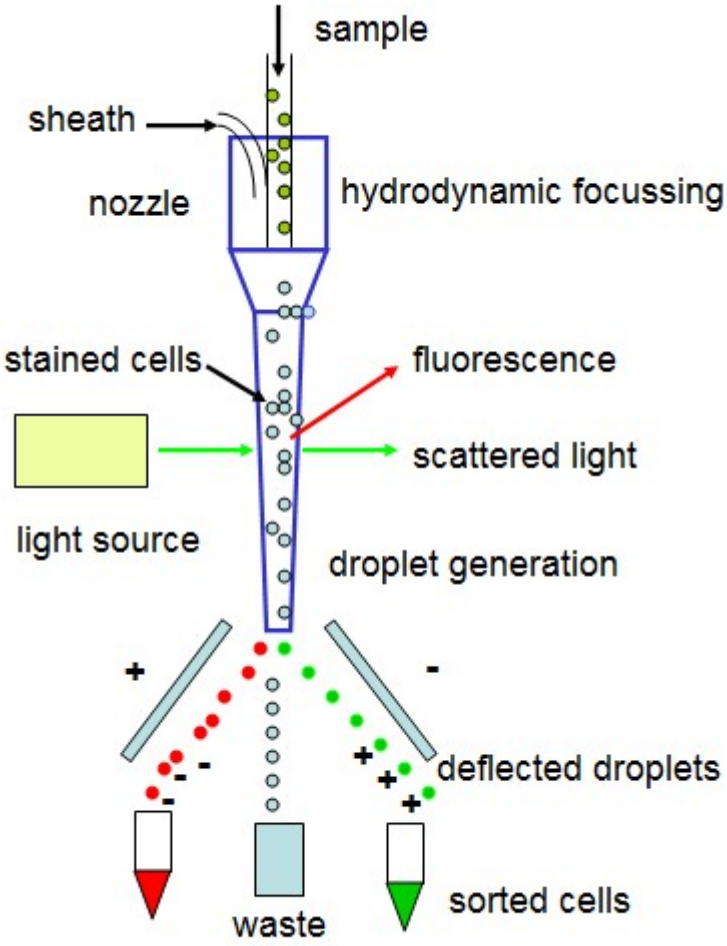

Figure 1-7 Diagram of FACS machine. Cells have been fluorescently tagged with either red or green antibodies, though not every cell expresses the epitope and therefore some are not tagged either color

Chapter 2
Synthesis of Alpha-helical Peptide Tethers and Characterization

This chapter describes the starting point of our rationally designed peptide, preliminary research of peptide synthesis, fabrication of NHS-ester and peptide bioconjugates that use the custom synthesized alpha helical peptide $K_3L_3A_{12}K_3$, and orthogonal fluorescently labeled peptide $K_3A_4L_2A_7L_2A_3K_3$. Here we apply the SPPS method described in Chapter 1. Subsequently, we attempt to functionalize these peptides with fluorescent groups for membrane localization as well as biotinylation, or, other modification for anchoring to the support. These conjugates were characterized using reversed-phase HPLC in tandem with electrospray ionization mass spectrometry (RP-HPLC-ESI-MS), Circular Dichrosim and Confocal Microscopy.

At this stage of our study, our aim was to construct NHS-esters-peptide conjugates and peptide-FITC for anchoring the lipid bilayer membranes to microspheres. The motivation for our approach of using alpha-helical peptides comes from the enhancement of the stability of tether-supported membranes described in Chapter 1. Popot and Engelman [40] reasoned that most hydrophobic spans could probably be thought of as α-helices when they were inserted into a membrane. In the peptide-based tethers mentioned above, peptides are inserted into the supported membrane, spanning the entire membrane with large contact areas within the hydrophobic parts of the bilayers. Our hypothesis is that the peptide will act as a membrane anchoring “molecular rivet”, providing the supported membrane with a biomimetic flexible interface and much higher stability.

This work describes peptide synthesis and the construction of NHS-Rhodamine, NHS-PEO_4-Biotin, NHS-Fluorescein conjugated peptides, as well as peptide-FITC for the

formation of solid-supported membranes on particles. We have used amine-based coupling to conjugate NHS esters to alpha-helical peptides ($K_3L_3A_{12}K_3$) at their amino terminus, and fluorescently labeled peptide $K_3A_4L_2A_7L_2A_3K_3$. The conjugates were characterized using Electrospray Ionization Mass Spectrometry (ESI-MS) after reversed-phase High Pressure Liquid Chromatography (HPLC) purification, afterwards the secondary structure of peptide was characterized using Circular Dichroism (CD). Lateral fluidity of the fluorescently tagged peptide will be analyzed via fluorescence imaging microscopy (Confocal Microscopy) and quantified using fluorescence recovery after photobleaching (FRAP) techniques in the following experiments.

2.1 Introduction

Popot and Engelman found that the folding of many integral membrane proteins (here, we refer to peptide helices spanning within the bilayers) can be understood as two energetically distinct stages. In the first stage, independently stable helices are formed across the hydrophobic region of the lipid bilayer. Secondly, the helices interact with one another to give a functional, globular membrane protein. Similarly, helix-helix peptides interactions participate in the stabilization of membrane proteins [40]. The length and hydrophobic properties are two key factors allow for scanning the sequence for stretches of peptide residues in lipid bilayers, which are expected to be at lower free energy across a membrane than in an aqueous environment. Burkhard's research indicates hydrophobicity values of alanine is close to zero when studied in the context of helical polypeptides (24 residues) and phospholipid bilayers [115], and careful sequence design

(described below) allows us to evaluate the connection between sequence, length and stability in the peptide anchor.

2.2 Methods and Materials

2.2.1 Solid phase peptide synthesis and Fmoc Cleavage

A wide variety of polyalanine as well as leucine-alanine peptides have been shown to adopt predominantly helical conformations in membrane environments. CD spectra show polyalanine-based peptides exhibiting fully helical conformations in SDS [115]. Similarly, lysine-flanked polyleucine or (LA) in sequences of sufficient length adopt transmembrane orientations. Related results indicate that sequences composed of 18 alanine (and/or leucine) residues can be accommodated in a transmembrane fashion. This observation confirms that lysine-flanked 18-residue helices match the hydrophobic thickness of POPC bilayers [115]. Chung and Thompson demonstrate that many different conformations of polyalanine-type sequences are present and interconnected by multiple equilibria in aqueous solutions [117].

We synthesized two kinds of peptides as target anchors: $K_3L_3A_{12}K_3$ and $K_3A_4L_2A_7L_2A_3K_3$. It is reasonable to assume that the size, shape, and conformation of peptides are strongly affected by changes in the solvent system. Although the inherent hydrophobicity of alanine allows both $K_3L_3A_{12}K_3$ and $K_3A_4L_2A_7L_2A_3K_3$ to exhibit transmembrane alignments, kinetically trapped configurations, such as for example small multimeric complexes, which do not efficiently insert into the lipid bilayers exist in a preparation- and time-dependent manner.

As a model for our studies, we selected a 24-residue peptide as target anchors, as shown in Figure 2-1. Here Lysine plays the role as “flank” to orientate peptide into lipid bilayers. To evaluate the progress of the synthesis, samples of resin were removed after construction of each helical region, and these were cleaved and analysed. Syntheses were performed using Fmoc SPPS protocols, as shown in Fig 1-10, via PS3 peptide synthesizer using continuous flow methods. To evaluate the effects of transmembrane helical insertion on synthetic efficiency, the stepwise synthesis of the full-length peptide was also attempted in an identical manner using only standard Fmoc amino acid derivatives.

Optimum cleavage conditions are dependent on the individual amino acid residues present, their number and sequence, the side chain protecting groups, and the type of linker attached to the resin. In the case, cleavage can be affected with TFA/water (95:5). TFA is an extremely corrosive liquid, great care must be taken when using this reagent, Proper eye protection, lab coat, and gloves are mandatory. Such steps are conducted in the fume hoods. We place dry resins in a flask and add TFA solution (TFA/water 95:5) (10-25ml/g resin). Stopper the flask and leave to stand for ~2 hours at room temperature with occasional swirling. We remove the resins by filtration under reduced pressure via a vacuum pump. We wash the resins twice with TFA and collect all filtrated solution and elutions.

We combine filtrates, and add 8-10 fold volume of MTBE (Methyl-tert bultylether) into the flask, rinse the container twice to transfer all peptide residues into a new flask. The peptide should precipitate in the MTBE. We transfer the suspension to a clean centrifuge tube and seal it. We centrifuge at a speed of 2500 rcf (force) for 20 minutes at

-4 ℃ and keep the precipitated fraction. We then repeat the ether wash and centrifugation steps twice. At this stage, we can store the dry peptides at -4℃, protecting fluorescent groups (if present) from light exposure.

2.2.2 Peptides, NHS esters and Solvent

Alpha helical peptide: $K_3L_3A_{12}K_3$ is synthesized and kept on the p-Benzyloxybenzyl Alcohol Resin (PL RINK Resin 75-150μm Polymer Laboratories) with a loading of 0.63 mmol peptide/g resin. The polymer matrix is copoly (styrene -1% DVB), 100-200 mesh. This is a standard resin for the Fmoc batch SPPS. Fmoc ((F)luorenyl-(m)eth(o)xy-(c)arbonyl) protect group is on the N-terminus of peptide, and Boc ((tert)-(B)utyl (o)xy (c)arbonyl) protect group is on the side chain of amino group of Lysine. Additionally, Fmoc-Lys(Dde)-OH (Novabiochem) is used to orthogonally protect the N-terminal Lys on the Wang-Resin (Thorn BioScience. Advanced ChemTech.) for $K_3A_4L_2A_7L_2A_3K_3$. The loading is 0.70 mmol peptide/g resin with a swollen volume of 7.0ml/g in DCM, and the polymer matrix is copoly (styrene -1% DVB), 100-200 mesh.

All the chemical structure schematics of Fmoc-amino acid, NHS esters, Biotin reagent and FITC are presented in Table 2-1.

NHS esters and FITC (Fluorescent reagent): NHS-Rhodamine, NHS-Fluorescein, NHS-PEO_4-Biotin, are from the Pierce Company. The chemical structure schematics are presented in table 3-3; NHS-Rhodanime (5-(and) 6-carboxytetramethylrhodamine succinimidyl ester) MW. 527.5 g/mol, Pierce Prod#46102 Lot GE96444 (Moisture and light sensitive); NHS-Fluorescein (5,(and 6)-carboxylfluoresecein, succinimidyl ester)

MW. 473.4g/mol, Prod#46100 Lot#GE96822 (Moisture and light sensitive) CAS 117548-22-8; NHS-PEO_4-Biotin Amine-reactive labeling reagent with a hydrophilic polyethylene oxide (= polyethylene glycol, PEG) spacer arm. MW 588.67g/mol; fluoresceine isothiocyanate (FITC), Molecular Weight: 389.38g/mol (Pierce Corp.)

Solvent: N, N-dimethyl formamide (DMF, Product No. 20673), Dichloromethane (DCM), 95% (v/v TFA/water= 95:5) trifluoroacetic acid (TFA), Methyl tert-butyl ether (MtBE), Methanol, Ethonal. (All chemicals with reagent grade, from Fisher Co. and Sigma Inc.)

2.2.3 Conjugations of Peptides and NHS esters

In the preliminary stage of SPPS experiments, we construct fluorescent labeling α-helical peptide conjugates from on several NHS esters. The N-hydroxysuccinimide (NHS) ester is a common activation chemistry for creating reactive acylating agents. NHS esters were first introduced as reactive ends of homobifunctional cross-linkers [146] (Bragg and Hou, 1975). Today, the majority of amine-reactive cross-linking or modification reagents commercially available use NHS esters. An NHS ester may be formed by the reaction of a carboxylate with NHS in the presence of a carbodiimide. To prepare stable NHS ester derivatives, the activation reaction must be done in nonaqueous conditions using water-insoluble carbodiimides or condensing agents, such as DCC. NHS ester-containing reagents react with nucleoophiles that release of

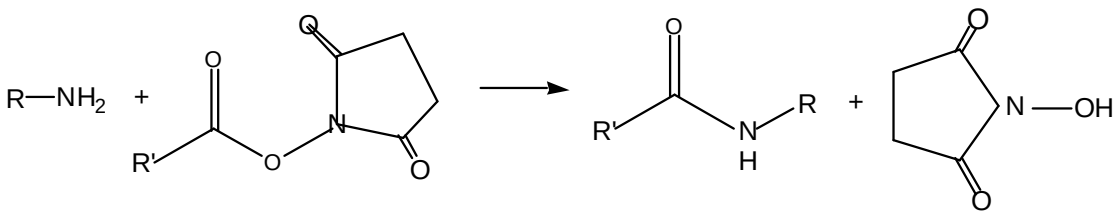

the NHS leaving group to form an acylated product. The reaction of such esters with a sulfhydryl or hydroxyl group does not yield stable conjugates, forming thioesters or ester linkages, respectively. Both of these bonds hydrolyze in solution [116].

Taking the conjugate reaction of NHS-Rhodamine and our peptide as an example, the peptides react with NHS-Rhodamine in organic solvent DMF at room temperature for 2~4 hours, the Fmoc group is removed by pyridine and then replaced with Rhodamine group. Afterwards, we get the peptides linked with rhodamine, and the peptides are still attached on the resin. Then we use 95% TFA to cleave the peptide from resin, and, simultaneously, the TFA cleaves the Boc group from the peptides. The chemical formula of two synthesized peptide and structure of starting resin are presented in Table 2-2. The schematic flowchart of starting material for NHS conjugation of peptide ($K_3L_3A_{12}K_3$), conjugates attached on resin and final products as $K_3L_3A_{12}K_3$ -Rhodamine conjugates are also shown in Table 2-3.

Using an approximate peptide-resin grafting density of 1.0 mmole peptide/g resin, we use ~30mg resin beads and control the molar ratio of peptide: NHS ester as 2:1. Accordingly, we measure appropriate amount of NHS ester reagents and add the peptide containing resin beads to 20 ml Dimethylformamide (DMF). The reaction vessel includes a funnel with quartz filter, letting beads swell freely in the organic solvent at room temperature for 2~4 hours. We dissolve NHS ester reagents with ~10 ml DMF, pour into a funnel, rinse the container of NHS esters two or more times to make sure all the reagents transfer into the reactor. For the coupling reaction, the contents are mixed

well and then incubated at room temperature for 2 hour.

We filtrate DMF solution through the glass filter by using vacuum pump to reduce the pressure in the reactor, remove nonreacted NHS- esters and take out the resin beads. We rinse the beads with dichloromethane (DCM) for 2~3 times, then rinse with dimethylformamide (DMF) for 2~3 times. Finally, we rinse with methanol for 2~3 times to dry the resin. We store the resin beads with the fluorescently labeled peptide at 4°C in a brown vial to protect them from light until they are ready to use. At this stage, the resin is clearly functionalized with the fluorescent group as the bead itself is fluorescent, even after repeated washing in solvent to remove unreacted fluorophores.

2.2.4 Fluorphore conjugation to peptide anchors

Orthogonal amine-protecting groups for the solid phase synthesis of branched peptide

Suitably protected lysine derivatives, such as Fmoc-Lys(Dde)-OH, Fmoc-Lys(Ddiv)-OH, and Fmoc-Lys(Alloc)-OH, allow the assembly of single sequence after Fmoc Deprotection. Chemical structures of these protecting groups are showed in Table 3-1 in detail. Selective removal of the orthogonal protection thus allows the assembly of another sequence in a similar manner to the addition steps of protected amino acids. As far for Fmoc-Lys(Dde)-OH, the N- Dde group is more susceptible to removal on either prolonged or repeated treatment with 20% piperidine in DMF, as well as susceptible to migration via intra-or intermolecular transamination pathways in the presence of free amines [124].

In terms of synthesis, we combined automatic PS3 synthesis (pre-synthesize peptide species $K_3A_4L_2A_7L_2A_3K_2$ with the orthogonal chemistry. We return to a new kind of resin: Fmoc-Leu-Wang resin to avoid the first amino acid coupling problems and increase the yield of peptide synthesis. Additionally, we conduct a manual synthesis, for coupling Fmoc-Lys (dde)-OH on the N terminus of peptide. After completion of automatic PS3 peptide synthesis, we conduct the ninhydrin test to monitor the existence of free primary amine group as follows. A small amount of ninhydrin solution (10% by weight ninhydrin in ethanol) is heated to 120°C. A few of resin are added to one test tube. When primary amines are present on the resin, ninhydrin solution turns blue; otherwise, the color of the solution remains unchanged.

We pre-swell the Resin-peptide ($K_3A_4L_2A_7L_2A_3K_2$) in DMF for 1 h in a reaction flask after Fmoc group deprotecting, wash the resin with DMF and filter away any excess DMF from the resin bed. We prepare a solution of Fmoc-Lys (Dde)-OH (0.4mmol), HTBU (0.4mmol) and Methylmorpholine (0.6mmol) in DMF (1.5ml). We leave the mixture for 2min. (Active reagent concentration 0.4M), then add the mixture to the resin bed, gently agitate the reaction suspension for 2h. We wash the resin with DMF three times, treat the resin with 20% (v/v) piperidine in DMF for 10 min, and remove any excess DMF from the resin bed. Subsequently, we place the resin-peptide in a flask and treat with 2% $NH_2NH_2 \cdot H_2O$ monohydrate in DMF (25mg/L) for 3 min at room temperature, filter the resin and repeat the previous step two more times. After completing the reaction, we wash the peptide-resin with DMF three times, collect the peptide-resin construct, wash with DCM (30ml), then let resin dry in hood. The peptide construct can

be cleaved from the solid support using standard TFA acidolytic mixtures as discussed before. Then, we obtained peptide species ($K_3A_4L_2A_7L_2A_3K_3$) [115] as anchoring molecules, and orthogonally modified [118] fluoresceine isothiocyanate (FITC) peptides allow us to detect the localization and distribution of anchors spanning the biomembranes, where Dde is cleaved by 2% hydrazine in DMF [119].

What's more, for the latest study, we chose fluorescein isothiocyanate as a more economical fluorescent dye ($200 for 100 mg). After N-terminal DDE group is removed, we label the fluorescent molecule onto the orthogonal site by incubating the resin-bounded peptide with FITC at room temperature overnight, keep reaction in dark. Later the tBoc group is removed from peptide and the peptide is cleaved from the resin by a mixture of 95% trifluoroacetic acid (TFA) peptide, and we precipitate the product in Methyl tert-butyl ether (MtBE), removing the precipitating solution with repeated centrifugation steps at -4℃.

For both cases, we place dry peptide-bounded resins in a flask and add TFA solution (TFA/water 95:5) (10-25ml/g resin). We stopper the flask and leave the solution standing for ~2 hours at room temperature with occasional swirling. We remove the resins by silica funnel filtration under reduced pressure via a vacuum pump, wash the resins twice with TFA and collect all filtrated solution and elution. Then, we combine filtrates, and add 8-10 fold volume of MTBE (Methyl-tert bultylether) into the flask, rinse the container twice to transfer all peptide residues into new flask. The peptide should precipitate in the MTBE, and we transfer the suspension to a clean centrifuge tube and seal it. We centrifuge with speed of 2500 rcf (force) for 20 minutes at -4 ℃ and reserve the

precipitates. Later, we repeat the ether wash and centrifugation steps twice. We remove all the ether supernatant and obtain precipitates (conjugated peptides). Finally we store the dry peptides at -4 ℃, protecting it from light. The flowchart of synthesis process of FITC-labeled peptide ($K_3A_4L_2A_7L_2A_3K_2$) is presented in Figure 2-1, and the schematic of FITC amine coupling mechanism is showed in Figure 2-2.

2.3 Techniques

HPLC Purification

As discussed in Chapter 1, reversed phase HPLC (RP-HPLC) consists of a non-polar stationary phase (generally made up of hydrophobic alkyl chains, C18) and an aqueous, moderately polar mobile phase (methanol/H_2O). The retention time is therefore longer for molecules which are more non-polar in nature, allowing polar molecules to elute more readily. Less polar (more hydrophobic) analytes are more attracted to the stationary phase, hence longer retention time and are eluted last.

Our samples are fractionized and analyzed on a C_{18} column at appropriate temperature, using a binary gradient elution (usually methanol/H_2O or acetonitrile/H_2O) with a fluorescent detector. The peaks area of the amino acids linearly correlated with their concentrations. Using HPLC purification, we could get predominantly concentrated peptide species at >95% purity.

EI-MS Characterization

In our project, samples are analyzed using liquid chromatography/electrospray ionization-mass spectrometry (HPLC-ESI-MS) with a C18 reversed-phase (RP) column

and a solvent system containing acetonitrile/H_2O (or MeOH/H_2O) at an appropriate flow rate (1~2.5 ml/min). Operating in the positive-ion mode, the sodium and/or proton adduct ions are generated in the ESI interface for alcohol, alkylphenol and amide ethoxylates, etc. Usually, coupled with MS analysis of each peak, a relatively simple RP-HPLC separation is sufficient to characterize many mixtures of peptides [121]. The spectra and analysis are shown in Figure 2-3~2-5.

2.4 Results and Discussion

We have demonstrated successful conjugation of α-helical peptide with several NHS esters and peptide-FITC conjugates to synthesize tether molecules. Conjugates are purified using HPLC, and the conjugates are characterized with RP-HPLC/ESI-MS; we aim to further probe the functional structure of peptides by CDs and Confocal scanning laser microscopy, which will be discussed in Chapter 4 and 5.

Identification of peptide

The relevant molecular weights for mass spectrometry are included below. The molecular weights of α-helical peptide $K_3L_3A_{12}K_3$, $K_3A_4L_2A_7L_2A_3K_3$ and amino acids Alanine (A), Leucine (L), Lysine (K) are 1979.48 g/mol, 2234.79 g/mol, 89.09 g/mol, 131.18 g/mol, and, 146.19 g/mol respectively. What's more, taking the molecular weight of NHS-Rhodamine, NHS-PEO_4-Biotin, NHS-Fluoresein and FITC into consideration, we can calculate the theoretical molecular weights of the desired conjugates as follows:

(a) Rhodamine-peptide 2392.97 g/mol

(b) PEO_4-Biotin-peptide 2454.14 g/mol

(c) Fluoresein-peptide 2338.87 g/mol

(d) Peptide-FITC 2624.16 g/mol

Other candidate peptide conjugate species are given in Table 2-4. The peptide characterization is carried out using reversed-phase HPLC with a C18 column in tandem with ESI-MS. The total time required to carry out this RP-HPLC/ESI-MS analysis is less than 15 minutes. The peptide bands are injected into the mass spectrometer, and the masses of the peptides are determined. For instance, taking the experimental results of the Rhodamine-peptide as examples (See Figure 2-3), the $[M+H]^+$ spectrum obtained from RP-HPLC/MS analysis reveals a dominant peak, which elutes between 8.472 and 8.543 min. This dominant peak contained a dominant $[M+H]^+$ ion of *m*/*z* 2256.4628. These $[M+H]^+$ ions correspond most closely to the with molecular weights 2250.81 g/mol, calculated for the $K_3L_3A_{10}K_3$ peptide conjugated with Rhodamine, with one lysine residue lost (Table 2-4). However, it is clear from the chromatogram that there are a large number of other peptide species formed.

Similar results were obtained for Fluorescein- and Biotin PEO_4- peptide conjugates, shown in the chromatograms in Figures 2-4. The fluorescein-peptide conjugates formed were spread over a greater number of species, however none of the species were consistent with $K_3L_3A_{10}K_3$-Fl found in the Fluorescein case, as would be expected since the same peptide starting material was used. In the analysis of the Biotin PEO_4- peptide conjugates a dominant peptide band of 2256.46 is consistent with $K_2L_3A_{11}K_3$-PEO_4-Biotin (2254.89: the large broad peak centered at 9.5 minutes is an artifact). Again this is inconsistent with the idea that the same bound peptide starting material was used for the conjugation, however,

perhaps other peptide permutations are present that we have not included. In particular, possibilities include peptides fragmented into shortened versions of the parent peptide via peptide-bond hydrolysis. According to the comparison in Table 2-4, considering the reduction of H_2O molecular weight when forming peptide bond, besides the molecular weights of amino acids Alanine (A), Leucine (L), Lysine (K), we can obtain the rough confirmation of peptide identification.

Figure 2-5 shows the MS spectra/Reverse phase-HPLC chromatogram of our synthesized peptide, it reveals a dominant peak with molecular weight 1963.26 g/mol, which means, we get a highly pure synthesized peptide species, ($K_3A_4L_2A_7L_2A_3K$). Figure 2-3 is the reverse-phase HPLC chromatogram of Rhodamine-peptide conjugates. This was some of the first successful results we obtained in the anchor peptide synthesis. X-axis stands for retention time, Y-axis records the strength of the detector signal, proportional to the concentration of species reveals a dominant peak, the dominant peptide band of 2256.46, corresponding to the highest peak 2256.4628 m/z in Mass spectrum, X axis is stands for mass-to-charge ratio where Y axis reflects the relative intensity of species. It shows 2256.4628 g/ mol in MW, maybe it is the most abundant species in the sample.

Why did we lose some amino acids in the peptide synthesis? It could be attributed to of experimental conditions in the synthesis microenvironment, instabilities of synthesized conjugates and probably, most important, the sequential amino acid coupling conditions and reaction times. The picture shows PEG pattern, 44.026 m/z between two adjacent mass peaks, it is caused by trap abundance in column, so we could not take the inconsistent data into consideration. In our experiment interfering peaks (m/s of 520.333, 564.359,

608.385 652.411, 696.438) were observed in every RP chromatogram corresponding to a percentage of can between 34-37% with a signal to noise ratio. These contaminants are enriched on the stationary phase of the trap column.

Successful peptide synthesis and fluorescently labeled species $KA_4L_2A_7L_2A_3K_2$

MS spectra give the information of molecular weight of synthesized peptide. The ESI/MS chromatogram of synthesized peptide shows that we get peptide species: $KA_4L_2A_7L_2A_3K_2$. They show that we have successfully synthesized the peptide and the fluorescently labeled species (Fig. 2-5). The percentage of FITC labeled peptide to unlabeled peptide was ~93%. The result shows the dominant species existing in target sample is with molecular weight 2349.6 g/mol, and a high purity in synthetic peptides is present before HPLC purification. Also, ($KA_4L_2A_7L_2A_3K_2$) show high helicity in both aqueous phase and liposomes (Figure 4-9), which enable it to form stable and hydrophobic self-assembled anchors within supported lipid bilayers. This is our starting molecule of choice for use as peptide anchors in the following experiments.

Circular Dichroism Spectra Analysis

As discussed in Chapter 1, CD can give the valuable information about secondary structure of peptides, as well as play an important role in the structural determinants of the shape and folding of peptide conjugation. Circular dichroism spectroscopy was conducted using an Olis DSM 20 CD spectrometer (Olis, Inc., Bogart, GA). To probe the peptide structure we employed circular dichoism spectroscopy of the peptide starting material and FITC conjugated species in micelles and liposomes. The CD spectra were

showed in figure 2-6. In each case, minima are seen near 225 nm that are indicative of high α-helical content. Secondary structure analysis of the unlabeled peptide yielded high α-helicity in both aqueous phase and liposome micelles, with ensemble average helicities of 94.2% and 89.0% respectively (red spectra and blue dotted line spectra). The top spectra (green) was from the $K_3A_4L_2A_7L_2A_3K_2$-FITC species embedded in liposomes. The helicity of this species was somewhat lower as the effect of FITC labeling likely perturbed the peptide structure, as the FITC group constituted a greater than 20% increase in molecular weight, adding a sizeable hydrophobic moiety to the N-terminal residue of the molecule. It is unclear if at this level of peptide to lipid ratio peptide aggregates form that perturb the intramembrane structure relative to freely-diffusing species. The negative peaks found at 209 and 222 nm present are characteristic of helix formation, and have been evidenced a multitude of studies of helical proteins and peptides.

Our peptide approaches perhaps what could be considered a “canonical” alpha helix domain, anchored in the hydrophobic region of the DOPC by lysines at the C- and N-termini [Anchor bechinger ref]. In this case the $A_4L_2A_7L_2A_3$ core forms a 2.7 nm long hydrophobic helical domain that is well-matched to the hydrophobic core of DOPC, a lipid bilayer structure experimentally determined to have a hydrophobic core thickness of ~2.72 nm when hydrated, proved to present helicity in structural models supported by CD data that would conceivably add hydrodynamic drag to the C-terminus.

Figures and Tables

Table 2-1 The chemical structure schematics of Fmoc-Ala-OH, Fmoc-Leu-OH, Fmoc-Lys-OH, Fmoc-Lyd(Dde)-OH, NHS esters, NHS-PEO4-Biotin and Fluoresceine Isothiocyanate (FITC)

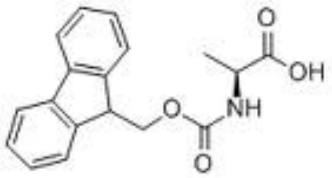

Fmoc-Ala(Boc)-OH, MW:311.34

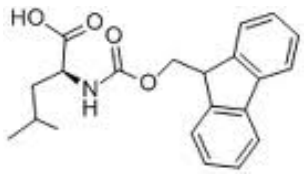

Fmoc-Leu(Boc)-OH, MW:353.42

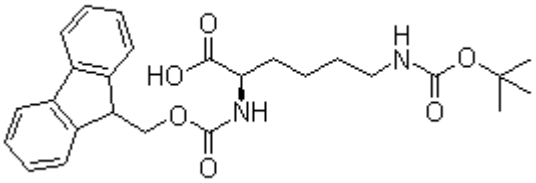

Fmoc-Lys(Boc)-OH, MW: 379.3

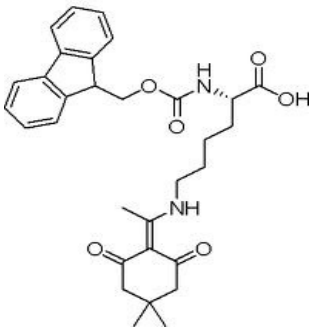

Fmoc-Lys-Dde ($C_{31}H_{36}N_2O_6$) MW: 532.64

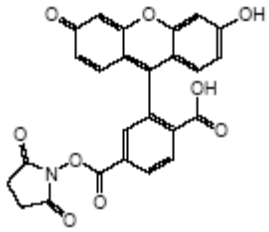

5-carboxyfluorescein succinimidyl ester

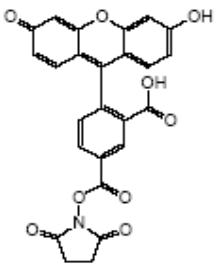

6-carboxyfluorescein succinimidyl ester

NHS-Fluorescein

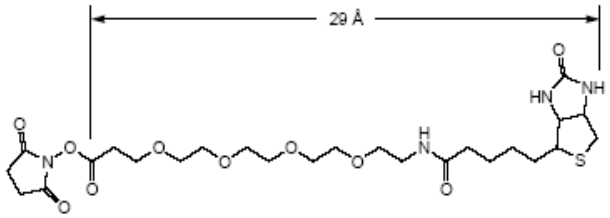

NHS-PEO_4-Biotin (Amine-reactive labeling reagent with a hydrophilic polyethylene oxide spacer arm)

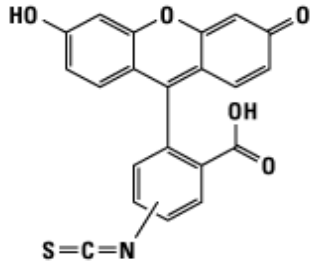

Fluorescein Isothiocyanate (FITC), MW: 389.38, Ex/Em 494/518 nm

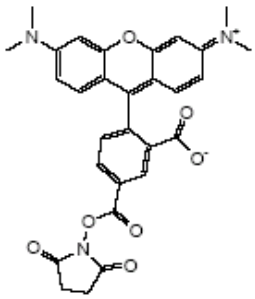

5-carboxytetramethylrhodamine

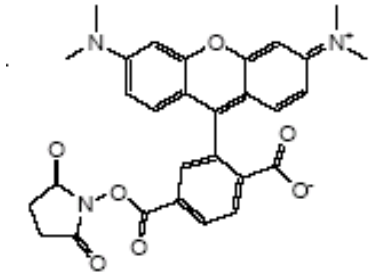

6-carboxytetramethylrhodamine

NHS-Rhodamine

Table 2-2 Peptide starting material ($K_3L_3A_{12}K_3$ with Fmoc, Boc groups, attached on resin), $K_3A_4L_2A_7L_2A_3K_3$ p-Benzyloxybenzyl Alcohol Resin (PL-RINK Resin) and Fmoc-Lys-Wang Resin.

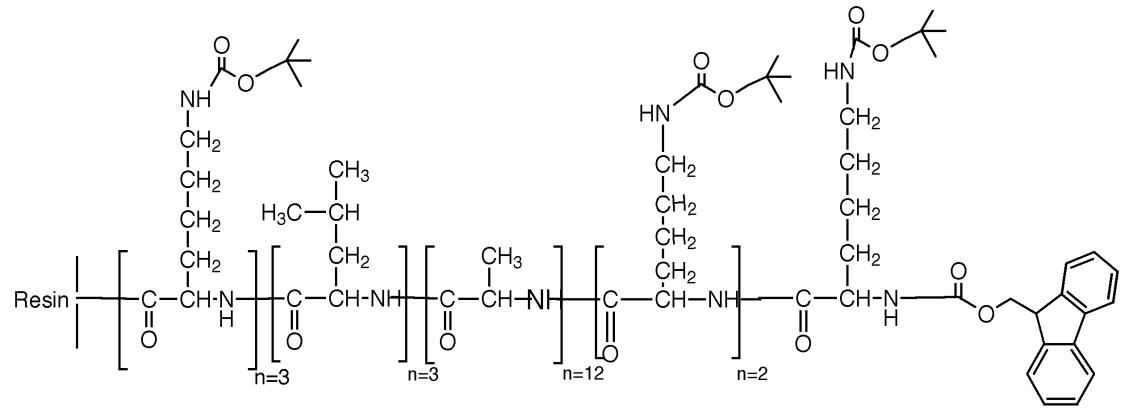

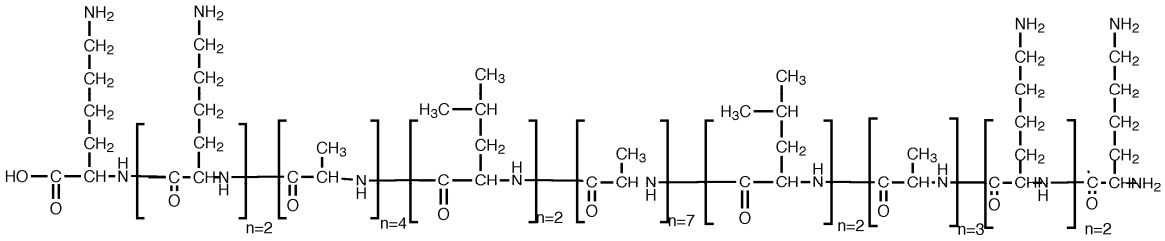

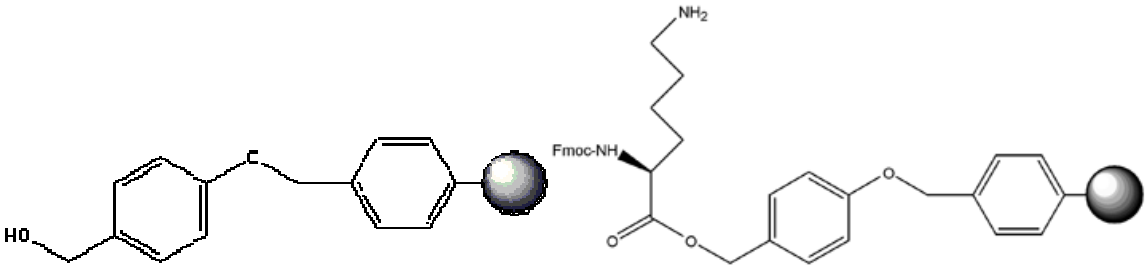

Table 2-3 The chemical structure of the idealized starting material, flowchart of synthesis process of $K_3L_3A_{12}K_3$-Rhodamine conjugates: Rhodamine conjugate attached on the resin and final product peptide $K_3L_3A_{12}K_3$-Rhodamine after tBoc de-protecting

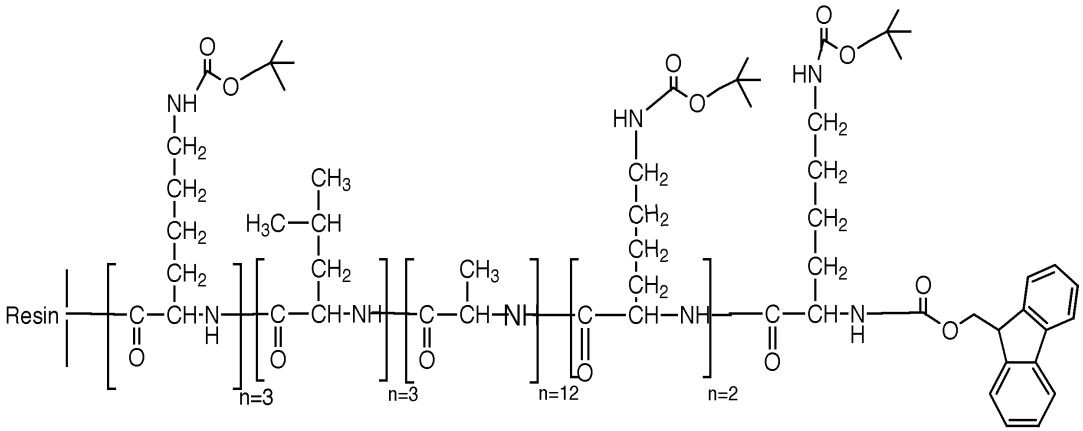

Peptide starting material ($K_3L_3A_{12}K_3$ with Fmoc, Boc groups, attached on resin)

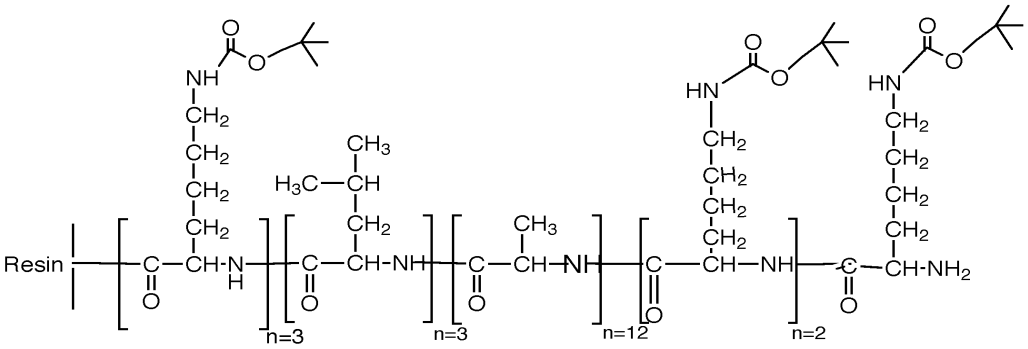

Fmoc protecting group on the site chain of lysine is moved by 20% piperinde/DMF, temperature

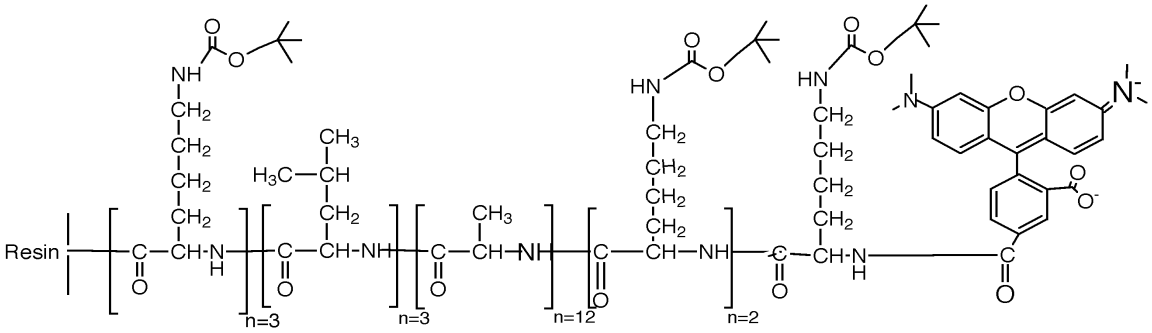

Peptide with Boc pretect groups, conjugated with Rhodamine, attached on the resin

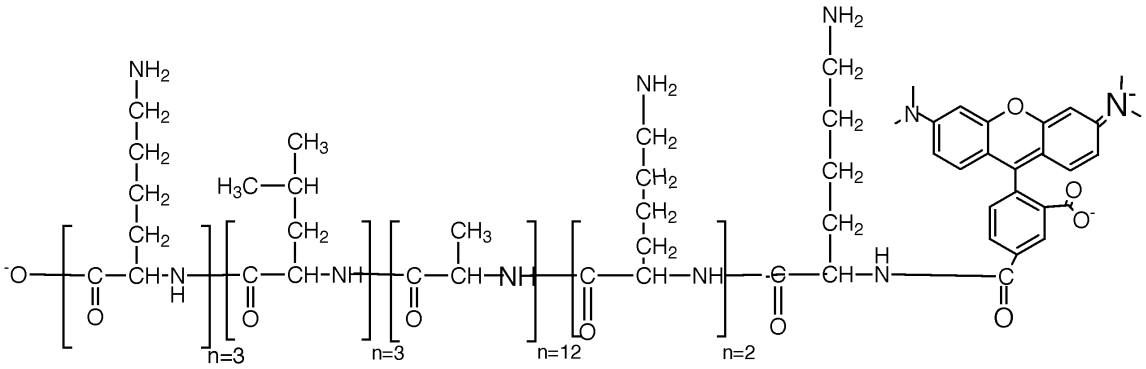

N-terminal Rhodamine labeled peptide conjugate ($K_3L_3A_{12}K_3$-Rhodamine)

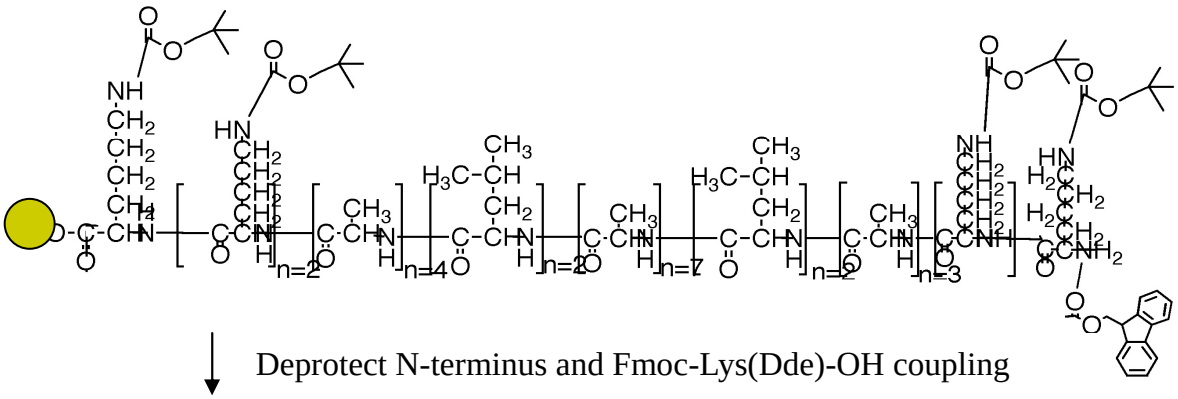

Deprotect N-terminus and Fmoc-Lys(Dde)-OH coupling

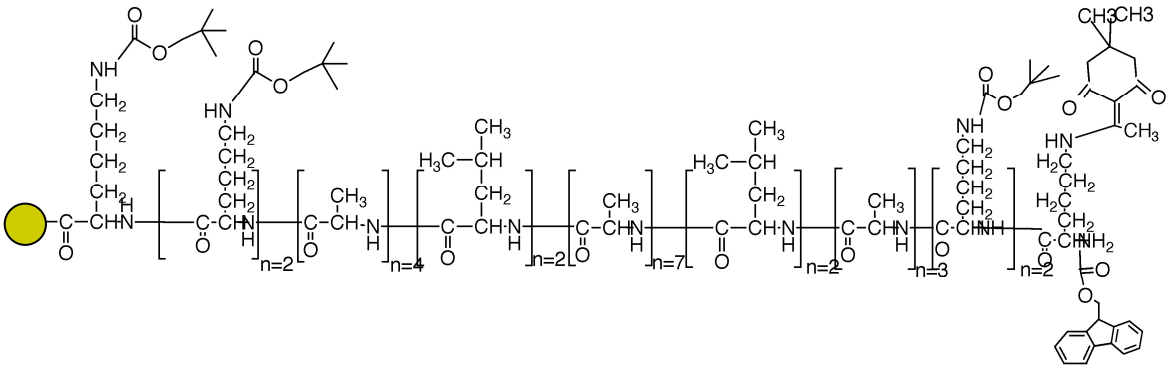

Deprotect Dde group with $NH_2NH_2H_2O$

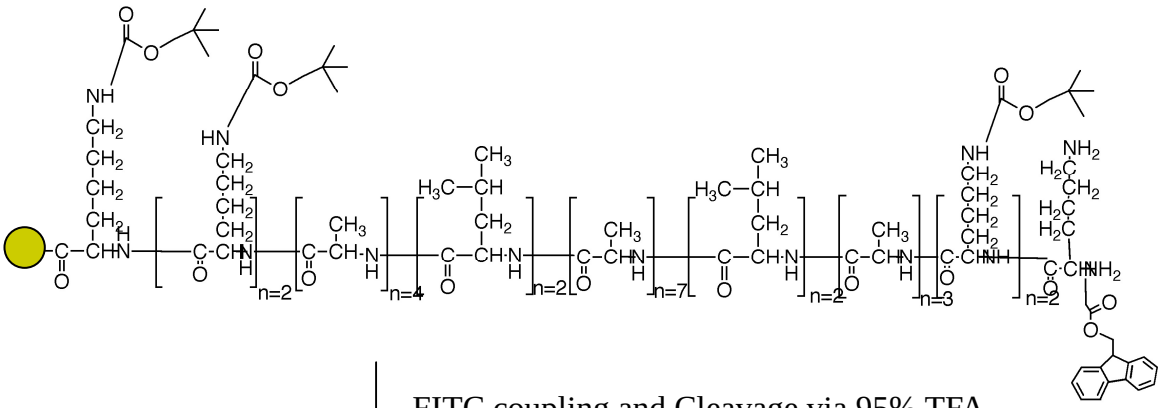

FITC coupling and Cleavage via 95% TFA

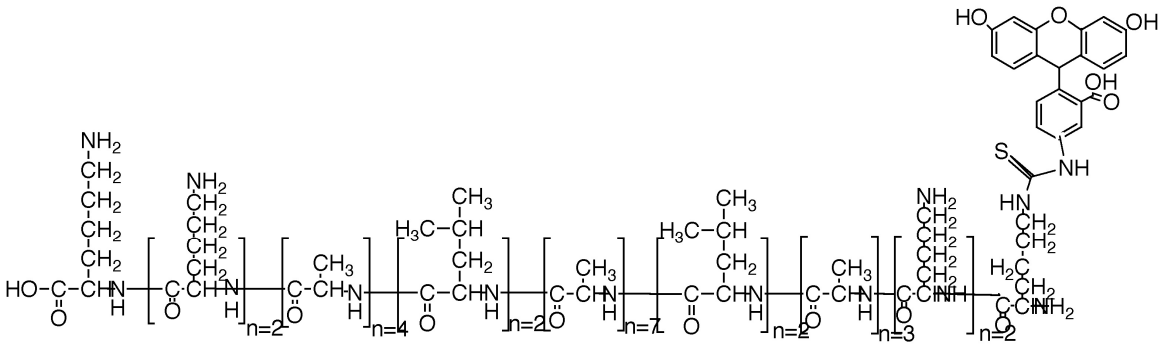

Figure 2-1 Flowchart of $K_3A_4L_2A_7L_2A_3K_3$-FITC conjugation Process: Swell pre-synthesize peptiede species $K_3A_4L_2A_7L_2A_3K_2$.bounded resin in DMF. Couple Fmoc-Lys(dde)-OH on the N terminus of peptide after Fmoc group deprotecting by 20% pipieridine/DMF. Treat resin with 2% $NH_2NH_2 \cdot H_2O$ monohydrate in DMF (25mg/L) for 3 min at RT to remove N-terminal DDE group on last lysine residue. Lable FITC to the orthogonal DDE site overnight. Cleave tboc from peptide and peptide from the resin by a mixture of 95% trifluoroacetic acid (TFA). Precipitate peptide in Methyl tert-butyl ether (MtBE) to get recrystallization at -4□, freeze dry and store at 4□ in dark.

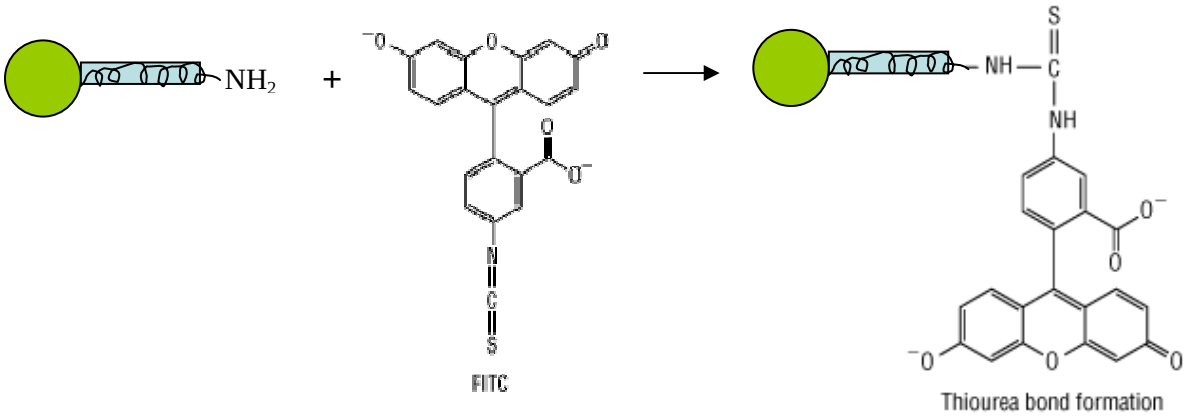

Figure 2-2 Schematic of FITC amine coupling with peptide Mechanism, FITC is the most simple reagents for protein fluorescent labeling, isothiocyanates react to amino groups on peptides, the derivatives of primary and secondary amines generally yield stable products, reaction is stable at pH 8-9. Peptides can be effectively labeled with several fluorophore tags per peptide protein molecule when reacted with a 15- to 20-fold molar excess of isothiocyanate-activated fluorophore.

Table 2-4 the calculated results of all permutaion of peptide conjugates ($K_3L_3A_{10}K_3$)

Permutation of peptide residues		Conjugated with Rhodamine MW (g/mol)	Conjugated with Fluorescein MW (g/mol)	Conjugated with PEO_4-Biotin MW (g/mol)
$L_3A_{12}K_3$	1594.96	**2008.46**	1954.36	2069.63
$K_3A_{12}K_3$	1639.99	2053.49	**1999.39**	2114.66
$K_3L_3A_{10}K_3$	1837.31	**2250.81**	2196.71	2311.98
$K_3L_3A_9K_3$	1766.23	**2179.73**	2125.63	2240.9
$K_2L_3A_{12}K_3$	1851.3	**2264.8**	2210.7	2325.97
$K_2L_3A_{11}K_3$	1780.22	2193.72	2139.62	**2254.89**
$K_2L_3A_{10}K_3$	1709.14	**2122.64**	2068.54	2183.81
$K_2L_2A_{10}K_3$	1595.98	**2009.48**	1955.38	2070.65
$K_2L_2A_9K_3$	1524.9	1938.4	1884.3	**1999.57**
$K_3L_2A_9K_3$	1653.07	2066.57	2012.47	**2127.74**
$K_3L_2A_8K_3$	1581.99	**1995.49**	1941.39	2056.66
$K_3A_{12}K_3$	1639.99	2053.49	**1999.39**	2114.66
$K_3A_2K_3$	**929.19**	1342.69	1288.59	1403.86
$KL_3A_{12}K_3$	1723.13	**2136.63**	2082.53	2197.8
$KL_3A_{11}K_3$	1652.05	2065.55	2011.45	**2126.72**
KL_3K_3	**870.17**	1283.67	1229.57	1344.84
KLA_4K_3	**928.17**	1341.67	1287.57	1402.84
$L_3A_{12}K_3$	1594.96	**2008.46**	1954.36	2069.63
$L_3A_{11}K_3$	1523.88	1937.38	1883.28	**1998.55**
$L_2A_6K_2$	**927.15**	1340.65	1286.55	1401.82
L_2AK_2	571.75	985.25	**931.15**	1046.42
L_2K_2	500.67	914.17	**860.07**	975.34
L_2A_2K	514.66	**928.16**	874.06	989.33

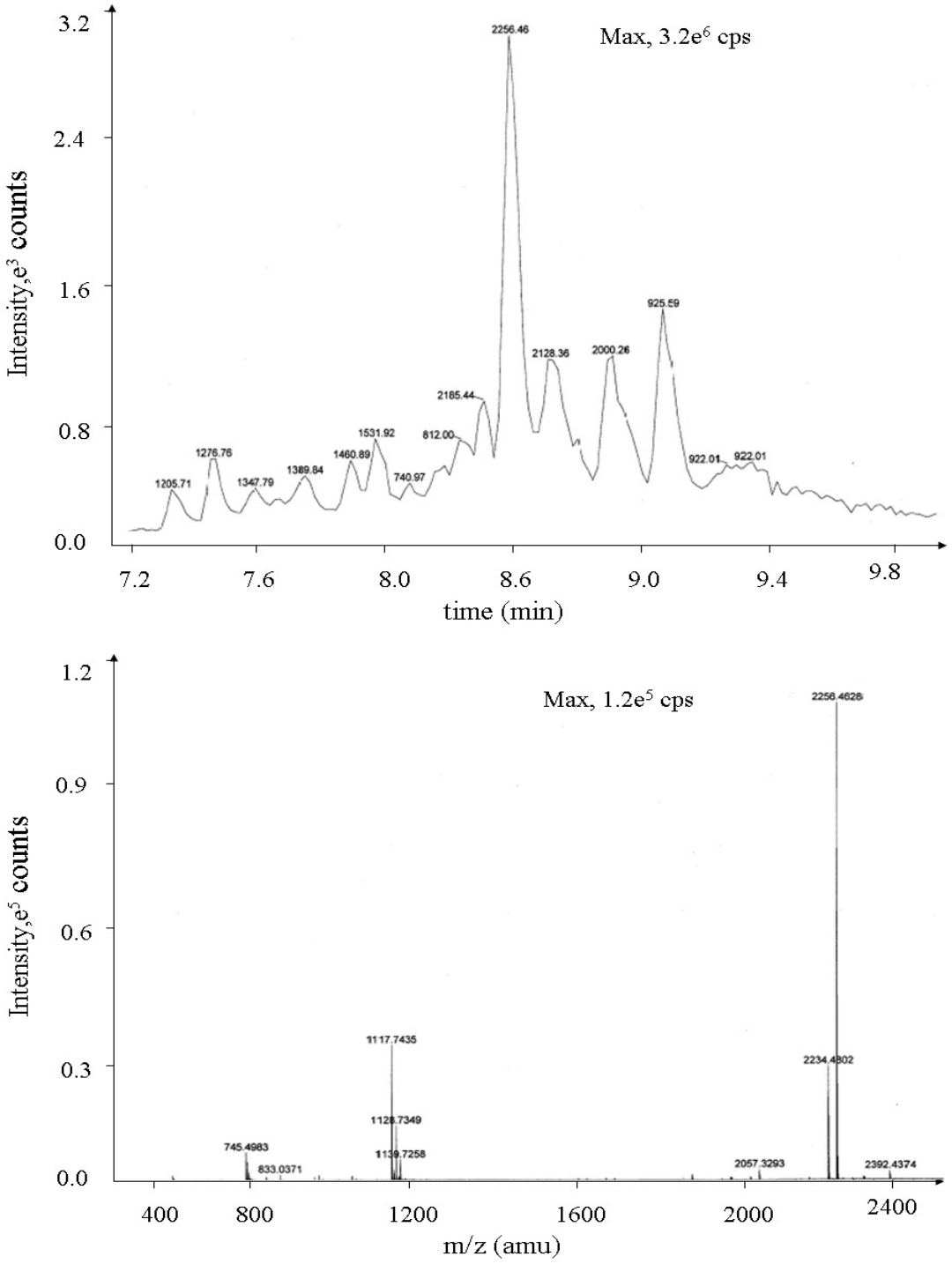

Figure 2-3 the HPLC reverse-phase chromatogram and corresponding the mass spectrum of Rhodamine-peptide conjugates, Polarity/Scan Type: Positive. Max. 3.2e6 counts. The highest peak of 2256.46m/z, elute from 8. 472 to 8.543 min. Polarity/Scan Type: Positive. Max. 1.2e5 counts. The highest peak of 2256.4628 m/z, representing the peptide species with molecular weight: 2256.4628 g/mol, that is $K_3L_3A_{10}K_3$ peptide species conjugated with Rhodamine

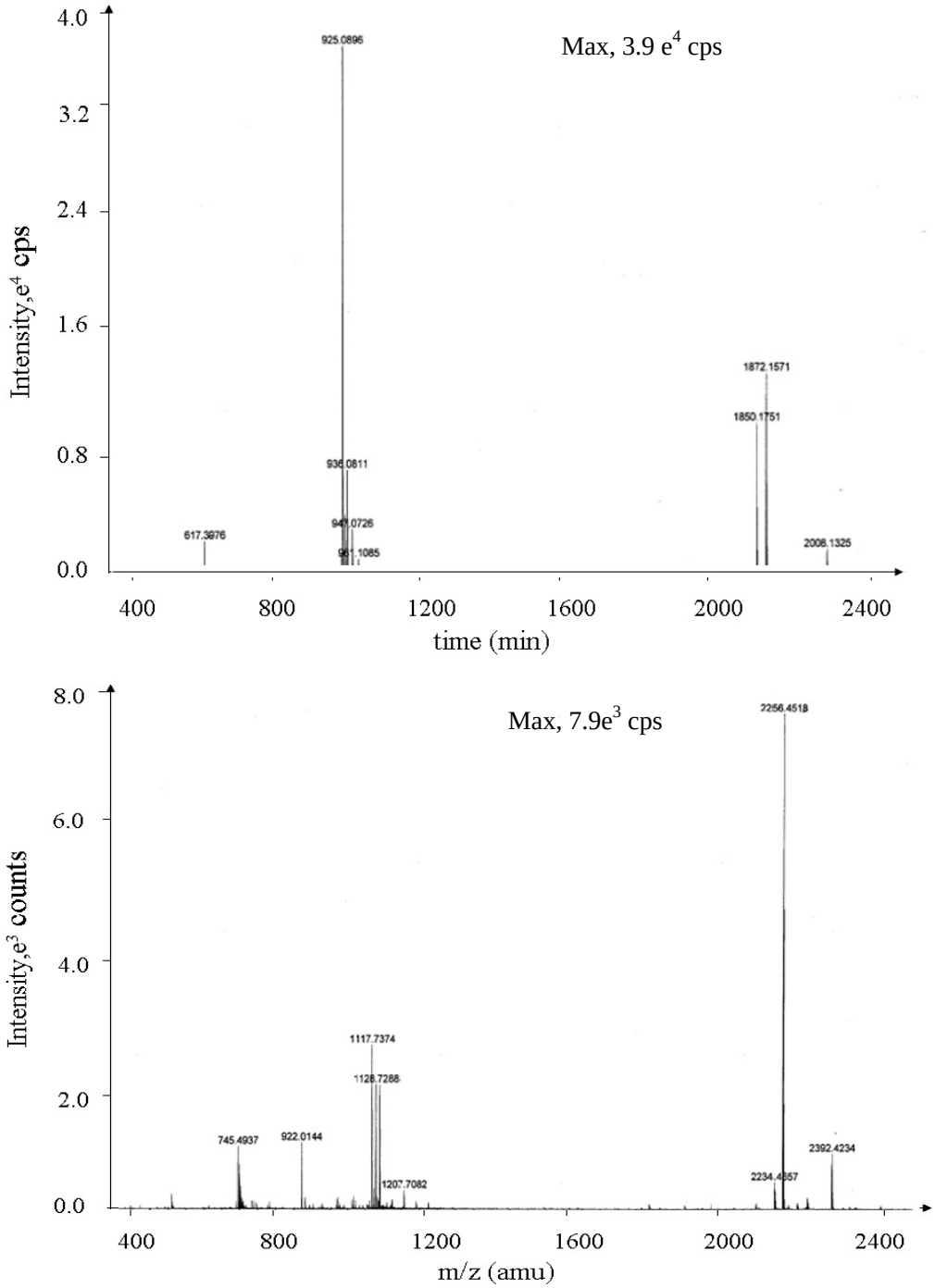

Figure 2-4 the mass spectrum of Fluorescein-peptide conjugates and PEO_4-Biotin conjugates, Polarity/Scan Type: Positive. Max. 7.94.0e^3 counts. (1) The highest peak of 925.0896m/z, elute from 9.039 to 9.110 min, two positive charges, representing the peptide species with molecular weight: 1848.18 g/mol, that is $K_3L_3A_{10}K_3$ peptide species conjugated with Fluorescein,(2) elute form 8.700 to 8.771 min, a dominant peptide band of 2256.46 is consistent with $K_2L_3A_{11}K_3$-PEO_4-Biotin (MW: 2254.89: the large broad peak centered at 9.5 minutes is an artifact).

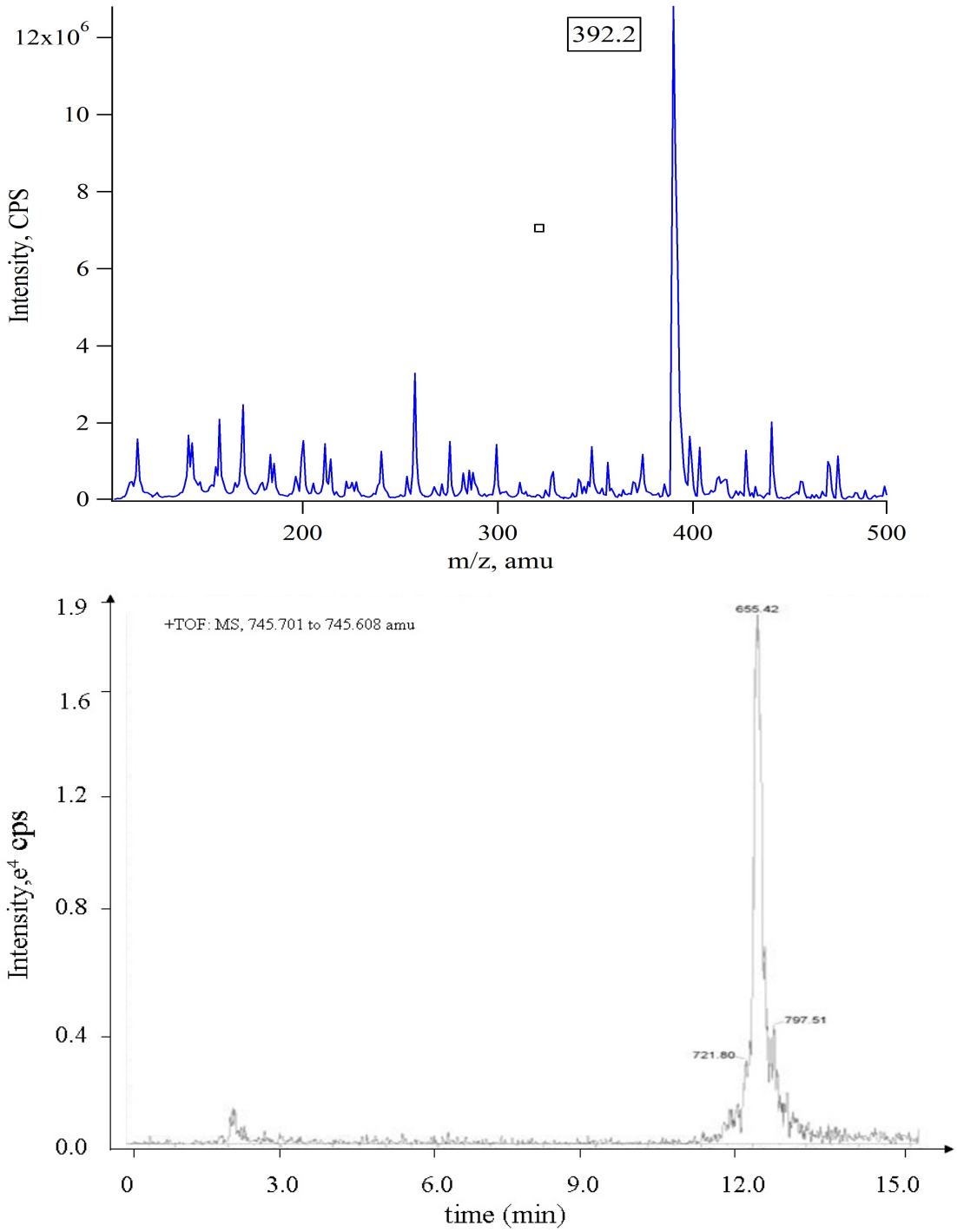

Figure 2-5. ESI-MS result of fluorescently labeled synthesized peptide, dominant species is at the mass peak 392.2 m/z, with six positive charges. Accordingly molecular weight 2349.6 g/mol, proven to be $KA_4L_2A_7L_2A_3K_2$-FITC. Mass Spectrum 0.004min to 0.575min, positive charged turbo pray. The ratio of FITC labeled peptide occupied 93.2% in all synthesized peptide species

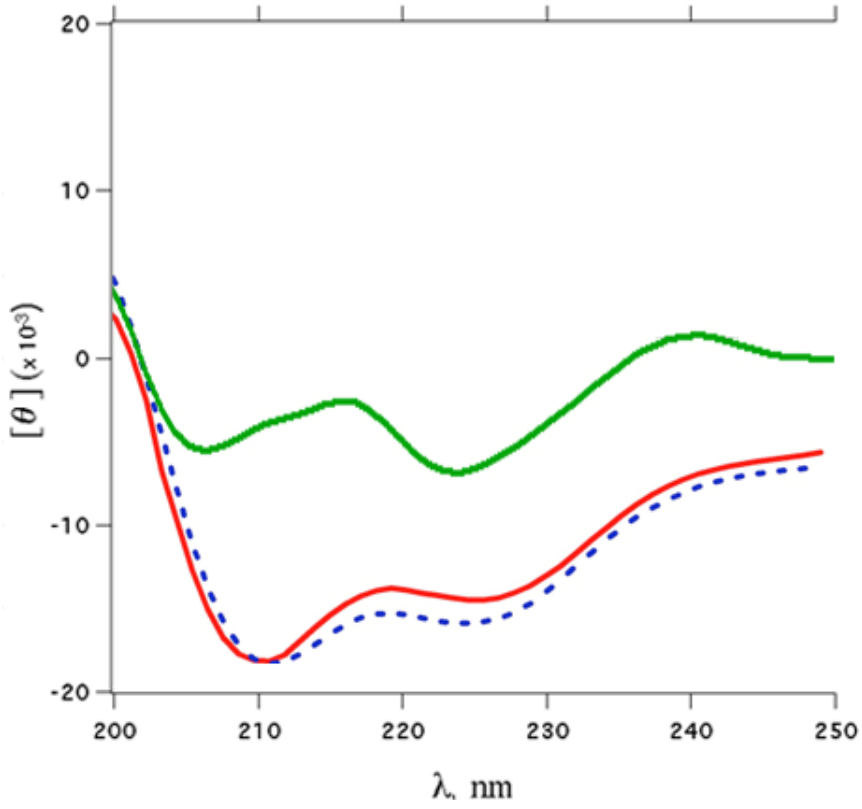

Figure 2-6. Circular dichroism spectra of the synthesized peptide in aqueous and lipid phase. Circular dichroism spectroscopy was conducted using an Olis DSM 20 CD spectrometer (Olis, Inc., Bogart, GA). CD spectra were obtained in Hepes A buffer at 1% OG concentration. The Peptide in water (0.2mg/ml), ensemble average alpha helicity is 94.2%. Broken line: Peptide within liposome (peptide: DOPC=1:30), ensemble average alpha helicity is 89.0%. Dot line: fluorescently labeled peptide spanning within lipid bilayers, ensemble average peptide alpha helicity is 74.6%, molar ratio of Peptide-FITC to DOPC is 1:10, peptide concentration is 0.2mg/ml. [98][122].

Chapter 3
Functionalization of Silica Bead Surface with Diverse polymers

Motivation

In the previous chapter we described in detail the synthesis of custom peptides, peptide-NHS esters and peptide-FITC conjugates, and characterized them for use as a suitable tethering alternative for supported bilayers. Our next goal was to functionalize a suitable solid surface to be used as a support for tethered membrane formation. We have synthesized the alpha-helical peptide tethers with terminal amine functionality in order to be able to crosslink them on a suitable surfaces. Silica was chosen as the starting material for the microparticles as it is hydrophilic and any non-specific hydrophobic interactions with the bare surface can be kept at a minimal level. Our goal is to immobilize these tethers on spherical microparticles and subsequently fabricate supported lipid membranes on them. Desirable properties of the particles include a specific biofunctionality (biotin binding ability in this case), a homogeneous and smooth surface to facilitate the uniform display of tether molecules, and satisfactory control over non-specific interactions of various molecules with the surface. In case that there could be non-uniform distribution of available reactive amine sites on these beads, especially for polystyrene based beads, we should make some modifications to get rid of the occasional cracks on the surface, because these cracks can be potential sites for lipid aggregation or other undesired structures. Another issue was the presence of unfolded peptide anchors and untethered polymer cushion on microbeads due to the intrinsic characteristics of solid surface and incubated molecules. In order to minimize these restrictions, especially the non-specific interactions with hydrophobic molecules or fluorescent probes, we set up to functionalize silica beads with different polymers according to our requirements and passivate them to

minimize non-specific adsorption and the formation of undesired structures.

3.1 Introduction

Silanization has been the most widely used method to modify the surface of microbeads and derivatize silica surfaces, generally, this method involves covalent linking of organic molecules to surface siloxy groups by silylation with methoxy or chlorosilanes. Before functionalization, extensive pretreatment of silica surface to completely dehydrate the surface followed by treatment with excess reactive silanes without a solvent or dissolved in anhydrous benzene or toluene is warranted [123]. The modified silica surface achieved in this manner contains molecules covalently linked to it but scattered distribution on the surface, at the same time, a lot of silanols exposed on the surface [125]. More compact density of these surface modifiers can be achieved by the formation of self-assembled monolayers (SAMs) on silica substrates. Amphipathic molecules, basic building blocks of SAMs spontaneously adsorb onto a solid surface from a solution to form a densely aggregated structure. Silica surface is highly hydrophilic and spontaneously absorbs atmospheric humidity leading to the formation of a thin water layer around micro-particle, the first step in the monolayer formation is the physisorption of the polar head groups on to the surface, then surface bound water layer hydrolyzes them into silanols. In organic phase the silanes is deposited on the surface contains tiny or no traces of water and hence the silanes cannot be completely hydrolyzed in the bulk solvent. If the surface adsorbed silane molecule contains more than one active group (e.g. Si-Cl_2 or Si-Cl_3 or Si-methoxy group). Figure 3-1 shows the sequence of

events discussed above for the case of lateral polymerization through intermolecular Si-O-Si bond formation to give strongly bound monolayers. Under uncontrolled conditions vertical polymerization can also occur, leading to the formation of aggregates on the substrate surface. Also, it is expected that curing the surfaces (heating the sample in air at 100-200ºC) can eliminate surface adsorbed water and cause covalent linking of adsorbed silanes with surface silanol groups [126], but there are contradicting views on this hypothesis. In this Chapter, we discussed some methods of solid substrates modifications. Figure 3-2 schematically presents the idea of designing of silica-suppoted proteoliposomes and PEG tethered polymer-supported lipid bilayers, aiming to space the lipid bilayer from the supporting solid substrate to allow for the reconstitution of integral membrane proteins.

3.2 Methods and Materials

NHS- PEG_{3000}-NHS, Fmoc-NH-PEG-NHS (RAPP Polymere), 6-Aminofluorescene, (Thermo Scientific Corp. MW: 347.3 g/mol) Methanol, Ethonal. (All chemicals with reagent grade, from Fisher Corp.), SATP (*N*-Succinimidyl S-Acetylthiopropionate, Pierce Corp.); EZ-Link NHS-PEO4-Biotinylation Kit; Ellman's Reagent (Pierce Inc., Product No. 22852), 50mM PBS buffer (40 g NaCl, 1 g KCl, 5.75 g Na_2HPO_4,1 g KH_2PO_4,1000 mL dH_2O, pH7.4), 5μm silica bead with free amine group, 20μm silica bead with reactive amine group N,N-dimethyl formamide (DMF, Product No. 20673), Dichloromethane (DCM), 95%(v/v TFA: water= 95:5)

3.2.1 Modification of Silica Microsphere Surface with NHS- PEG_{3000}-NHS

We decided to derivatize the silica bead surface by the formation of self-assembled monolayers as it can give quite compact and uniform distribution of the desired functionality on silica bead surface. In our project, NHS- PEG_{3000}-NHS is used as the building block of the cushions. This anchors to amine terminal functionality on the bead surface, which can be exploited further to attach molecules of our choice to further derivatize the silica surface. The presence of one terminal amine functionality presents a possibility for the use of N-hydroxysuccinimide (NHS) based reagents. NHS based reagents are highly reactive towards nucleophilic amine groups. The reaction links the molecule of interest to the amines and hydrolyzed NHS ester molecule. Another advantage of derivatizing the surface with amine terminated SAMs that the further chemistry can be carried out in aqueous phase. This is crucial for our system as in some cases we aim to functionalize our beads with streptavidin, which can unfold and loose its ability to bind biotin in an organic solvent.

We will use Biotin-PEG-NHS linkers to attach to the top of SAMs later. This was followed by treatment with excess PEG-NHS to block any unreacted sites and also to make the surface completely passive to non-specific adsorption. The biotin-derivatized surface was then coated with fresh fluorphore-labeled streptavidin when it was required.

Procedure for NHS-PEG_{3000}-NHS Modification of Solid Surface

1. Immediately before reaction, dissolve 2 mg of NHS-PEG_{3000}-NHS in 4 ml of PBS buffer (2mg/ml concentration).

2. Add 10mg 5μm silica beads into 3ml of PBS buffer. Sonicate the suspension mildly to

make beads distribute evenly in solution.

2. Vortex the beads included solution. Combine 800 μl of 5μm silica beads with 200 μl of the NHS-PEG_{3000}-NHS solution. Mix contents and incubate reaction at room temperature for 15 minutes. (Default reaction uses 66 nmol primary amine group and 10 nmol NHS-PEG3000-NHS, a 6.6:1 molar ratio of NHS-PEG_{3000}-NHS to free amine).

3. After incubtation, centrifugally separate NHS-PEG_{3000}-NHS -modified silica beads from buffer and wash beads with 1 ml of the PBS buffer. Vortex beads in PBS buffer and mix them well in solution.

4. Repeat step 3 for three times.

5. Store NHS-PEG_{3000}-NHS -modified silica beads in 1ml PBS buffer. Use the cushioned beads for next experiments.

3.2.2 Fmoc Assay for Estimation of available amino groups on microbeads

Materials

Silica beads in PBS buffer (5 μm diameter, ~5×10^{10} beads/g) are obtained from Bangs Laboratories, Inc., Carmel, IN. Succinimidyl 4-hydrazinonicotinate acetone hydrazone, methylene chloride, diisopropyl ethylamine (DIEA), acetic anhydride, acetonitrile, all oligonucleotides are high performance liquid chromatography (HPLC) concentration. All other reagents are obtained from NovaBiochem, Aldrich or Sigma. All solutions are prepared with sterile and nuclease free DI-water.

Procedures for Functionalize silica beads with Fmoc-NH-PEG$_{3000}$-NHS and Amino (or Thiol) Loading Measurement on Beads.

The beads are washed with ethanol prior to derivatization with silane reagents: 5 μm silica beads (2 mg) are washed with 5 mL ethanol (HPLC grade). The beads are then suspended in 5 ml PBS buffer (pH 7.4) and shaken for 1 hr at room temperature followed by washed 5 times with 1 ml ethanol and 3 times with 1 ml PBS buffer, dried, and stored at room temperature. 10 mg silanized beads are suspended in methylene chloride (10 mL) followed by addition of 200 μL (1.2 mmol) of diisopropyl ethylamine (DIEA).

After a brief sonication, 2 mg Fmoc-NH-PEG-NHS is added into the 4mL suspension and the reaction mixture was shaken for 1 h at room temperature. The beads are then washed 5 times with 10 ml methylene chloride and 5 times with 10 mL acetonitrile. Unreacted amino (or thiol) groups were capped with a mixture of 0.2*M* acetic anhydride and 0.2*M* DIEA in methylene chloride (10 mL for 1 g of beads). The suspension was shaken overnight at room temperature. The beads are washed 5 times with 10 mL methylene chloride and 5 times with 10 mL acetonitrile.

For the purposes of ranging from microsphere quality control to accurate determination of thermodynamic and kinetic parameters such as equilibrium constants and kinetic rates, we incubated the 5μm silica beads with Fmoc-NH-PEG-NHS to obtain Fmoc group decoration around silica beads, overall reaction ratio was 2mg Fmoc-NH-PEG-NHS reagent/1mg bead. To estimate available amino groups, the Fmoc protecting group was removed and its absorbance was measured as follows: After capping, the 10ml silica beads were suspended in a solution (4 mL) of 20% piperidine in DMF

(dimethylformamide) and shaken for 30 min in glass vial. The beads were then centrifuged, the supernatant was collected and its absorption at 301 nm was measured. The number of reactive groups per bead (i.e., the bead loading) was calculated from

$$C = A/\varepsilon l$$

(*C=conc. of Fmoc molecules* ε=7800 for Fmoc at 301nm)

Reactive amino groups/bead=Fmoc molecules/number of beads (there are 1.565×10^{10}beads/g) [133]

As discussed in later sections, we switch to cross-linker application to passivate and modify the solid surface. By using appropriate covalent crosslinker, the silica surface could be decapped, passivated and carboxylated as "bold surface". BS^3 crosslinker (Bis[sulfosuccinimidyl] suberate) is a water soluble homobifunctional protein/peptide cross-linker. The BS^3 protein crosslinker possesses amino reactive Sulfo-NHS esters on both ends of the molecule and can be used to prepare antibody-peptide conjugates, which allow us to decorate the surface and anchor our target peptide onto the surface later. For cross-linking and constructing peptides complexes, as well as for covalently orienting antibody to an immobilized peptide on supported solid surface. The flowchart for passivation of solid surface is showed in Figure 3-5.

3.2.3 Aminofluorescene Assay for optimal proteolipobead staining conditions via FACS technique

To determine the optimal proteolipobead staining conditions, 5μm microspheres after NHS-PEG_{3000}-NHS treatment are stained with 6-Aminofluorescein using different

incubation times and dye concentrations to determine optimal staining conditions. Maximal labeling was attained within 1.5 h with 0.5 mM fluorescent dye in DCM, we optimize the proteolipobeads staining condition by getting the curve as a function of incubation time, which shows optical incubation time is ~90 min (Figure 3-7). The flowchart was dispalyeded in Figure 3-9.

Conjugation of 6-aminofluorescein to the beads in solution was measured with a flow cytometer instrument. We used constant laser power of 15 mW, and photomultiplier tube (PMT) gain of 580 for all measurements, intensity was recorded for at least 5,000 beads. Following hybridization in solution, a small amount of beads was added to 1 mL specific buffer (in FACS compatible test tube), and mean channel fluorescence (MCF) of FITC is obtained via analysis of the PLB histogram. We plotted the MCF of FITC fluorescence versus the different staining times of various samples. To further quantify the PLB FITC intensity we used FITC MESF (Molecules of Equivalent Soluble Fluorochrome) calibration beads, which will be discussed in details in Chapter 4. A standard fluorescence curve was established using different concentrations of a known amount of fluorescent concentration. The amount of dye-labeled silica bead was then determined using that standard curve. In the same manner, we optimized the proteolipobeads staining condition by getting the curve as a function of incubation time, which showed the optical incubation time was to stain the bead for ~90 min, with 2mg/ml proteoliposome concentration at room temperature. This result was demonstrated in Figure 3-7

3.2.4 Fluorescent Streptavidin addition to biotinylated bead surface

In Gilchrist and Sharma's work, Streptavidin was attached to Biotin-PEG_{3400} tethered beads by incubating the beads with a solution of streptavidin in phosphate buffer (pH 8.0). In our experiment, a 10 mg beads were dispersed in 200µl fluorescent streptavidin (streptavidin-AlexaFluor 633) stock (0.01 mg/ml) and incubated for 2 hours at room temperature with gentle mixing protected from light. Beads were then washed 3 times with PBS buffer (pH 7.4) to remove excess unbounded peptide and imaged via Confocal Microscopy, which showed uniform stain by SA-AF632. In future work, as a test for specific biotin labeling by streptavidin-AF633, a set of PEG (different chain length) passivated beads will be investigated, also treated with streptavidin-AF633 under similar conditions as comparison.

Comparison of various PEG passivation to functionalized beads for surface modification

One of the important goals of surface modification was to minimize non-specific interactions of the lipids with silica surface. For the purpose we passivated the beads with PEG_{3000}. In order to verify that we had achieved control over non-specific interactions with the surface, silica beads at different stages of surface modification were incubated with lipid formulations (DOPC/POPC/BODIPY). Different surfaces that were tested were: bare silica, Di-NHS-PEG_{3000} coated, and streptavidin-AF632 functionalized. In a typical run, 2 mg of beads were mixed with 20µl of fluorescently doped liposomes solution (lipid concentration 2 mg/ml) and incubated for 1 hour at room temperature. Fluorescent lipid diO was present in the liposome formulations at a ratio of 1:1000 (probe:lipid). Excess

liposomes were washed by PBS buffer and removed by centrifugation. Beads were analyzed by Confocal Microscopy.

Confocal Microscopy

Confocal microscopy was used to image the fluorescently tagged bead surface. As well known, it is a very powerful fluorescence imaging technique as it includes the ability to control over the illuminated spot size and depth of field, ability to reject out of focus fluorescence and ability to image extremely thin sections of a sample at nanometer level, as well as couples of more advanced features not feasible in regular fluorescence microscopes.

Samples were imaged using Leica TCS SP2 AOBS Spectral Confocal Microscope System equipped with Argon ion and HeNe lasers. 1024x512 frames pixel was applied and 63x/1.4 oil immersion objective was used. Texas-Redwere was excited at 594 nm. Rodamine and fluorescein were excited at 488 nm. FITC was excited at 488 nm using argon laser and a detection window of 500 – 600 nm was used. β-Bodipy lipid was excited using 488 nm excitation line of Argon laser and images were taken with the detection window of 502 – 615 nm. AF632- streptavidin was excited using 633 nm excitation and images were taken with the detection window of 650 – 750 nm. Pinhole aperture was set at airy value of 1 (sometimes, set pinhole as 1.5 airy for FRAP), which was equivalent to an ~500 nm vertical slice of the bead.

3.3 Results and Discussion

In order to use hydrophilic silica beads we needed to modify the surface to provide it the suitable functionality and properties for followed proteoliposome coating. We employed the DiNHS-PEG3000 molecule, which could be cushion during the process of lipid bilayers constructing on supported silica surface. What have to point out is the incubation time of DiNHS-PEG3000 with beads, 15~20 min is optimal right before the following lipid bilayers construction. Longer stain time perhaps cause self-aggregation and cracks left on the micro-beads. A potential advantage of using DiNHS-PEG3000 is that the ease and feasibility of incubation, mild reaction environment and high possibility of interaction between amine and NHS to anchor alpha helical peptide tethers at the terminal group further stabilizing the assemblies. As far for spherical silica beads, we had much larger surface area to volume ratio and we needed to optimize the NHS-PEG_{3000}-NHS concentration and incubate time accordingly. Figure 3-4 shows the confocal images of different 5 μmproteolipobead with fluorescent dye in lipid molecules after different surface modification, including PEG passivation, Streptavidin linked and SATP Modification. In comparison with bare silica beads, and parallelly compare the coverage status and signal strength to investigate the modification level and feasibility. Figure 3-3 demonstrate the chain length, cross-sectional area of lipid and peptide tether, which enable us to study the structure and configuration of peptide anchored supported lipid bilayers at microsopic level.

Functionalization of Silica Surface with Fmoc-NH-PEG_{3000}-NHS

In order to determine the surface density of available amine group on the silica beads,

Fmoc-NH-PEG_{3000}-NHS binding assay was performed. 2 mg Fmoc-NH-PEG_{3000}-NHS was added to 1mg 5 μm silica beads, coupled onto the surface and released NHS ester. Fmoc protecting group were deblocked from the surface of bead in 20% piperidinde/DMF. The beads were centrifuged and the supernatant was collected, and its absorption at 301 nm was then measured. The number of reactive groups per bead (i.e., the bead loading) was calculated from the equation: $\boldsymbol{C= A/\varepsilon l}$. By monitoring the absorption at 301 nm and using an extinction coefficient of 7800 for Fmoc at 301nm, the total number of reactive amino groups/bead can be calculated. To get accurate estimation of amino sites on the bead surface, Fmoc group concentration was required above saturation level. This was verified by the experimental observation that the absorption at 301 nm did not drop to zero, indicating that there was still excess free Fmoc group in the supernatant.

Figure 3-6 has the UV-Vis absorption spectra for the Fmoc assay ranging from 189 nm to 589 nm, which shows an obvious independent peak in the Fmoc-group absorption at 301 nm upon incubation with silica beads. For the surface area and volume of a 5μm silica bead, $A=4\pi R^2=70.582\mu m^2$, $V=4/3\pi R^3= 63.892\mu m^3$, there number of micro-beads for 1g 5μm silica bead is 1.565×10^{10}beads/g. Based on the absorption difference of 0.01, read from the standard curve (Fig. 3-8), Fmoc density on surface was calculated to be 0.0129 mg/mg beads, which was calculated to be 2.59×10^{15} molecules/mg beads, this corresponds to 1.655×10^{8} molecules per bead. Assuming that we can tag all the surface amino groups with Fmoc-NH-PEG_{3000}-NHS molecules, this translates into an amine binding capacity of 0.0602 μg/mg beads. This number is comparable to the amine binding capacity of commercially available beads in Sharma's work (0.038 μg/mg beads) [3]. It

could give important information to predict coverage of the bead surface in later work.

As far for the Amino (or Thiol) loading measurement on beads, in terms of the established formula $C = A/\varepsilon l$: (1) for 2mg Fmoc-NH-PEG-NHS/ml buffer, the mean value of A_{301nm} is 0.146 after 10 times diluted, Reactive amino groups/bead= 2.25×10^9/bead. (2) for 4mg Fmoc-NH-PEG-NHS/ml buffer, the mean value of A_{301nm} is 0.375 after 10 times diluted, reactive amino groups/bead= 5.78×10^9/bead. (3) for saturation of Fmoc-NH-PEG-NHS in reaction solution, the maximum value of reactive amino groups/bead= 9.7705×10^9/bead correspondingly. Assuming each polymer has one available free amino group on the surface, the maximum value of #PEG/unit surface of bead=$1.384\times10^8/\mu m^2$

Test of staining time of polymers to functionalized beads at different stages of surface modification

Our goal is to fabricate lipid bilayers on these modified silica surfaces. To test the loss of NHS activation due to hydrolysis over time in aqueous solution, a fixed quantity of silica beads were incubated with identical concentrations 6-aminofluorescein at successive time points. Figure 3-7 shows the relative MCF signal strength in flow cytometry histogram for different incubation time using 6-aminofluorescein fluorescence as probe. Minimal conjugation was achieved after 15 min, maximum conjugation was achieved at 90 min, after 90 minutes the hydrolysis of NHS leads to decreased conjugation.

Conclusions

The main conclusions for this chapter are the following:

1. We have successfully coated the silica bead surface with Di-NHS- PEG_{3000}, Fmoc-NH-PEG_{3000}-NHS, and streptavidin-AF632. Conditions for SAMs self-assembly on silica beads were optimized in terms of (i) concentration, (ii) stain time, (iii) and bead treatment. We have eliminated this spontaneous formation of bilayers on bare silica surface by completely passivating it with a layer of polyethyleneglycol (PEG) of molecular weight 3000.
2. We determine the surface density of available amine group on the silica beads, homogeneity of Fmoc group distribution was verified by specific labeling with fluorescent FITC and confocal imaging. As far for the amino (or thiol) loading measurement on beads, amine binding capacity of bead is 0.0602 µg/mg beads, 1.655×10^{8} molecules NH_2/bead, and was found to be approximately one PEG_{3000} molecule per 42.6 nm^2.
3. Stained 5µm microspheres after Fmoc-NH-PEG3000-NHS treatment with 6-Aminofluorescene for different incubation timeto determine the optimal proteolipobead staining conditions as function of time. Silica surface was successfully tagged with fluorescent streptavidin (SA-AF632). This surface showed uniform staining by fluorescent streptavidin as verified by confocal imaging.

Figures and Tables

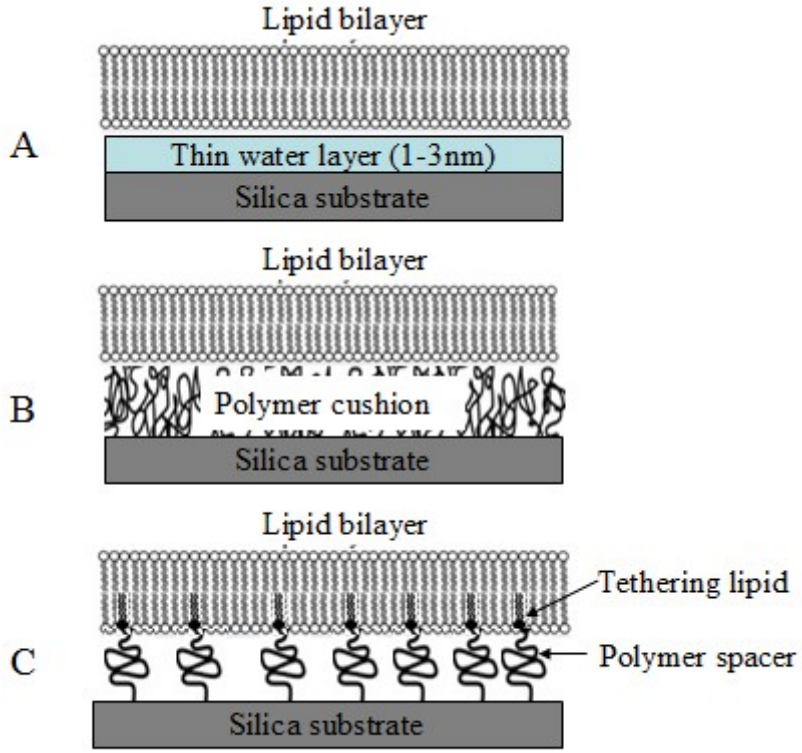

Figure 3-1. Theoretic Schematics of various examples of supported lipid bilayer, A) Free floating on a silica support, the thickness of water layer encapsulated is 1-3 nm (Chapter 1) B) Cushioned by a polymer tether, suppored on silica surface C) Tethered to the support through a polymer [115], Figure 3-1C showed the schematic of our work by using transmembrane peptide anchor instead of lipid tethering into the lipid bilayers.

A:

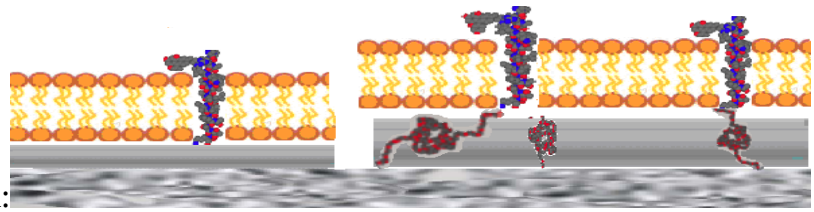

B: NHS-PEG$_{3000}$-NHS

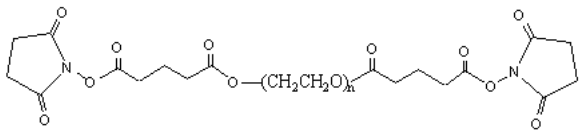

Figure 3-2 Design of a tethered polymer-supported lipid bilayer: (A) Left for silica supported sample; Right for tethered sample Polymer-supported lipid bilayers are designed to space the lipid bilayer from the supporting solid substrate to allow for the reconstitution of integral membrane proteins. The linear polymer is covalently attached at its two ends to the substrate and membrane lipids. Two layers represent the structure of a lipid: DOPC, Red rope represents a spacer (polyethyleneglycol) for tethering lipid bilayers. (*B*) Chemical structure of the linker NHS-PEG$_{3000}$-NHS [115]

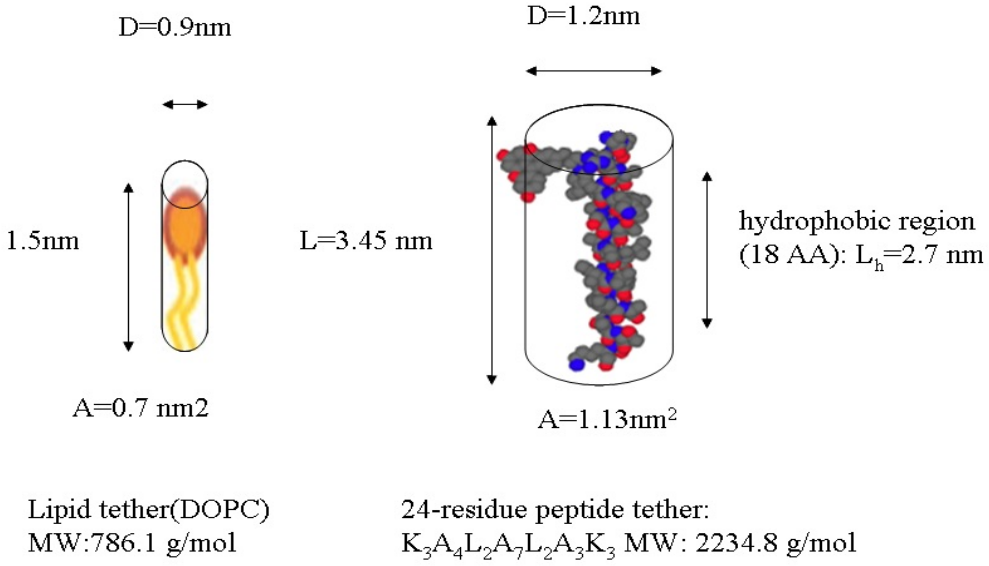

Figure 3-3. Comparison of lipid molecule tether and custom peptide tether. Helical diameter, cross-sectional area, chain length, hydrophobic region of the peptide is shown in an elliptical envelop for comparison. The dimensions are not exact and have been roughly estimated by using Chem3D.

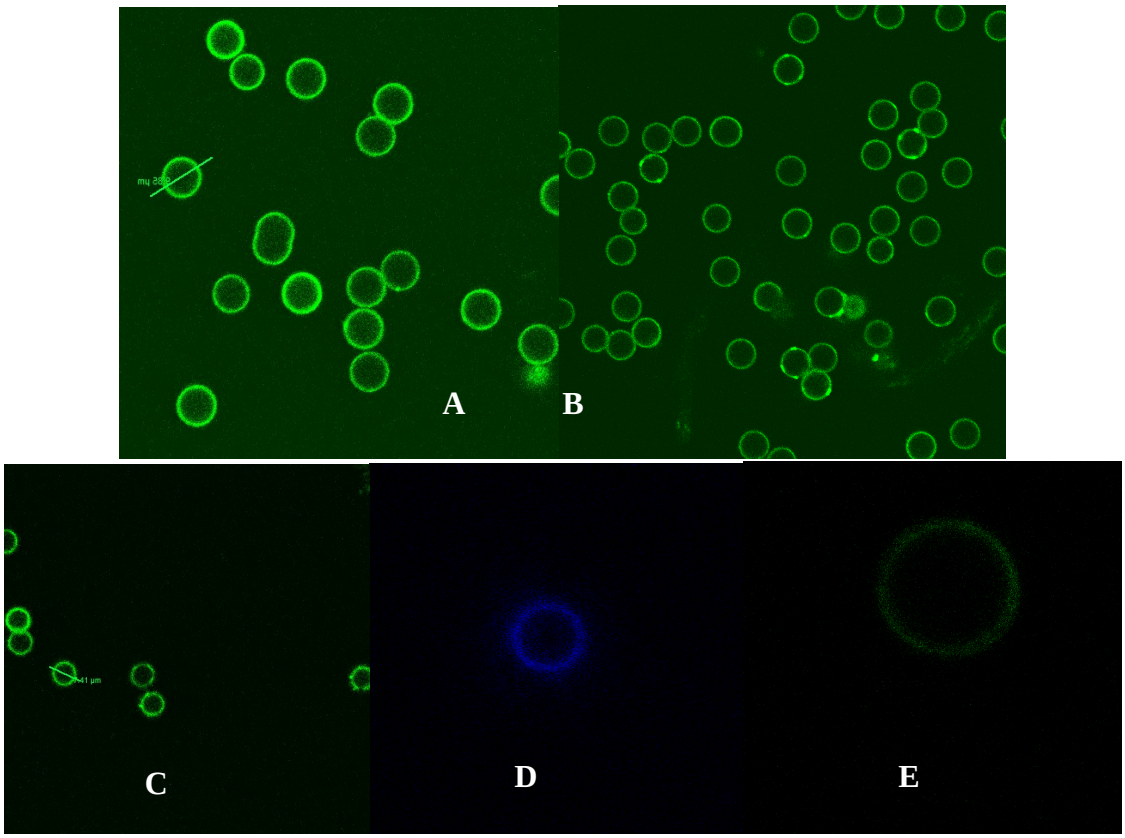

Figure 3-4. Study of non-specific interaction of fluorescent lipid molecules to 5 μm silica bead with different surface modification. Each image shows an overlay of green channel with transmission channel for one particular set. A) Bare silica surface labeled with FITC, B) proteoliposomes coated silica surface (peptide:lipid=1:32 in molar ratio), labeled with FITC, C) NHS-PEG3000-NHS functionalized silica surface coated with proteoliposomes (peptide:lipid=1:32 in molar ratio); D) AF632-Strevadin coated bead E) diO:DOPC=1:1000 incubated bead. Some lipid aggregates identified on the bead surface. 1024×1024 pixel. Excitation line 488 nm. Emission from 508nm to 650nm.

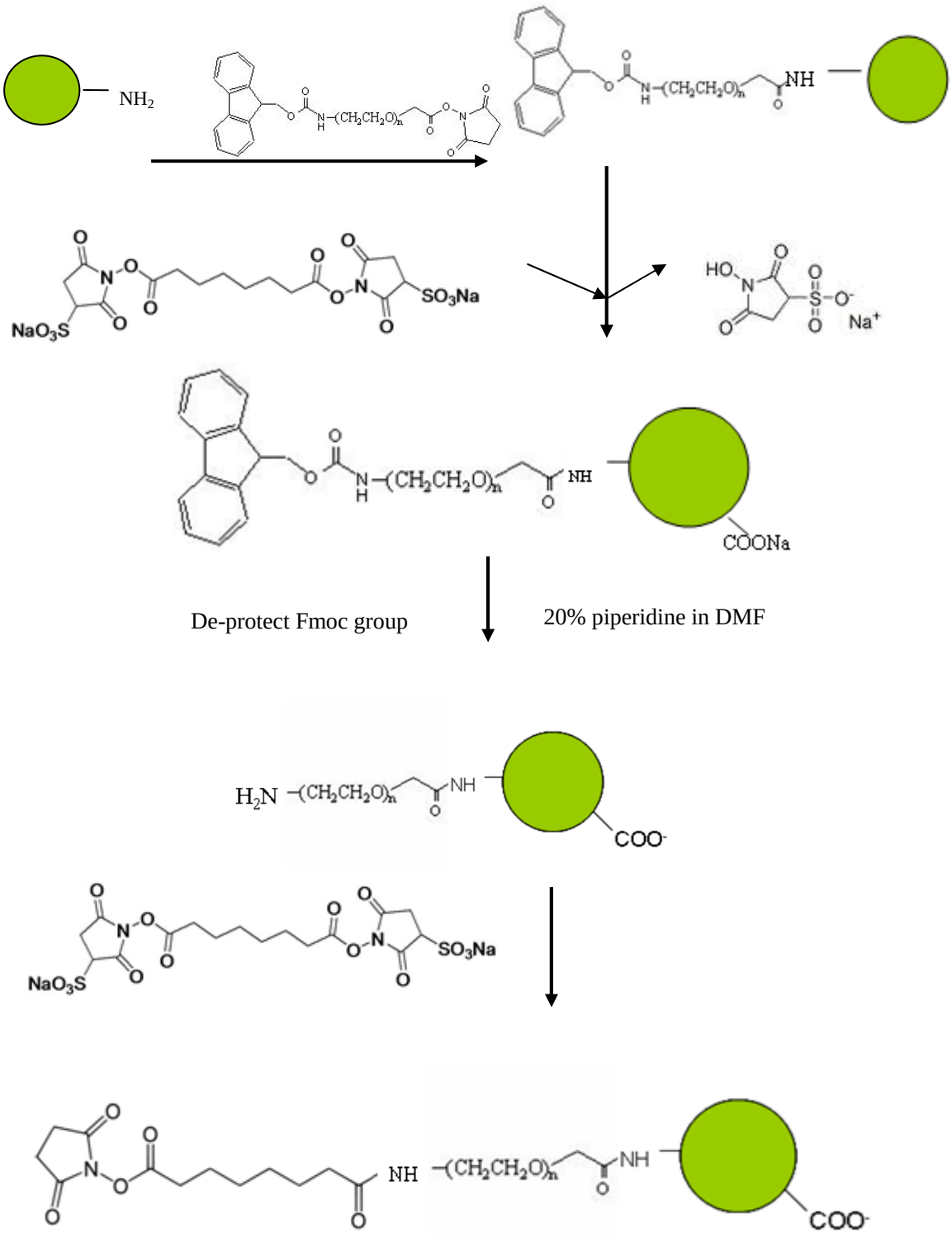

Figure 3-5 Flowchart of Fmoc-NH-PEG-NHS modification, Fmoc de-protect, BS3 cross linker and Construct labeled peptide into Lipid Bilayers onto the surface of beads

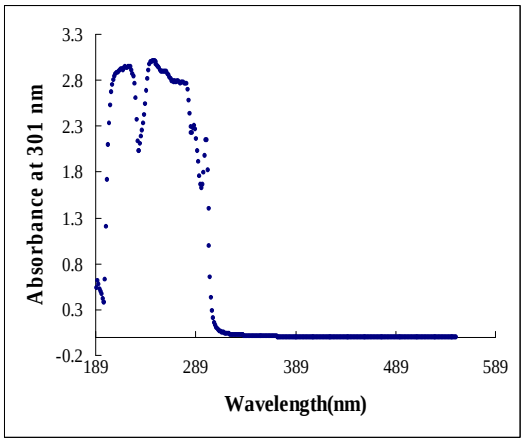

Figure 3-6. Fmoc scanning Spectra from 180nm to 590nm to verify the absorption at 301nm, there was an obvious sharp peak existing at 301nm, gave excellent separation ratio from other bulk peaks, facilitated for estimation of available amino groups on microbeads. Biomates35 Mode spectra photometer, 0.5mg/ml trace concentration for Fmoc group.

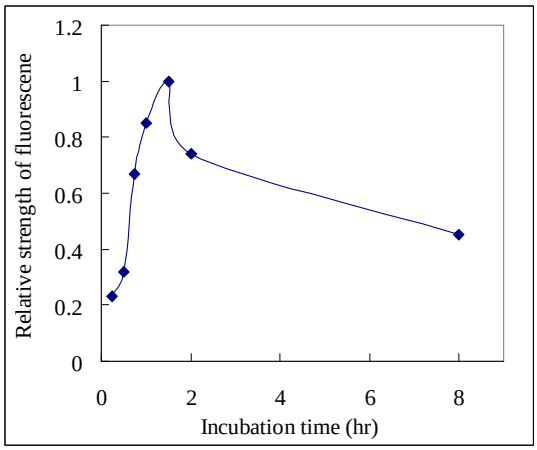

Figure 3-7 The curve of relative fluorescene of 6-Aminofluorescein tagged beads as the function of incubation time using FACS technique, dye concentration is at 0.2mg/ml, incubate at room temperature, ranging from 15min to 8 hr. When incubated bead for 90 min, the strength of fluorescence achive relatively maximum value

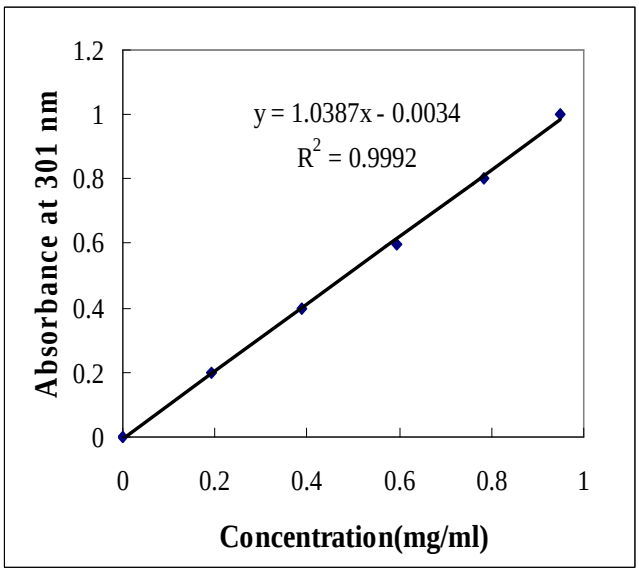

Figure 3-8. Standard Curve of Fmoc absorption at 301nm: y=1.0387x-0.0034, R^2=0.9992, A_{301nm}=0.146, concentration of Reactive amino groups/bead is 2.25×10^9/bead, A_{301nm}=0.375, concentration of Reactive amino groups/bead is 5.78×10^9/bead. The maximum (saturation) value tested of Reactive amino groups/bead is 9.7705×10^9/bead.

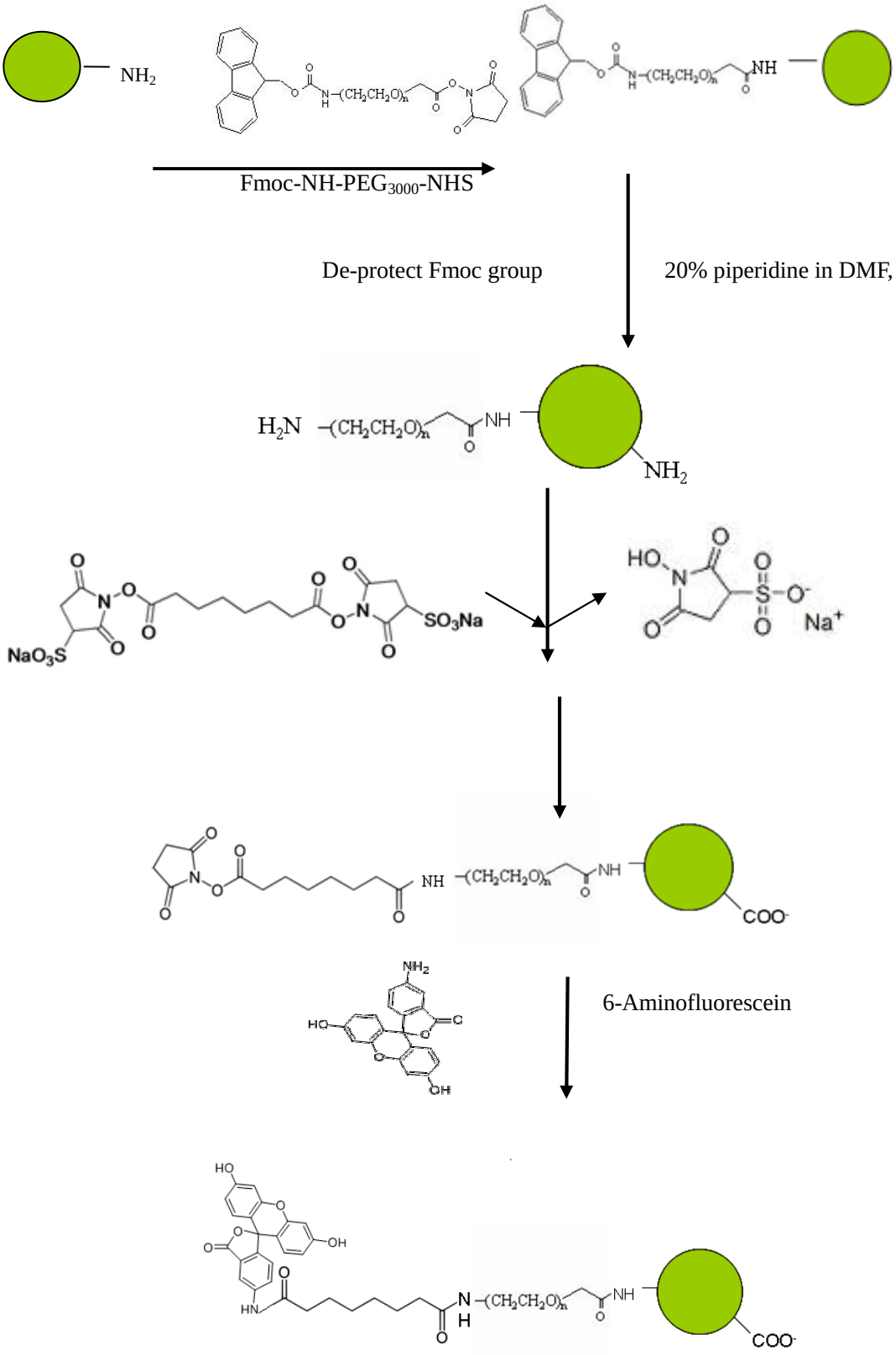

Figure 3-9 Flowchart of Chemistry protocol for Aminofluorescein assay of Fmoc-NH -PEG-NHS modified bead

Chapter 4
Fabrication of Solid-Supported Membranes on Silica Beads using Peptide Conjugates as Integrated Anchors

4.1 Introduction

Provided that the lipid composition is similar to the native environment, the activity of membrane proteins can be rejuvenated after they are reconstituted into lipid bilayers. As is well known, solid-supported lipid layers are considered as model systems for biological membranes. Supported membranes have gained a lot of importance due to their potential applicability in various areas, serving as a model of biological cell membranes and hence are promising candidates for the design of biomimetic interfaces. The fact that *in vivo*, lipid bilayer membranes accommodate a variety of transmembrane proteins, makes supported membranes an ideal candidate to be used for *ex vivo* reconstitution of these biomolecules from native cellular sources.

Supported membranes are generally fabricated by unrolling lipid vesicles onto a suitable surface. The Langmuir-Blodgett deposition technique is also used to transfer a monolayer, or a bilayer, on to a suitable substrate. The supporting surface could be modified or unmodified silica, quartz, glass, and it can either be planar or spherical. Fabrication of supported membranes on spherical particles has various advantages compared with flat geometry, including increases in the surface to volume ratio, ease of purification and processing, hence leading to more versatility in terms of applications. Various groups have shown that lipid membranes spontaneously form on spherical silica beads when these are exposed to lipid vesicles, known as lipobeads. Supported membrane is separated from the supporting hydrophilic surface by a thin water layer (10-30 Å). Lipid bilayer can be simply adsorbed onto the surface or tethered through intermediate molecules ranging from polymers to peptides.

Lipobeads are mechanically stable compared with lipid vesicles and easily adapted to various functions [50]. It is crucial to preserve the lateral fluidity of the lipids within the supported membranes, while constructing thermodynamic and mechanically stable structures. Instead of using larger membrane proteins as ‘anchor’ molecules, alpha helix peptide anchors have some advantages, including manipulating the biomembrane with external perturbations [130], controlling the stability of biomembrane through peptide sequence and size [131], and conjugating peptides with various reporter groups. Moreover, we can study the helical partitioning into the membranes by monitoring the CD spectra when helical peptides are interacting with lipid billayers.

Here we are reporting on the fabrication of supported membranes on silica surfaces using alpha-helical peptides as an anchoring moiety, as well as poly(ethylene glycol) (PEG) as polymer cushions. There are many reasons that make peptide compounds appropriate anchoring moieties for lipobeads. First, we can control the spanning range within biomembrane via control the sequence of peptide. Secondly, when the peptides are fluorophore-labeled we can detect the localization and distribution more easily and quantify the density of anchors in the biomembrane. Thirdly, we can control the volume of accommodation underneath the lipid bilayers by changing the chain length of poly(ethylene glycol) linkers to the substrate. Moreover helical peptides possesses a much larger surface area of interaction with the lipid bilayer making it a much stronger “molecular rivet” for holding the supported membrane on the supporting structure. The presence of the amino acid lysine on the backbone of peptide sequence provides possibility of fluorescence labeling and/or tagging other molecules on the surface of the

molecule external to the lipid bilayer, forming the basis for ligand displays or sensing systems.

Our work differs from previous research in the sense that we have used custom fluorophore-labeled peptides as an anchoring moiety, giving rise to new types of tethered lipobead systems. From our experience with polystyrene beads, we have seen that nonspecific adsorption of the lipids and fluorophores to the surface is a very crucial issue and it makes it impossible to confirm the formation of supported membranes around such particles. The silica particles that we utilized have hydrophilic surfaces and low levels of non-specific binding of free fluorophores and labeled proteins relative to polystyrene surfaces. More importantly, as we have discussed, silica microspheres are ideal substrates for the fusion of liposomes to form supported membranes (as lipobeads). We can eliminate spontaneous formation of bilayers on bare silica surface by completely passivating it with a layer of polyethyleneglycol (PEG) of molecular weight 3000 and allow for templated supported bilayer formation with functionalized PEG (discussed in chapter 4). To this end, NHS-PEG_{3000}-NHS was employed as the polymer spacer to obtain more submembrane space for cytosolic or extracellular domains in our present study, as well as form covalent crosslink “nucleation” sites for the formation of tether supported lipid bilayers. Details about synthesis and characterization of peptide conjugates have been provided in chapter 3.

This chapter describes the fabrication of new tether-supported lipid bilayers on silica particles of 5 μm diameter. We fused peptide-containing liposomes on bare silica beads and also NHS-PEG_{3000}-NHS cushioned silica beads, to form fluid lipid-bilayer assemblies

on these structures. Confocal microscopy was utilized to localize FITC labeled peptides in the assemblies and examine biomembrane surface coverage levels. Fluidity of the untethered peptides in the tether-supported lipid bilayer assemblies was characterized by using fluorescence recovery after photobleaching (FRAP) measurements.

4.1.1 Construction of peptide anchored lipid bilayers on silica beads

Researchers have long been focused on studying membrane-membrane interactions for understanding cellular surface processes. In most cases, liposomes were utilized as model systems for biological cell membranes. Fluid-supported lipid bilayers are first prepared by vesicle fusion to a cleaned glass substrate using vesicles that display short sequences on their surfaces [2]. One of the first reasons for utilizing supported membranes was to be able to have a geometrically well-defined planar surface for characterization studies.

Initially, planer supported membrane system was essentially a Langmuir-Blodgett (LB) monolayer of lipid on alkylated glass, and was not suitable for incorporation of membrane protein due to steric issues and the lack of fluidity of the lipids, which inspired the design of supported lipid bilayer membrane systems. The replacement of lipid bilayers for monolayer means, sequentially transfer two monolayers of phospholipids (such as DPPC, DMPC and DOPC) from the air-water interface to solid substrates. These lipid bilayers constructs not only were useful in studying membrane-membrane interactions but also from the standpoint of investigating the lateral diffusion of lipids as well as other macromolecules associated with the membranes. This was accomplished

using fluorescence recovery after photobleaching (FRAP) to probe lipid dynamics. Supported lipid bilayers have since become increasingly important as a model for cellular membranes. Various other methods have been utilized to construct supported membranes on suitable surfaces. One of the most widely utilized methods involves fusion of lipid vesicles on suitable hydrophilic glass or silica surface to coat it with lipid bilayers. Here we adopt this method, which could be able to reconstitute peptide tether moiety into supported lipid bilayers using vesicles containing membrane proteins (proteoliposomes).

In 2009, Tieleman et al. [134] combined the use of X-ray diffuse scattering and molecular dynamics simulations to determine the orientation of alamethicin in model lipids (DOPC), and inserted helical peptide as transmembrane tethers. The measured thickness of lipid liayers ranges from 6.34 to 7.82 nm according to the concentration and properties of peptide adopted. For our designed 24-residue peptide $K_3A_4L_2A_7L_2A_3K_3$, the length of an alpha helical turn is 0.54 nm and 3.6 nm residues consist one turn. Therefore, we could predict the length of our peptide tether molecules: ~3.4nm, which is at the similar size of those studied in Tieleman's work. Histova's studies suggested that lysines flanking decrease the hydrophobicity of the lipid bilayers (TM domain) during reverse phase HPLC purification, and have small effects on peptide solubility and on peptide secondary structure, but they significantly affect protein–protein interactions in SDS and abolish peptide dimerization.[135] Their work pointed out that caution should be exercised when modifying lipid bilayers domains and peptide design to render them more manageable for biophysical studies as these might severely affect their native properties. However, in the rational design of peptide anchors no such constraints exist

and it is favorable to suppress peptide dimerization with lysines flanking the hydrophobic core region.

There have been serious limitations in the applicability of supported membranes of various architechtures. In particular, lipid bilayers fabricated on hydrophilic surfaces are separated from the substrate by an ultra-thin (10-20 Å) layer of water, which is insufficient to impart the essential fluidity to the lipids to supply native environment for TM protein or other biological molecules. Extraneous parts of the membrane proteins can interact with the supporting surface and get immobilized, losing their mobility and function. Lateral mobility plays an important role in the activity of membrane proteins, and thus, immobilization of these biomolecules within lipid membranes to supporting surface is undesirable. There have been several attempts to address this problem with a general approach to separate the bilayer from the supporting surface by a polymer cushion. [4] Due to defects formed upon formation, bilayers formed on such polymer cushions were not very successful [21][66]. Wagner developed one strategy of forming supported membranes was further modified by using a tethering molecule at the end of polymer spacer [66], a part of the polymer tether is integrated into the lower leaflet of the supported bilayer and other end is covalently linked to the surface (Figure 2-7). The soft polymer cushions offer a lubricating layer between the supported surface and the membrane, encapsulate more molecules in the enveloped volume, as well as enable the ‘self-healing’ of surface defects. So far, primarily single lipid [66] or a cholesterol [136] linked to a hydrophilic polymer or a hydrophilic oligomer molecule have been used as the part of tether integrated into the supported bilayer. Most commonly used polymer spacer is

polyethylene glycol (PEG) polymers or oligomers.

Two decades ago, spherical geometry has been more and more widely used for supported solid substrate. The first reported study concerning the formation of bilayers on spherical silica beads was given by Bayerl et al.[49]. We chose to fabricate supported bilayer on spherical geometry instead of a flat interface, as there are certain advantages to this approach. Firstly, it allows much more surface area to work with compared with the flat geometry. Second, in spherical geometry there is a possibility of achieving the compartmentalization of an aqueous space between the bilayer and the supporting surface. This is a very crucial aspect as it can allow us to encapsulate a number of molecules, varying from simple tracer molecules to the highly complicated signaling proteins in the enveloped volume. Primary motivation behind the work was to recreate the model membrane systems consisting two lipid layers of well-defined shape (preferably spherical in order to understand the role of membrane curvature) and a size range comparable to that of biological cells. In order to address the issues related to the close proximity of the bilayer to the supporting surface, Sackmann [48] and Bayerl [49] modified these structures with a polymeric cushion, which separates the supports the bilayer from the glass surface.

In Sharma's research [84], bacteriorhodopsin tethers were attached on streptavidin-conjugated beads and subsequently lipid-bilayer assemblies were formed on these structures, and a detergent-based bilayer reconstitution method resulted in the desired assemblies. As other closely related research, Sodrosky and coworkers [137] constructed lipid bilayers on paramagnetic particles by detergent dialysis of Biotin-DOPE doped lipid formulations, paramagnetic beads were coated with 1D4 antibody and

streptavidin acted as anchor for the membrane reconstitution around beads through immobilization of biotin-DOPE. In Bunjes' research, they monitored the reaction at solid/solution interface by fusion of vesicles prepared from a fluid lipid mixture with and without reconstituted proteins. It showed an ideal tethered bilayer model and a successful incorporation of ATPase into these membrane matrices [138].

Inspired by previous research, our aim is to use alpha-helical peptide complexes with predominantly hydrophobic side chains to enhance their stability and biological feasibility of lipobeads for the study of membrane proteins and their interactions with cells. In this work, we have made use of a fluorescent peptide derivative optimized for its use in anchoring lipid bilayers. Moreover, the some fraction of the peptides conjugate to NHS-PEG_{3000}-NHS, giving rise to *in vitro* models will be incorporated into lipid bilayer (DOPC) supported by microbeads. Figure 4-1 presents our supposed structure of a peptide-anchored lipid bilayer located on the surface of a silica microsphere.

4.1.2 Alpha helical peptide as a membrane tether and NHS-PEG_{3000}-NHS as polymer cushion

For a 23-residue peptide molecule $K_3A_4L_2A_7L_2A_3K$, the overall length of alpha helix is ~3.45 nm, however, the 18-residue hydrophobic core matches the hydrophobic region of DOPC lipid bilayers, which have been determined experimentally to be ~2.7 nm in length. As mentioned above, the chemical component of lipid membrane itself is the key factor to determine the membrane fluidity DOPC, formally named 1,2-dioleoyl-*sn*-glycero-3-phosphatidylcholine, is a kind of phospholipid with two C18

chain hydrophobic tails and a choline headgroup. Tristram-Nagle and coworkers [134] proved a simulation which was also performed with the area per molecule for DOPC constrained to 72 $Å^2$. Besides that, in their recent work using neutron scattering data, an area of 67.4 $Å^2$ was obtained [141]. The effective hydrophobic thicknesses have been suggested to be 26.8 Å-28 Å for DOPC and the decay lengths equaled to 6.0 Å for Alm/DOPC [134]. Uhrikova and coworkers' applied Luzatti's method to determine the bilayer thickness and the bilayer surface area per DOPC at the bilayer-water interface. Both the d(L) and A(L) increase with the CnOH chain length n at CnOH : DOPC = 0.3 molar ratio: d(L) = (3.888 ± 0.066) + (0.016 ± 0.005)·n (in nm), A(L) = (0.6711 ± 0.0107) + (0.0012 ± 0.0008)·n (in nm^2) [142].

Concerning the length of spacers from the substrate to biomembrane, the extramembrane region of a large membrane protein such as ATPase is on the order of ~5nm. Accordingly, if we employ NHS-PEG_{3000}-NHS as polymer cushion we could get substrate to biomembrane spacings of ~4.7 nm when the polymer is in the "mushroom regime", expected to be the dominant structure when the polymer is grafted to the surface in aqueous solution ((Flory radius: $R_F = aN^{3/5}$;N= 68 and a = 0.35 nm for -CH_2CH_2O-: "mushroom regime"). Whan fully extended the NHS-PEG_{3000}-NHS could extend out to ~24 nm from the surface.

As mentioned earlier, the use of membrane-spanning molecule to tether the bilayers has been limited to a lipid or cholesterol molecules. Our approach is to utilize alpha helical peptide, a transmembrane peptide, as a tethering molecule, NHS-PEG_{3000}-NHS as polymer cushion. This polymeric network is covalently linked to lipid bilayers (DOPC)

supported on modified silica surface, by crosslinking to lysines or the N-terminus of the labeled peptide. By using peptides as tethered molecules, we could control the spanning range within the biomembrane, detect the localization and distribution more easily than using sizable protein, and investigate the fluidity and mobility via conjugating with various reporter groups. Our strategy is to recreate this peptide-tethered polymeric network to support the lipid bilayers formed on spherical particles (Figure 4-1).

4.2 Materials and Methods

1,2-dioleoyl-*sn*-glycero-3-phosphocholine(DOPC), which purchased from Avanti Corp., fluoresceine isothiocyanate (FITC), (Thermo Scientific Corp. MW: 389.38g/mol.) DiNHS-PEG3000 (RAPP Polymere), 6-Aminofluorescein, (Thermo Scientific Corp. MW: 347.3 g/mol), SATP (*N*-Succinimidyl S-Acetylthiopropionate, Pierce Corp.), Quantum^{TM} FITC-5 MESF Premix (Bangs Lab.), Starting designed peptide with symmetrical sequence: $K_3A_4L_2A_7L_2A_3K_3$ [2]; EZ-Link NHS-PEO_4-Biotinylation Kit; Ellman's Reagent (Pierce Inc., Product No. 22852), 50mM PBS buffer (40 g NaCl, 1 g KCl, 5.75 g Na_2HPO_4,1 g KH_2PO_4,1000 mL dH_2O, pH7.4), 5μm silica bead with free amine group, 20μm silica bead with reactive amine group. N,N-dimethyl formamide (DMF, Product No. 20673), Dichloromethane (DCM), 95%(v/v trifluoroacetic acid (TFA): water= 95:5) NHS-PEO_4-Biotin, Methyl tert-butyl ether (MtBE), Methanol, Ethonal, Chloroform. (All chemicals with reagent grade, from Fisher Corp.)

4.2.1 Liposome Reconstitution

The peptide liposomes are constucted by hydration of a dried peptide/lipid film, first forming MLVs and then liposomes via sonification. We then fuse the peptide proteoliposomes onto 5μm silica beads. First we dissolve peptide/DOPC lipid film in PBS buffer, vortex the mixture, and sonicate the dispersion in ice-cold bath, the lipid is strongly agitated with probe sonication and peptide capsulated, obtain the peptide proteoliposomes in clear solution. As far for spacer-tethered sample, we functionalize the beads after mild sonication to ensure good dispersion with NHS-PEG_{3000}-NHS for 15min at room temperature. However, longer reaction time is not recommended because the hydrolysis of surface-PEG_{3000}-NHS will not enable functionalization. To make lipobeads ncubate the functionalized beads and non-functionalized beads (as control beads) with liposomes for more than 1hr at room temperature. Then the lipobeads that mimic lipid bilayers supported by micro-beads, untethered and tethered with polymer cushions were obtained. The flowchart of proteolipobead formation for our experiment is shown in Figure 4-2.

Protocol for Proteoliposome Fusion on Silica Substrates

Lipid constituents were first dissolved in chloroform at 10 mg/ml total lipid concentration. DOPC was the main constituent and was present in all the lipid formulations used. The lipid solution was then subdivided into parts containing 2mg of total lipid stock and transferred into 4ml glass vials. Chloroform solvent was evaporated using vacuum overnight and then the lipid films we stored under Argon. Different lipid film involved peptide was made (molar ratio of peptide to lipid range from 1:32, 1: 48 to

1:64). Vials containing lipid films were stored under argon at -20°C until required. To form multilamellar vesicles (MLVs), 2-mg lipid formulation was hydrated using PBS buffer (pH 7.4) at 2 mg/ml and the suspension was subjected to 5 cycles with vortexing and rinsing by buffer. Centrifugated the bead, Removed the supernatant, and resuspended the pellet. In this stage, multi-Lamellar vesicles (MLV) were obtained. Small unilamellar vesicles (SUVs) were formed by extruding MLVs through polycarbonate membranes (Avanti Mini-Extruder) or by sonicating the MLV suspension to optical clarity using a probe sonicator (Biologics Inc. Ultrasonic Homogenizer, 150W model, microtip, 40% Power, 15 min). Size of the vesicles was verified using Malvern Zetasizer Nano ZS. For sonication, placed the MLVs in an ice-cold water bath, sonicated the dispersion. During the sonication process, the lipid was strongly agitated by ultrasonication. Finally, we get the proteoliposomes in clear solution, which are termed small unilamellar vesicles (SUVs).

For parallel experiments, we functionalized the microbeads with Di-NHS-PEG_{3000} for 15min at room temperature in advance, then we incubate the functionalized microbeads and non-functionalized beads with proteoliposomes for more than 1hr at room temperature with gentle shaking every 20 min. Rinse and get rid of excess proteoliposomes not fusioned onto the beads, we get the mimic lipid bilayers supported by microbeads, with and without polymer cushions.

4.2.2 NHS-PEG_{3000}-NHS as Polymer Cushion in Fabrication of Supported Membranes

In Castellana and coworkers' work, the supported membranes is achieved by fusing vesicles containing polyethylene oxide oligomers conjugated to phosphatidylethanolamine (PEG-PE) lipids to glass substrates [50]. The PEG-PE lipids within the bilayer serve two functions. They increase the bending elastic modulus of the membrane and increase the headgroup hydration layer thickness [99]. Other means of tethering membranes involve the use of ligand-receptor interactions [129] and the direct anchoring of transmembrane proteins to the substrate followed by lipid film fusion. The binding of biotin-presenting vesicles to streptavidin monolayers followed by PEG-facilitated vesicle fusion has been suggested to provide a supported bilayer with a polymer cushion [129]. There are multiple papers in the literature to support the idea of using PEG as cushion, separating the lipid bilayers away from supported surface.

Formation of non-tethered lipid bilayer on silica beads

As a reference set, supported bilayer was formed on silica particles without any tethering molecules. This was achieved by incubating 5μm silica microspheres (2mg beads) with 200μl of sonicated proteoliposomes solution (2mg/ml lipid) in PBS buffer for 75~90 min. Proteoliposomes spontaneously coated the clean silica surface to form a lipid bilayer at room temperature. Excess unbounded proteoliposomes were separated by 6000rpf centrifugation and successive washing with fresh 10mM PBS buffer (pH 7.4). These samples were stored at 4°C until required.

Formation of supported membrane using NHS-PEG_{3000}-NHS tethers

As mentioned above, lipid bilayer around silica particles were formed by fusion of intact lipid vesicles which coated silica surface with lipid bilayer inserted by a thin water layer around 10–20 Å [50]. In the previous stage we fabricated lipid bilayers around silica beads using the approach mentioned. Lipid vesicles (SUVs) were obtained by either sonication or extrusion through polycarbonate membranes as explained before. 200µl vesicle solution (2mg/ml lipid in 50mM PBS buffer pH7.4, molar ratio of peptide to DOPC is 1:32, 1:48 and 1:64 separately) was used to incubate a 1 mg of PEG treatmented beads. The mixture was incubated at room temperature for 2 hours with gentle mixing in between to ensure even dispersion of the beads. Excess liposomes were separated by centrifugation (6000rpf; 1min; 3 times) and beads were washed with fresh PBS buffer in 3-5 spin-rinse cycles.

NHS-PEG_{3000}-NHS treatment was performed on the beads as follows: A small quantity of beads (~4mg, in suspension) was made up in 50mM PBS buffer solution at 50% (w/v) concentration after being mildly bath sonicated to get proper dispersion in the presence of solution, NHS-PEG_{3000}-NHS was dissolved in 50mM PBS buffer at 2mg/ml (w/v) concentration. Beads coated with NHS-PEG_{3000}-NHS in PBS buffer for 15min at room temperature. Excess PEG reagent was separated by centrifugation (6000rpf; 1min; 3 times) and beads were washed with fresh PBS buffer in 3-5 spin-rinse cycles. Beads were recovered by centrifugation and successive rinsing with PBS buffer. At 20 minutes after NHS-PEG_{3000}-NHS coupling, the peptide proteoliposomes were added to be crosslinked to the PEG_{3000}-NHS via coupling to peptide amino groups. This yields microsphere-PEG_{3000}-$K_3A_4L_2A_7L_2A_3K_2$-FITC conjugates that anchor the biomembrane in

tethered proteolipobeads.

In order to test if the proteoliposomes were immobilized to the beads in intact manner we conjugated FITC dye in the liposomes in the stage of peptide synthesis (at molar ratio of peptide to lipid 1:32, 1:48 and 1:64). Proteoliposomes loaded with fluorescein-conjugated peptides were used for incubation with NHS-PEG_{3000}-NHS functionalized beads or plain silica beads using the protocol mentioned above.

4.2.3 Characterization of Silica Supported Bilayers and Tethered Lipid Bilayers

Using liposome formulations, peptide proteolipobeads were constructed via liposome fusion onto 5 micron amino-terminated silica microspheres. Two types of proteolipobead systems were examined, (1) untethered peptide lipobeads with a thin water layer separating the biomembranes from the substrate and (2) tethered biomembranes connected to the substrate via homobifunctional crosslinking from surface amines to peptide lysines via NHS-PEG_{3000}-NHS.

4.2.4 Analysis of membrane fluidity using FRAP

Confocal microscopy is a powerful tool to study the lateral fluidity and spatial distribution of the fluorescently tagged peptide within supported membranes. Furthermore the confocal fluorescence recovery after photobleaching (FRAP) technique is used to characterize the mobility of peptide spanning within a supported membrane. In this work, we use confocal microscopy as a tool to study the lateral fluidity and spatial distribution

of the fluorescently-tagged peptide within supported membranes. The fluorescence recovery after photobleaching (FRAP) technique is used to characterize the mobility of peptide spanning within a supported membrane. Here the left graph in Figure 4-4 presents data collected during a FRAP experiment. A baseline of fluorescence is collected (1) the photobleaching occurs so that the amount of fluorescence is reduced dramatically (2) Over time, the amount of fluorescence in the photobleached area increases as unbleached molecules diffuse into this area (3). Later, there is a stabilization of the amount of fluorescence recovery (4) and a flat line is obtained. The lateral mobility is determined by the slope of the curve. The steeper the curve is, the faster the recovery, and the more mobile the molecules.

Membrane Fluidity for DOPC

Membrane fluidity appears essential for the dynamics and functions of membrane proteins, either enzymes, transport proteins, trans-membrane peptide spannings or receptors. Membrane fluidity plays an important role in cellular functions and membrane proteins interactions; generally, due to the effect of protein crowding in the membrane and to constraints from the aqueous matrix, lateral diffusion of membrane proteins is slower than theoretical assumptions. It is well known that the bilayer core is much more fluid than the surfaces. The "viscosity" calculated for the surface could be 1-2 P, but in the midplane it could be 10 times lower, that means, the lateral diffusion coefficient in the bilayer core is 10 times higher than the surfaces [139].

Analysis of membrane fluidity using FRAP

Quantified lateral fluidity of supported membrane by studying the fluorescently tagged peptide using fluorescence recovery after photobleaching (FRAP) techniques. It was accomplished by bleaching a small region (e.g. 1µmx1µm) on one side of the bead (See Figure 4-3) and monitoring the fluorescence recovery back into the bleached region. A typical recovery curve for the bleached region has been shown in Figure 4-3 along with a schematic with analysis parameters relevant to the discussion below. In order to estimate the diffusion coefficient of the fluorescent lipid encapsulated with FITC-peptide, to describe the amount of fluorescence as a function of time in mathmatics, Klonis et al [103] have reported this in a simple mathematical formulation for fluorescence recovery with time as:

$$F(t) = \alpha F_p \sum_{n=0}^{\infty} [(\frac{(-K)^n}{n!}) \frac{1}{(1 + n(1 + \frac{2t}{\tau_D}))}] + (1 - \alpha) F_o$$

In general cases, diffusion coefficient can be determined by this formula.

Where:

F(t) = Fluorescence intensity of the bleached spot at time t after bleaching

F_p = Prebleach intensity

F_o = Intensity immediately after bleaching

$\alpha = \frac{F_\infty - F_o}{F_p - F_o}$ Fraction of the mobile species or recovery fraction

K = Parameter related to the degree of bleaching

$$\frac{F_o}{F_p} = \frac{(1-e^{-K})}{K}$$

The τ_D parameter is related to Diffusion coefficient as –

$D = \omega^2 / 4\tau_D$

Where ω is $1/e^2$ of the Gaussian radius of the bleached spot.

Parameters K and α were calculated from the above relationships. These values were used in the above formulation to get a best fit for the experimental data by using different values of τ_D by a trial-and-error method. The best-fit value of τ_D was then used to estimate D as represented above. As our bleached spot was 1 µm wide by 1 µm thick, we used a value of 1 µm as an approximation of ω. In general cases, diffusion coefficient can be also by determined by this formula. $D= \beta\omega^2/4\tau_{1/2}$, where $\tau_{1/2}$ stands for the half time of recovery. Figure 4-4 showed the snapshots of the opposite ends of the lipobead studied for fluorescence recovery after photobleaching (FRAP) in different stage, including pre-bleach event, bleach and post bleach. The regions of interests (ROIs) shown in 4-4 were ratioed to remove the photobleaching transient from the FRAP data.

Confocal Microscopy

Confocal microscopy was used to image the formation of fluorescently-tagged supramolecular structures on the silica bead surface. Samples were imaged using Leica TCS SP2 Confocal Microscope System equipped with argon ion and HeNe lasers. FITC was excited using 488-nm line of argon laser and images were taken with a 63x oil immersion objective with the detection window set between 500-550 nm. Pinhole aperture was set at Airy value of 1.5

Photobleaching studies were done using built-in protocol of the Leica SP2 system. Image plane was set at the equator of the bead and a 512x32 pixel format was used (zoom value 16; scan speed 400Hz, 488-nm, normal AOTF 2%, Bi-Directional scan), which enabled the fast imaging (0.2 sec/frame) of two equatorially opposite ends of the bead. After 5 pre-scans a region of 1µmx1µm on the bead was subjected to 20 fold laser intensity (AOTF 40%) for the duration of one scan. This resulted in bleaching of the selected region on the sample. Recovery of fluorescence was monitored for 60-sec at normal laser intensity (AOTF 2%). Data was collected for the normalized fluorescence intensity of the bleached region throughout the sampling time and analyzed using *Mathematica* to estimate the value of time constant τ_D, thus yielding the diffusion coefficient, D.

4.3 Results and Discussion

The fluorescence intensity distribution around the peptide proteolipobeads was studied using confocal microscopy. Figure 4-6 illustrates representative 3D reconstructions from CLSM of peptide proteolipobead supported lipid bilayers consisting of DOPC and the $K_3A_4L_2A_7L_2A_3K_2$-FITC species (peptide:lipid=1:10 in mass ratio; peptide:lipid=1:32 in molar ratio). Highly uniform supported lipid bilayers were formed in the supported bilayers at the peptide to lipid ratio shown. An in-depth analysis of surface coverage and was conducted based on analysis of the equatorial z-sections of N=20 randomly selected microspheres of each type, examining the lipobead structures obtained using peptide to lipid molar ratios of 1:32, 1:48 and 1:64. This data is

summarized in panel E of figure 4-6. The untethered lipobeads were indicated in by the diagonal pattern bars and the PEG tethered lipobeads were given by the dotted pattern bars. In both the tethered and untethered case the lipid coverage was greater than or equal to 88%.

The coverage was slightly lower in the polymer-cushioned tethering case. If the time delay after NHS-PEG_{3000}-NHS functionalization of the amine terminated microspheres was extended until the terminal NHS groups were deactivated by hydrolysis (~3 hours), liposome fusion was minimal and sparse (data not shown). This is consistent with our earlier work with microspheres of this type that were functionalized with PEG_{3400}–biotin chains, in this case near complete passivation to liposome fusion was evidenced and negligible amounts of supported lipid bilayers were formed. To quantify the NHS hydrolytic degradation, the time dependent conjugation of 5-aminofluorescein was examined, confirming the timescale of NHS hydrolysis (see the previous chapter). Taken together, this data is consistent with the formation of homobifunctional crosslinks to give microsphere-PEG_{3000}-$K_3A_4L_2A_7L_2A_3K_2$-FITC tethering, where the peptide serves as an anchoring construct in polymer cushioned supported biomembranes. The polymer cushion spacing between the silica surface and tethered biomembrane is ~4.4 nm, as calculated from the Flory radius of PEG_{3000} ($R_F = aN^{3/5}$;N= 68 and a = 0.35 nm for -CH_2CH_2O-: “mushroom regime”).

Figure 4-4 presented the data of FRAP experiment in FRAP ROI (ROI-1) and reference ROI (ROI-2) channels of the imaging plane in the confocal microscope. We selected a rectangular area for photobleaching, as comparison, and selected unbleached

area of the same size to investigate the intrinsic photobleaching during image aquisition. Two curves of fluorescence versus time in ROI-1 and ROI-2 channel were obtained, represented bleached and unbleached region respectively. After dividing ROI-1 by ROI-2, a single FRAP curve for further analysis was generated, $\tau_{1/2}$ stands for the half time of recovery. The two FRAP curves shown in 4-3 and 4-4 present two kinds of typical (raw) FRAP data for this study; untethered and tethered PLB samples. The half time of recovery is 20.65 sec for untethered sample and 16.0 sec for the tethered sample. Correspondingly, the calculated values of diffusion coefficient were 0.01219 and 0.01574 μm^2/sec respectively. The results at first glance tell us that peptide within tether-supported lipid bilayers have a faster recovery than that within untethered lipobeads, where the lubricating “polymer cusion” layer offers a better mobility for the embedded peptides. (See Figure 4-1).

Results for the calculations of fluidity measurements for larger sample sizes are presented in Figure 4-7 for the PEG_{3000}-tethered peptide PLBs (red dotted bar pattern) and untethered silica-supported PLBs as a reference (blue diagonal bar pattern). The sample size was over 40, and the mass ratio of peptide to lipid was 1:10, 1:15 and 1:30 (molar ratio was 1:32, 1:48 and 1:64) respectively. Also, the fraction of the beads showing successful FRAP was found to be ~0.40 based on a total of ~200 beads that were analyzed. A small percentage of beads (~5%) exhibited the desired fluidity on one location and no or minimal fluidity on another location. This indicated that there could be local regions of fluidic membrane coexisting with other lipid aggregate structures on the

surface of a single bead. The mean diffusion coefficients are 0.0134±0.0004 for the untethered sample versus 0.0158±0.0004 $\mu m^2/s$ for the tethered, polymer-cushioned sample, a greater than 18% increase due to the effect of polymer cushioning (1:10 peptide to lipid mass ratio). At the levels of peptide loading we examined, the diffusivity was significantly higher in the polymer-cushioned case, with p-values of $p<0.001$ in each case. This is not unexpected, as there are a wide range of precedents for the positive influence of polymer cushioning on membrane protein mobility and function in supported membranes. Other studies have examined the diffusivity of smaller membrane-embedded peptides in lipid bilayers, for comparison, we have list a few pertinent examples in Table 4-1. We note that in each case the lipid composition differs, as well as the peptide to lipid ratio. Lipid diffusivities, in general, are an at least an order of magnitude larger (5 - 0.1 $\mu m^2/s$) than those of peptides and up to two orders of magnitude of higher than proteins, by virtue of the fact that their diffusion is confined to one leaflet of the bilayer with lower membrane embedded volumes. The toxin Gramicidin D shares this single leaflet characteristic, a cyclic decapeptide of well-characterized structure, shown to possess a diffusivity that is 4 times larger than $K_3A_4L_2A_7L_2A_3K_2$-FITC, yet of the same order of magnitude. Possibly the most relevant case is that of $AKKL_{18}GKK$-FITC, a 24-mer with highly similar structure studied by Gambin et al. in giant unilamellar vesicles (GUVs) at 1:1000 peptide to lipid molar ratios in SOPC. The diffusivity was greater than 18-fold larger than that of our peptide in polymer-cushioned supported bilayers with DOPC, however the level of peptide loading was at least two orders of magnitude higher in our studies, significantly increasing the levels of peptide-peptide interactions, furthermore,

the use of the GUV system presumably precluded peptide-substrate interactions that would slow diffusion. Another relevant study was performed by Merzlyakov et al., involving a rhodamine-labeled 33-mer based on the transmembrane domain of the FGF-receptor, conducted in planar supported bilayers at 1:2000 peptide to lipid ratio. Under these conditions the 33-mer exhibited a three-fold smaller diffusivity than for our 23-mer under study. This is not altogether unexpected if we compare the two structures. Our peptide approaches perhaps what could be considered a “canonical” alpha helix domain, anchored in the hydrophobic region of the DOPC by lysines at the C- and N-termini [115]. In this case the $A_4L_2A_7L_2A_3$ core forms a 2.7 nm long hydrophobic helical domain that is well-matched to the hydrophobic core of DOPC, a lipid bilayer structure experimentally determined to have a hydrophobic core thickness of ~2.72 nm when hydrated. [134] In contrast, the 33-mer has a significantly longer rhodamine-labeled 9-residue region protruding out from the postulated hydrophobic domain, also assumed helical in structural models supported by CD data, which would conceivably add hydrodynamic drag to the C-terminus.

.

Discussion about Lateral Fluidity

In general cases, diffusion coefficient can be determined by this formula. $D= \beta\omega^2/4\tau_{1/2}$, where $\tau_{1/2}$ stands for the half time of recovery. The mean diffusion coefficient is 0.0127~0.01438 (untethered sample) and 0.0140~0.0169$\mu m^2/s$ (tethered sample). In the FRAP studies, no evidence was seen for larger multimeric peptide complexes with longer recovery times. To probe for the presence of substantial peptide-peptide interactions

influencing peptide mobility, we examined the diffusivity of $K_3A_4L_2A_7L_2A_3K_2$-FITC peptides within untethered and tether-supported lipid bilayers at two-fold lower peptide to lipid mass ratios (1:20). Although these FRAP measurements were carried out near the limits of obtaining adequate signal to noise ratios in the pPLBs (1:20 mass ratio ≈ 1:60 peptide to lipid mole ratio), significantly greater diffusivity was evidenced when polymer cushioning (tethering) was employed at these conditions. The increased diffusivity was likely due to changes in the viscosity of the lipid bilayers by decreasing the concentration for peptide and also by presumably by less peptides anchoring the supported lipid bilayers and thus less obstacles in the diffusion path. For the untethered case the diffusivity increase was much less pronounced. By comparison, as the lipobead concentration of peptide decreased by half (molar mass ratio of peptide to lipid ranged from 1:30 to 1:60), the diffusivity of lipid bilayers increased by ~16.4%; over the same interval the diffusivity of lipid bilayers increased ~7.5% for the untethered case. The data is not altogether inconsistent with the formation of discrete dimeric or multimeric peptide complexes under the conditions studied, although the repulsion of the flanking lysine residues is designed to suppress this effect. Further studies are warranted to address this issue more carefully.

The influence of the PEG_{3000} bilayer-to-substrate tethering layer versus a thin water layer was also evidenced in the statistically significant ~14% increase of mobile fraction, α, in the polymer cushioned case relative to the untethered lipobeads, shown in Figure 4-7. Within the lipid bilayers, for the (rarely seen) perfect case, the recovery fraction is unity (α=1), meaning that the microscale region sampled in the FRAP experiment is

100% mobile; in contrast, α=0 means that no fluorescence recovery (no mobility) occurs. For practical cases, the value of the recovery fraction is between 1 and 0. There are a few factors that are expected to affect peptide lateral mobility that directly influence the mobile fraction: 1) strong interactions with the substrate surface that lead to peptide immobility or "pinning", 2) covalent tethering of labeled peptides in the polymer-cushioned case and 3) immobile regions in the bilayer due to peptide aggregation and 4) incomplete bilayer formation leading to discontinuous (yet fluid) supported bilayer regions isolated from lateral diffusion on the larger length scale of the measurement (also consistent with immobilized, unfused peptide proteoliposomes). In the polymer-cushioned case, there is a likely a trade-off between steric inhibition of peptide pinning by the cushion (increasing α) and covalent anchoring (decreasing α). In the upper-bound scenario where the micropheres are smooth and completely covered with activated PEG_{3000}-NHS (R_F = =4.4 nm; $A_{PEG3000}$ = 60.8 nm^2), and after homobifunctional crosslinking, 100% of the PEG_{3000}-tethers are connected to peptides with embedded area of ~1.2 nm^2, less than 2% of the total supported biomembrane area is anchored. From this analysis we conclude that the level of covalent anchoring, while effective for constructing tether supported biomembranes, is too low to significantly affect the mobile fraction and the increase in α due to tethering in the PLBs is from favorable steric inhibition of peptide pinning by the polymer cushion.

Differences between Peptide and Protein anchors

The cross-sectional area per protein molecule for a membrane protein such as

Bacteriorhodopsin is 8.75nm^2 [144]. However, for our peptide, the diameter of alpha-helix is ~1.2nm, with the cross-sectional area per peptide anchor of only ~1.13nm^2, comparable to lipids (such as POPC, DOPC, SOPC) with cross-sectional area per lipid molecule of ~0.7 nm^2. However, unlike lipids, our peptides span both leaflets of the lipid bilayer and are easily customizable with functional groups (fluorphores or ligands) relative to transmembrane proteins and lipid anchors. [134]

The Effect of Polymer Length on the Two-Dimensional Lateral Mobility

From Cremer's work, we could see that: The longer of polymer length (PEG_{550}, PEG_{2000}, and PEG_{5000}), the more mobile fraction and mobility on the two-dimensional lateral mobility of fluorescently labeled Annexin V, which matched our finding: that polymer spacer arm provide more sizable accommodation for peptides and gave rise to greater mobility within lipid bilayers [143].

In this section, we completed the fabrication of solid-supported membranes on silica beads using peptide conjugates as integrated anchors, established several supported membrane systems and characterized them, especially investigated the key property: lateral fluidity.

We developed the idea of the use of PEG tethered peptide anchors for lipobead assemblies, customized and synthesized the desirable peptide anchor, and added the fluorophore probe reporter under SPPS control for flexibility and practicality. We have successfully used the NHS-PEG_{3000}-NHS molecules as tethering agents, where the NHS end was crosslinked to peptide amines, attached to functionalized silica beads and

tagged peptide was incorporated in the tether supported lipid bilayer separated from the surface by PEG_{3000} spacer. In a parallel batch, silica beads were directly exposed to proteoliposomes w/out DiNHS-PEG_{3000} stock solution in PBS buffer. No significant difference was observed in the proteoliposome coverage for the DiNHS-PEG_{3000} pretreated beads as analyzed by FITC staining as was explained above. Confocal analysis of the complexes showed homogenous distribution of the lipid probe in the case of both type of lipobeads. The diffusion coefficient and mobile fraction of the fluorescent lipid were estimated using FRAP analysis and were comparable to the reference cases of transmembrane peptides other lipid bilayers. We believe that the peptide tether-supported membranes will be more stable compared to the non-tethered membranes on silica support, as well as more suitable for the surface funtionalization of lipobeads with ligands for the synthesis of sensor systems.

Figures and Tables

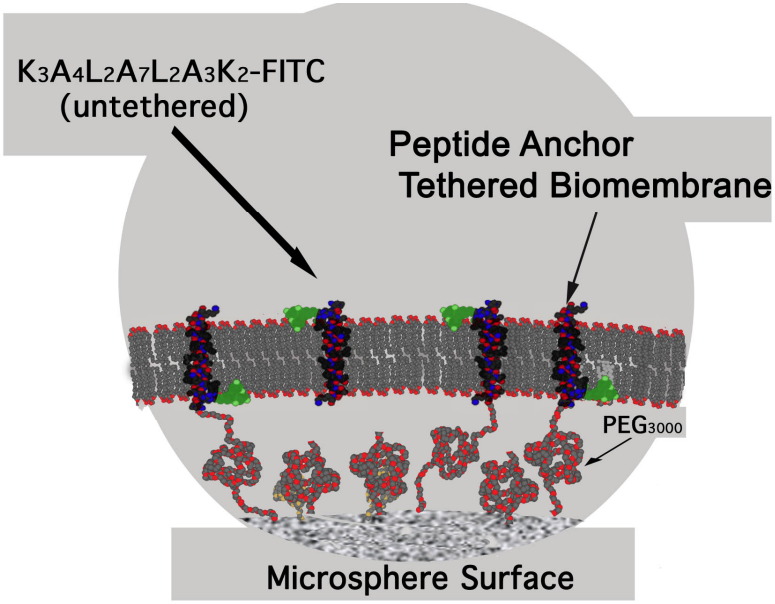

Figure 4-1. Schematic structure of a peptide anchor tethered biomembrane, termed a peptide proteolipobead. The rationally designed peptide labeled with fluorescent dye ($K_3A_4L_2A_7L_2A_3K_2$-FITC), hydrophobic spanning within DOPC lipid bilayers, shown tethered with PEG_{3000} spacer arm.

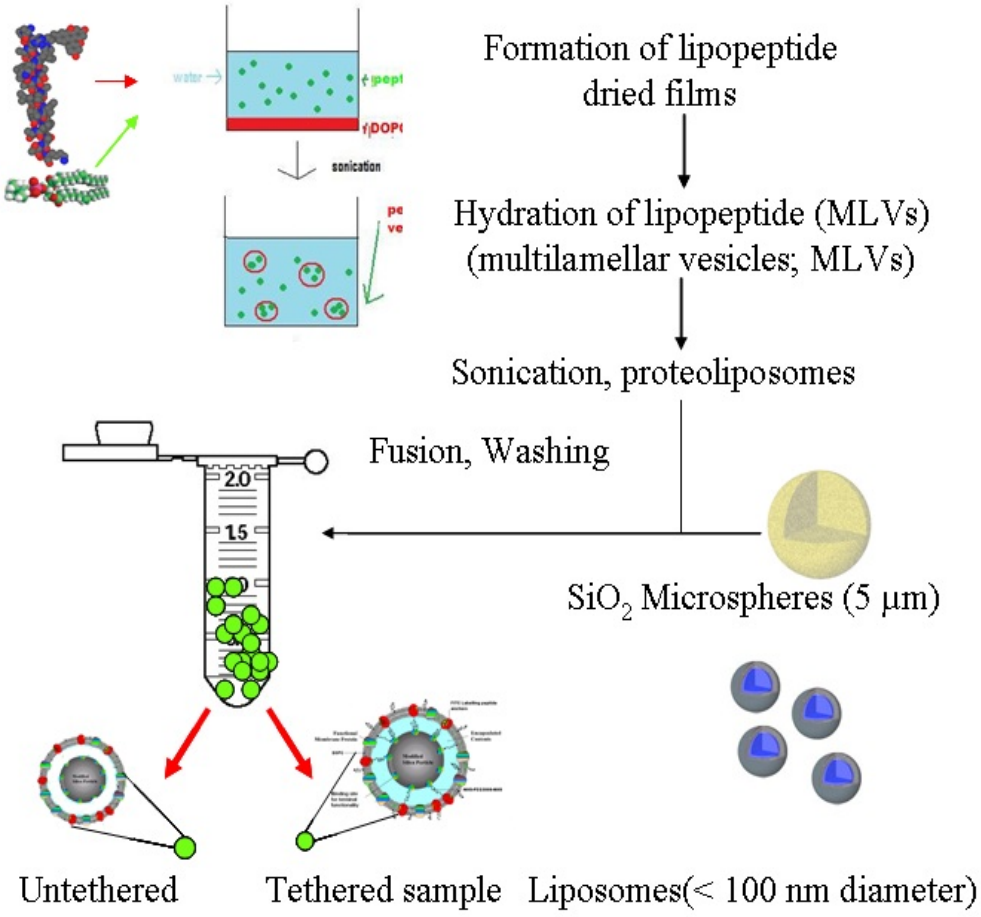

Figure 4-2. Flowchart of Proteolipobead Formation. Dissolve peptide-FITC and DOPC (1mg lipid/ ml) via chloroform in brown vials and evaporate it to get dry film, hydration in pH 7.4 PBS buffer and sonication, fusion onto 5 µm microspheres. Left: fuse $K_3A_4L_2A_7L_2A_3K_2$-FITC proteoliposomes onto silica beads for 90 min at room temperature, denoted untethered sample. Right: incubate proteoliposomes onto beads functionalized with NHS-PEG_{3000}-NHS for 15 min to form microsphere-PEG_{3000}-$K_3A_4L_2A_7L_2A_3K_2$-FITC crosslinks, denoted tethered sample.

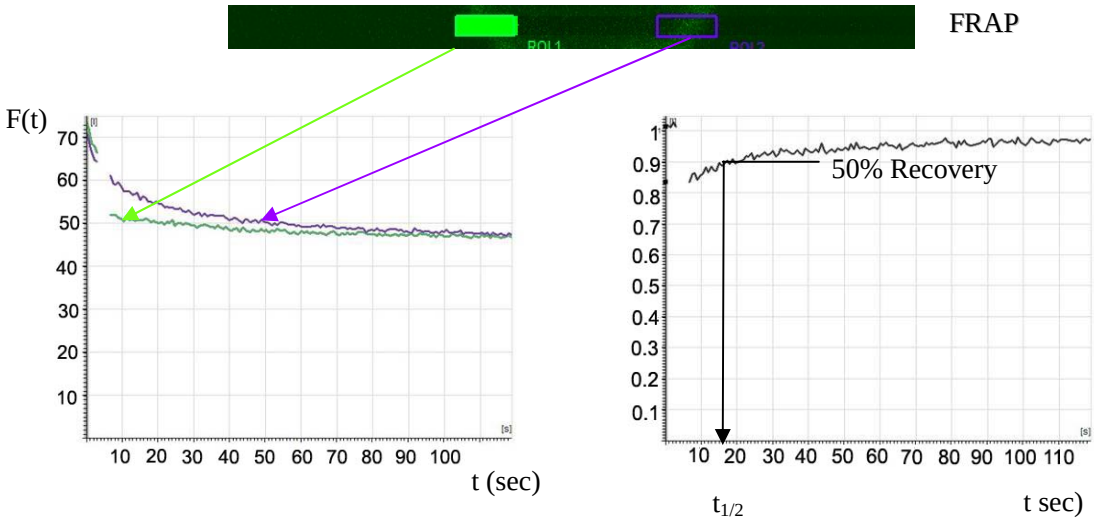

Figure 4-3 Snapshots of the equatorially opposite ends of the bead studied for fluorescence recovery after photobleaching, presenting the data of FRAP experiment in ROI channels of confocal microscope. All settings are the same as figure 5-5. Left: ROI-1 channel (Green): bleached region (AOTF 2%, Gain 795, excitation line 488 nm, detection 500-583 nm) ROI-2 channel (Purple): unbleached region with the same size used to correct for the background photobleaching process. Divided RO1 by RO2, one graph standing for FRAP calculation curve were presented on right side. $t_{1/2}$ stands for the half time of recovery, 16 secs; diffusion coefficient in lipid is 0.012 μm^2/sec.

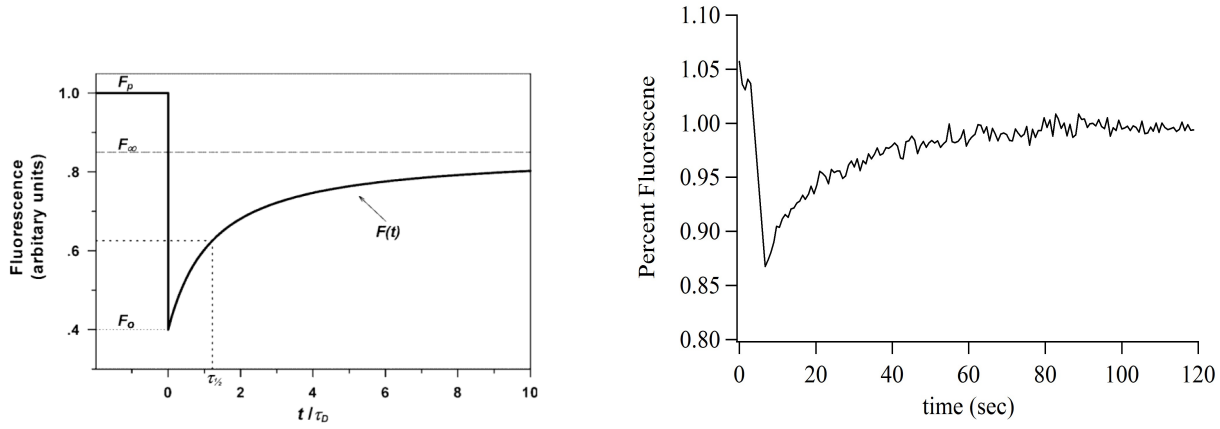

A **B**

Figure 4-4. Schematics of time variation of the normalized fluorescence intensity of the bleached spot. (FRAP curve data obtained by using Confocal Imaging): (A) Theoretical FRAP data, F_p for pre-bleach intensity, F_o for post bleach intensity, F_∞ for the steady level of recovery intensity (dashed line) , the value of mobile or recovery fraction equals to $\alpha = (F_\infty - F_o)/(F_p - F_o)$; $\tau_{1/2}$ is indicated by the dotted line. (B) FRAP data of NHS-PEG_{3000}-NHS tethered supported proteolipobeads (peptide-FITC: DOPC=1:32 in molar ratio). Recovery fraction is 0.728, $t_{1/2}$ is 15.08 sec, diffusion coefficient is 0.01658 $\mu m^2/S$. Viewed at 512*32 pixels, 3 frames pre-bleaching, 2 frames bleaching, 120 post-bleaching. Excitation line 488nm, Emission fluorescence measured from 500 nm to 550 nm.

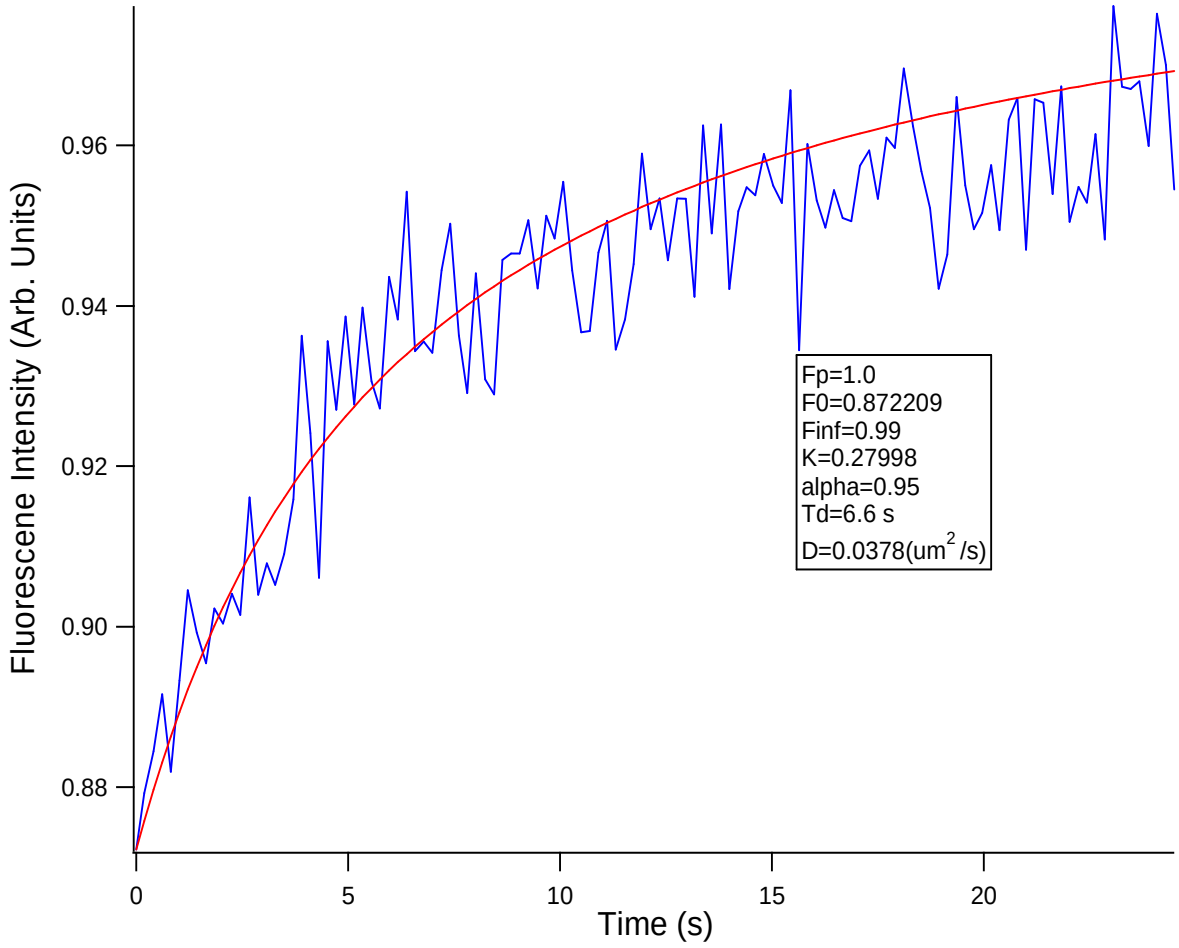

Figure 4-5 Mathematica simulation of typical FRAP data: the post-bleach recovery curve (blue line) was cut off and simulated via Mathematica 8.0 (red line). According to Yguerabide's study, the value of diffusion coefficient could be determined from other parameters. F0=0.8722, Fp=1.0, Finf=0.99, alpha=0.95, K=0.27998, t_D=6.6s, the value of diffusion coefficient is D=0.0378μm^2/s.

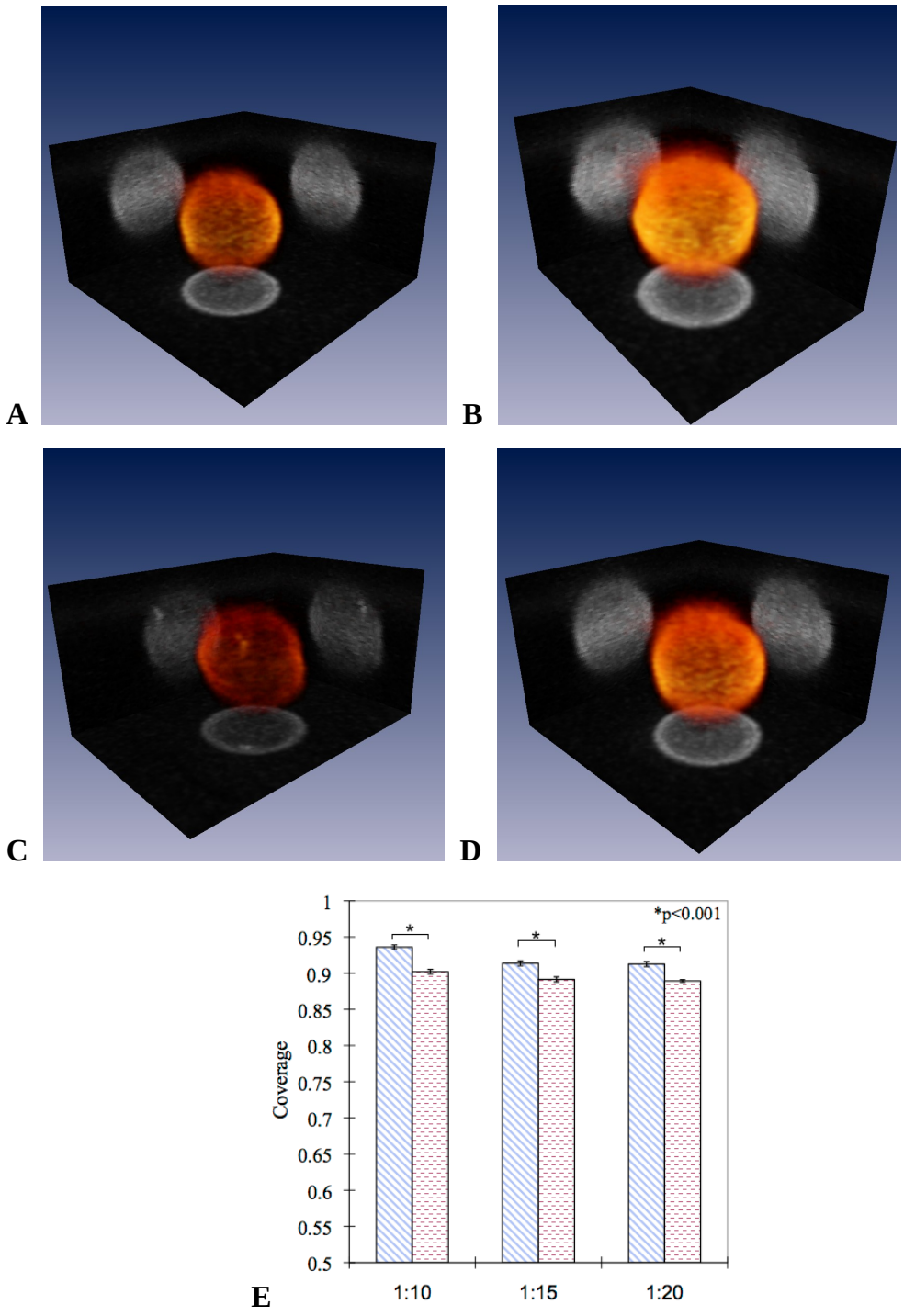

Figure 4-6. Representative 3D Reconstructions of Confocal Image Stacks of 5µm $K_3A_4L_2A_7L_2A_3K_2$-FITC proteolipobeads (peptide:lipid=1:32 in molar ratio), excitation wavelength 488nm, Detection window 500-550 nm; Projection views from Amira 3.0 software 3D rendering: (A) silica supported bead, (B) silica supported bead (C)

NHS-PEG_{3000}-NHS-tethered bead (D) NHS-PEG_{3000}-NHS-tethered bead. Panel E is the lipid coverage fraction metric (Diagonal patterned bars: tethered -PEG_{3000}- cushioned lipobeads bead. Dotted patterned bars: untethered lipobead sample), measured from equatorial lipobead z slices (N = 40); values are given ± standard error ($\sigma/\sqrt{N}$); p values were less than 0.001 based on ANOVA and Tukey's Multiple Comparison Test for compared tethered and untethered sample in three cases.

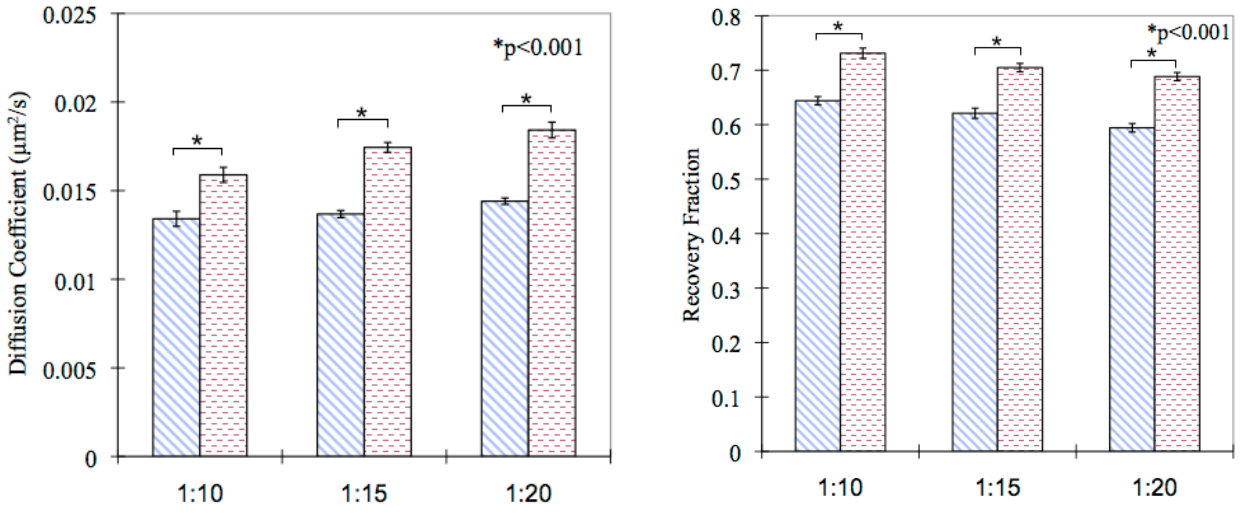

Figure 4-7. FRAP data Analysis: Mean value of Diffusion coefficient and recovery fraction. The mass ratio of peptide to lipid was 1:10, 1:15 and 1:20 (molar ratio was 1:32, 1:48, 1:64) respectively. (Diagonal patterned bars: tethered -PEG_{3000}- cushioned lipobeads bead. Dotted patterned bars: untethered lipobead sample), N = 40; values are given ± standard error ($\sigma/\sqrt{N}$); p values were less than 0.001 based on ANOVA and Tukey's Multiple Comparison Test for compared tethered and untethered sample in three cases.

Table 4-1. Comparison of Transmembrane Peptide and Lipid Diffusion Coefficients in Supported Lipid Bilayers

Peptide + Major Lipid	**D ($\mu m^2/s$)**
$AKKL_{18}GKK$-FITC (GUVs 99%SOPC 1:1000)[REF]	0.31±0.02
FGFR TM Peptide in (supported membrane, 99%POPC 1:2000, 33mer) [REF]	0.0055±0.0001
Gramicidin D (POPC, cyclic decamer) [11]	~0.07
$K_3A_4L_2A_7L_2A_3K_2$-FITC in untethered supported membrane (peptide: DOPC=1:10 (mass))	**0.0134±0.0004**
$K_3A_4L_2A_7L_2A_3K_2$-FITC tethered solid supported membrane (peptide: DOPC=1:10(mass))	**0.0158±0.0004**

Chapter 5
Conclusions and Future Work

Conclusions

In this work, we describe a directed-assembly approach for producing surface-supported bilayers with transmembrane helices. Our work has realized the reconstitution of the peptide-anchors tethering supported lipid bilayers, developing methods for investigating the properties of peptides and exploiting lipobeads for sensing and ligand display systems. The novelty in this approach is the rational design and incorporation of the peptides into the lipid bilayers at the aqueous/lipid film interface, allowing for precise control over peptide concentration and orientation. Major conclusions of this thesis project are summarized below:

- We have successfully synthesized alpha-helical peptide and complexes with high purity using SPPS chemistry and reverse phase HPLC purification, characterized the tether molecules, conjugated peptide with fluorescein isothiocyanate to synthesize fluorescently labeled peptide. MS Characterization of the conjugates revealed predominantly single site labeling with fluorescein isothiocyanate as required for their use as an anchoring agent. Alpha helical content was analysised via Circular Dichroism, exhibiting a high alpha helical content for stable spanning into lipid bilayers. The tether conjugation was identified using Confocal Image assay and was found to be in agreement with the conclusions of the previous studies. In this stage, we've successively synthesized fluorophore-labeled peptide conjugates for use as anchoring contructs in

supported membranes.

- Surface of the silica beads was successfully modified with diverse polymers in order to immobilize the peptide conjugate tethers. Modification of micro-beads was executed for more stability and feasibility, including available Fmoc assay for estimation of available amino groups on microbeads. We have used amine-based coupling to conjugate NHS- PEG_{3000}-NHS to silica surface. The modified beads were further incubated with proteoliposomes tagged with FITC to facilitate localization via fluorescence imaging.
- Tether supported lipid bilayer membranes (proteolipobeads) were constructed successfully on NHS- PEG_{3000}-NHS functionalized silica particles (5μm). This is a novel use of alpha helical peptide based anchors to tether lipid bilayers on spherical particles. We used the liposome fusion self-assembly route to form supported lipid bilayers around the particles. The fluidity of the supported membranes was analyzed using the FRAP technique, furthermore, the mobility of the peptides were found to be significantly higher than peptides in untethered lipid bilayers on plain silica particles, as well as comparable to diffusivity value reported in literature for the other transmembrane peptides in lipid bilayers.
- We have shown that PEG-lipids that are covalently tethered to the surface of silicate substrates at appropriate concentrations form viable cushions for supported lipid bilayers. We characterized the peptide tethers and the lipobead structures with various methods including confocal microscopy and CD spectroscopy. Our results demonstrate that peptide supported lipid bilayers,

exhibiting high lateral mobility, are suited for the construction of novel *in vitro* biomembrane systems.

Future work

Our motivation of this project is to build stable lipid microenvironment with native-like proerties. So far we have successfully fabricated peptide-based tethers to anchor the supported bilayer structures onto the bead surface, and tetherted the supported lipid bilayers via NHS-PEG-NHS for enhancing stability and fluidity. Future work in the light of above discussion will be addressed as following:

1 Establish optimal conditions for the formation of membrane structures;

2 Develop stability assays and compare different membrane systems,

3 Incorporation of functional membrane proteins into the supported lipid bilayers;

4 Characterazation of the properties for other functional groups;

These constructs can then be used to reconstitute various membrane proteins in the tether-supported lipid bilayer for enhanced stability and functionality under a wider range of processing conditions required for applications of interest.

1. Establish optimal conditions for the formation of membrane structures

Besides the reaction conditions (stain time, environment, media, reagent concentration) for supported lipid bilayers, the routes of formation will be taken into consideration, such as detergent method, streptavidin-biotin inter-locked method for

anchoring onto beads. Different methods for membrane formation should be compared and discussed.

2 Stability assay and comparison among different membrane systems

We successfully fabricated tether supported lipid membrane from the point of view of stability enhancement. This is essential as the un-tethered lipid bilayer structures can potentially fall apart in various processing environments and lateral diffusivity could be compromised. Hence it is important to investigate the stability of the constructs and compare them with the membranes with/out any tether supports. In future work, we will construct different supported membrane systems with peptide anchors, tethered and un-tethered, and then compare the stability and fluidity of them, including subjecting the assemblies to elevated temperatures and testing shear stress effects.

3 Incorporation of functional membrane proteins into the suppoted lipid bilayers

To verify that the native environment of mimic lipid bilayers, we will incorporate functional membrane proteins into the suppoted lipid bilayers and test the properties of functional molecules. The membrane proteins could be chosen from the candidate large pool and may include: intramembrane proteases, bacteriorhodopsin, G-protein coupled receptors, or photosynthetic reaction centers.

For example, we could conjugate synthesized peptide with biotin-PEG to construct

biotin-PEG-peptide based tethers, fabricate supported membranes on on 5μm (or 20μm) beads. These beads will be pre-coated with streptavidin, then fluorescently-tagged reaction centers will be incorporated into the supported lipid bilayer assemblies.

4 Characterization of the properties for functional groups

Once we incorporate the membrane protein in the functional form in stabilized lipid assemblies on microparticles, such a solid surface will have a specific display of functionality in an inert matrix. Such a surface carrying membrane proteins via specific tags anchoring can then be developed into a specific recognition or screening device based on the functionality of the reconstituted membrane protein. Normally, the inserted membrane proteins are pre-conjugated with fluorescent tags. As discussed above, by investigating the localization, activity, stability, chemical properties and mobility of fluorescent probe conjugated to transmembrane protein (MPs), we could assay the affect of fabricated membrane on spanning protein.

In details, future work will be focused on several aspects: (1) to optimize the conditions of reactions, including conjugation, probe labeling, proteoliposomes fusion, etc; (2) using other surface modification methods to improve the stability and validity of supported membrane, such as adopting specific affinity adsorption between strevavidin and biotin, protein receptor and ligand; (3) to use Confocal microscopy to study the lateral mobility characteristics and localization of tagged tethers (4) to utilize NMR for chemical and physical characterization of anchor peptides; (5) to monitor the

proteoliposome fusion process in real-time; and (6) to design other suitable peptides and integrate the peptide anchors into supported membranes and characterization them. Nonetheless, it is also possible to design longer affinity spacer molecules to expand the submembraneous space (different chain length of PEG, and different type of polymer cushion).

That is to say, future work will switched to two main aspects: (i) different methods for investigation (ii) different systems for study, especially for NMR characterization of other functional systems.

NMR chemical and physical characterization of anchor peptides

Furthermore, we will inspect the peptide-based anchors in detail using NMR, in both micelles and proteoliposomes. NMR spectra, on the basis of peptide backbone C-13 chemical shifts and dipolar couplings, can provide information concerning alpha-helical structure in micelles and liposomes and also about bioconjugation, which could supply us sufficient data to evaluate the detailed chemical and physical properties of anchors, in particular examining the impact of conjugation on peptide structure.

Fabrication of other tether-supported membrane systems

Accordingly we aim to develop an efficient methodology for the evaluation of other candidate peptides that are proven to be useful for tethering yet contain other functionalities such as tailor-made glycopeptides used to build mimics of cell-surface glycoproteins and the glycocalyx.

Bibliography

[1] Kevin R. MacKenzie, *Folding and Stability of α -Helical Integral Membrane Proteins,* Chemical Review, American Chemical Society, Department of Biochemistry and Cell Biology, Rice University, Houston, Texas 77005

[2] Motomu Tanaka and Erich Sackmann, Polymer-supported membranes as models of the cell surface, Nature, **437**, 656-663

[3] Manoj K. Sharma. A Lane Gilchrist, *Design of Supramolecular Complexes for Stability Enhancement of Membrane Protein-Based Biomaterials*, Dissertation Submitted to the Graduate Faculty in Engineering in Partial Fulfillment of the Requirements for the Degree of Doctor of Philosophy

[4] Sackmann, E., *Supported membranes: scientific and practical applications*. Science, 1996. **271**(5245): p. 43-8.

[5] Benkoski, J.J. and F. Hook, *Lateral Mobility of Tethered Vesicle-DNA Assemblies.* J. Phys. Chem. B, 2005. **109**: p. 9773-9779.

[6] Yoshina-Ishii, C., et al., *General method for modification of liposomes for encoded assembly on supported bilayers.* J Am Chem Soc, 2005. **127**(5): p. 1356-7.

[7] Raymond S. Tu. Matthew Tirrell, *Bottom-up of biomimetic assemblies,* Advanced Drug Delivery Review **56**(2004)1537-1563

[8] Lowenstam, H.A. & Weiner, S. (**1989**) *On Biomineralization* (Oxford Univ. Press, Oxford, U.K.)

[9] Weiner, S, & Addadi, L. **(1997)** *J. Mater. Chem.* 7,689-702

[10] Mann, S., Webb, J. &Williams, J.P. (**1989**) *Biomineralization: Chemical and Biological Perspectives* (VCH, New York)

[11] Sarikaya, M. & Aksay, I. A. (**1995**) *Biomimetics: Design and Processing of Materials* (AIP Press, Woodbury, NY

[12] Addadi, L.& Weiner, S. (1992) *Angew. Chem. Int. Ed. Engl.* **31**,153-169

[13] Rajendra Prasad (Edited) *Manual on Membrane Lipids Membrane blue book,* Springer Lab Manual, page1-15.

[14] Wiener, M. C.; White, S. H. *Biophys. J.* **1992**, 61, 437

[15] Bangham, A.D., *Liposomes: realizing their promise.* Hosp Pract (Off Ed), 1992. **27**(12): p. 51-6, 61-2.

[16] Gregoriadis, G. and A.T. Florence, *Liposomes in drug delivery. Clinical, diagnostic and ophthalmic potential.* Drugs, 1993. **45**(1): p. 15-28.

[17] Lasic, D.D., *Liposomes: From Physics to Applications.* **1993**, Amsterdam: Elsevier Science.

[18] Ollivon, M., et al., *Vesicle reconstitution from lipid-detergent mixed micelles.* Biochim Biophys Acta, 2000. **1508**(1-2): p. 34-50.

[19] Lesieur, S., et al., *Size analysis and stability study of lipid vesicles by highperformance gel exclusion chromatography, turbidity, and dynamic light scattering.* Analytical biochemistry, **1991**. 192(2): p. 334-343.

[20]Paternostre, M., et al., *Solubilization and reconstitution of vesicular stomatitisvirus envelope using octylglucoside.* Biophysical journal, **1997**. 72(4): p. 1683-1694.

[21] Tamm, L.K. and H.M. McConnell, Supported phospholipid bilayers. Biophysical journal, 1985. 47(1): p. 105-113.

[22] J.-L. Rigaud ,Brazilian Journal of Medical and Biological Research (2002) 35: 753-766

[23] Cornelius F (1991). Functional reconstitution of the sodium pump. Kinetics of exchange reactions performed by reconstituted Na/K-ATPase. *Biochimica et Biophysica Acta*, 1071: 19-66.

[24] Rigaud JL, Pitard B & Lévy D (1995). Reconstitution of membrane proteins into liposomes: application to energy-transducing membrane proteins. *Biochimica et Biophysica Acta*, 1231: 223-246.

[25] Papahadjopoulos, D., ed. *Liposomes and Their Uses in Biology and Medicine. Ann. N.Y. Acad. Sci., 308*. 1978.

[26] Szoka, F., Jr. and D. Papahadjopoulos, *Comparative properties and methods of preparation of lipid vesicles (liposomes).* Annu Rev Biophys Bioeng, 1980. **9**: p. 467-508.

[27] Ollivon, M., et al., *Vesicle reconstitution from lipid-detergent mixed micelles.* Biochim Biophys Acta, 2000. **1508**(1-2): p. 34-50.

[28] Lasic, D.D., *Liposomes: From Physics to Applications*. 1993, Amsterdam: Elsevier Science.

[29] Ringsdorf, H., B. Schlarb, and J. Venzmer, *Molecular Architecture and Function of Polymeric Oriented Systems: Models for the Study of Organization, Surface Recognition, and Dynamics of Biomembranes.* J. Angew. Chem., 1988. **27**(1): p. 113-148.

[30] Liu, S. and D.F. O'Brien, *Stable polymeric nanoballoons: lyophilization and rehydration of cross-linked liposomes.* J Am Chem Soc, 2002. **124**(21): p. 6037-42.

[31] Graff, A., M. Winterhalter, and W. Meier, *Nanoreactors from Polymer-Stabilized Liposomes.* Langmuir, 2001. **17**(3): p. 919-923.

[32] Allen, T.M., *The use of glycolipids and hydrophilic polymers in avoiding rapid uptake of liposomes by the mononuclear phagocyte system.* Adv. Drug Delivery Rev., 1994. **13**(3): p. 285-309.

[33] Woodle, M.C. and D.D. Lasic, *Sterically stabilized liposomes.* Biochim Biophys Acta, 1992. **1113**(2): p. 171-99.

[34] Allen, T.M., *The use of glycolipids and hydrophilic polymers in avoiding rapid uptake of liposomes by the mononuclear phagocyte system.* Adv. Drug Delivery Rev., 1994. **13**(3): p. 285-309.

[35] Brown DA, London E: *Structure and origin of ordered lipid domains in biological membranes.* J Membrane Biol 1998, **164**:103-114.

[36] Steven G Boxer, *Molecular transport and organization in supported lipid membranes,* Current Opinion in Chemical Biology 2000, **4**:704–709

[37] Tanford, C. *The Hydrophobic Effect; Wiley*: *New York,* **1980**

[38] Terrettaz S, Stora T, Duschl C, Vogel H. 1993. *Protein-binding to supported lipid membranes: investigation of the cholera toxin–ganglioside interaction by simultaneous impedance spectroscopy and surface plasmon resonance*. Langmuir **9**:1361–1369.

[39] Steven G Boxer, *Molecular transport and organization in supported lipid membranes,* Current Opinion in Chemical Biology 2000, **4**:704–709

[40] Popot, J. L.; Engelman, D. M. *Biochemistry* **1990**, 29, 4031

[41] Deisenhofer, J.; Epp, O.; Miki, K.; Huber, R.; Michel, H. *J. Mol. Biol.* **1984**, 180, 385.

[42] Nagle, J. F.; Wiener, M. C. *Biophys. J.* **1989**, 55, 309.

[43] Wiener, M. C.; Suter, R. M.; Nagle, J. F. *Biophys. J.* **1989**, 55, 315.

[44] Henderson, R.; Baldwin, J. M.; Ceska, T. A.; Zemlin, F.; Beckmann, E.; Downing, K. H. *J. Mol. Biol.* **1990**, 213, 899.

[45] Chiaki Yoshina-Ishii, Steven G. Boxer, et al. *Langmuir* **2006,** *22*, 5682-5689

[46] White, S. H.; Wimley, W. C. Annu. ReV. *Biophys. Biomol. Struct.* **1999**, 28, 319.

[47] Booth, P. J.; High, S. Mol. *Membr. Biol*. **2004**, 21, 163.

[48] Radler, J., H. Strey, and E. Sackmann, *Phenomenology and Kinetics of Lipid Bilayer Spreading on Hydrophilic Surfaces*. Langmuir,1995. **11**(11): p. 4539-4548.

[49] Bayerl, T.M. and M. Bloom, *Physical properties of single phospholipid bilayers adsorbed to micro glass beads. A new vesicular model system studied by 2H-nuclear magnetic resonance*. Biophys J, 1990. **58**(2): p. 357-62.

[50] Edward T. Castellana, Paul S. Cremer, Solid supported lipid bilayers: From biophysical studies to sensor design. Surface Science Reports 61 (2006) 429–444

[51] Von Tscharner, V. and H.M. McConnell, Physical properties of lipid monolayers on alkylated planar glass surfaces. Biophys J, 1981. 36: p. 421-427.

[52] Tamm, L.K. and H.M. McConnell, Supported phospholipid bilayers. Biophys J, 1985. 47(1): p. 105-13.

[53] Terstappen GC, Angelo R. 2001. *In silico research in drug discovery.* Trends Pharmac. Sci. **22**(1): 23–26.

[54] Plant AL. 1999. *Supported hybrid bilayer membranes as rugged cell membrane mimics*. Langmuir **15**: 5128–5135.

[55] Terrettaz S, Stora T, Duschl C, Vogel H. 1993. *Protein-binding to supported lipid membranes: investigation of the cholera toxin–ganglioside interaction by simultaneous impedance spectroscopy and surface plasmon resonance*. Langmuir **9**:1361–1369.

[56] Lang H, Dushcl C, Vogel H. 1994. *A new class of thiolopids for the attachment of lipid bilayers on gold surfaces.* Langmuir **10**:197–210.

[57] Bieri C, Ernst OP, Heyse S, Hofmann KP, Vogel H. 1999. *Micropatterned immobilization of a G protein-coupled receptor and direct detection of G protein*

activation. Nat. Biotech. **17**:1105–1108.

[58] Stora T, Lakey JH, Vogel H. 1999. *Ion-channel gating in transmembrane receptor proteins: functional activity in tethered lipid membranes*. Angew. Chem. Int. Edn **38**(3): 389–392.

[59] Schmidt EK, Liebermann T, Kreiter M, Jonczyk A, Naumann R, Offenhausser A, Neumann E, Kukol A, Maelicke A, Knoll W. 1998. *Incorporation of the acetylcholine receptor dimer from Torpedo californica in a peptide supported lipid membrane investigated by surface plasmon and fluorescence spectroscopy*. Biosens. Bioelectron. **13**(6): 585–591.

[60] Cornell BA, Braach-Maksvytis VLB, King LG, Osman PDJ, Raguse B, Wieczorek L, Pace RJ. 1997. *A biosensor that uses ionchannel switches*. Nature **387**: 580–583.

[61] Boden N, Bushby RJ, Clarkson S, Evans SD, Knowles PF, Marsh A. 1997. *The design and synthesis of simple molecular tethers for binding biomembranes to a gold surface*. Tetrahedron **53**(31): 10939–10952.

[62] Jenkins ATA, Boden N, Bushby RJ, Evans SD, Knowles PF, Miles RE, Ogier SD, Schonherr H, Vancso GJ. 1999. *Microcontact printing of lipophilic self-assembled monolayers for the attachment of biomimetic lipid bilayers to surfaces*. J. Am. Chem. Soc. **121**(22): 5274–5280.

[63] Duschl C, Knoll W. 1988. *Structural characterization of Langmuir–Blodgett multilayer assembles by polariton surface field-enhanced raman spectroscopy.* J. Chem. Phys. **88**:4062–4069.

[64] Sackmann E, Tanaka M. 2000. *Supported membranes on soft polymer cushions: fabrication, characterization and applications*. Trends Biotechnol. **18**: 58–64.

[65] Wong JY, Park CK, Seitz M, Israelachvili J: *Polymer-cushioned bilayers. II. An investigation of interaction forces and fusion using the surface forces apparatus*. Biophys J 1999, **77**:1458-1468.

[66] Wagner ML, Tamm L: *Tethered polymer-supported planar lipid bilayers for reconstitution of integral membrane proteins*. Biophys J 2000, **79**:1400-1414.

[67] Prucker O, Naumann CA, Ruhe J, Knoll W, Frank CW: *Photochemical attachment of polymer films to solid surfaces via monolayers of benzophenone derivatives.* J Am Chem Soc 1999,**121**:8766-8770.

[68] Cooper MA, Hansson A, Lo¨ fa° s S, Williams DH. 2000. *A vesicle capture sensor chip for kinetic analysis of binding to membrane-bound receptors*. Anal. Biochem. **277**:

196–205.

[69] Jenco JM, Becker KP, Morris AJ. 1997. *Membrane-binding properties of phospholipase C-beta1 and phospholipaseCbeta2: role of the C-terminus and effects of polyphosphoinositides, G-proteins and Ca2*. Biochemistry **327**: 431–437.

[70] Spinke J, Yang J, Wolf H, Liley M, Ringsdorf H, Knoll W. 1992. *Polymer-supported bilayer on a solid substrate*. Biophys. J.**63**: 1667–1671.

[71] Beyer D, Elender G, Knoll W, Kuhner M, Maus S, Ringsdorf H, Sackmann E. 1996. *Influence of anchor lipids on the homogeneity and mobility of lipid bilayers on thin polymer films.* Angew. Chem. **35**(15): 1682–1685.

[72] Wiegand G, Jaworek T, Wegner G, Sackmann E. 1997. *Studies of structure and local wetting properties on heterogeneous, micropatterned solid surfaces by microinterferometry.* J. Colloid Interface Sci. **196**(2): 299–312.

[73] Srivastava, L.K., et al., Reconstitution of affinity-purified dopamine D2 receptor binding activities by specific lipids. Biochim Biophys Acta, 1987. 900(2): p. 175-82.

[74] Bangham, A.D., Liposomes: realizing their promise. Hosp Pract (Off Ed), 1992. 27(12): p. 51-6, 61-2.

[75] Wimley, W. C.; White, S. H. *Nat. Struct. Biol*. **1996**, 3, 842.

[76] Tossi, A.; Sandri, L.; Giangaspero, *A. Biopolymers* **2000**, 55, 4. 1999,

[77] Shai, Y.; Oren, Z. *Peptides* **2001**, 22, 1629.

[78] Lear, J. D.; Gratkowski, H.; DeGrado, W. F. *Biochem. Soc. Trans*. **2001**, 29, 559.

[79] Skehel, J. J.; Cross, K.; Steinhauer, D.; Wiley, D. C. *Biochem. Soc.Trans*. **2001**, 29, 623.

[80] Kuroiwa, T.; Sakaguchi, M.; Mihara, K.; Omura, T. *J. Biol. Chem.* **1991**, 266, 9251.

[81] Chen, H.; Kendall, D. A. *J. Biol. Chem*. **1995**, 270, 14115.

[82] Nilsson, I.; von Heijne, G. *J. Mol. Biol.* **1998,** 284, 1185.

[83] Davis, N. G.; *Model, P. Cell* **1985,** 41, 607.

[84] Manoj K. Sharma, Harsha Jattani, and M. Lane Gilchrist, Bacteriorhodopsin conjugates as anchors for supported membranes. Bioconjugate Chemistry, 2004. 15(4): p.

942-947.

[85] Nikhil D. Kalyankar, Manoj K. Sharma,, Shyam V. Vaidya, David Calhoun, Charles Maldarelli, Alexander Couzis, and Lane Gilchrist*, Arraying of Intact Liposomes into Chemically Functionalized Microwells, Langmuir 2006, 22, 5403-5411

[86] Janet R. Kumita‡, Oliver S. Smart§, and G. Andrew Woolley *Photo-control of helix content in a short peptide*,PNAS April 11, **2000** vol. 97 no. 8 3803–3808

[87] Nadya I.Tarasova,* Rishi Seth, Sergey G. Tarasov, Teresa Kosakowska-Cholody, Christine A. Hrycyna,# Michael M. Gottesman,# and Christopher J. Michejda, *Transmembrane Inhibitors of P-Glycoprotein, an ABC Transporter* J. Med. Chem., **48** (11), 3768 -3775, 2005.

[88] http://www.biotech.uiuc.edu/centers/Proteomics/Proteinscience/spps.htm

[89] Singer SJ, Nicolson GL. 1972. *The fluid mosaic model of the structure of cell membranes*. Science **175**(23): 720–731.

[90] R. B. Merrifield (1963). "Solid Phase Peptide Synthesis. I. The Synthesis of a Tetrapeptide". *Journal of the American Chemical Society* **85**: 2149

[91] Gierasch, Lila M (2006), "Editorial: Passing of a gentle giant of peptide science: in memoriam, R. Bruce Merrifield", *Biopolymers* **84** (5): 433–4

[92] Biemann K, Contributions of mass spectrometry to peptide and protein structure. *Biomed Environ Mass Spectrom*. 1988 Oct;**16**(1-12):99-111.

[93] Steven A. Hofstadler, Ray Bakhtiar, and Richard D. Smith, Electrospray Ionization Mass Spectroscopy: Part I. Instrumentation and Spectral Interpretation

[94] Clauser KR, Baker P, Role of accurate mass measurement (+/- 10 ppm) in protein identification strategies employing MS or MS/MS and database searching. Burlingame AL Anal Chem. 1999 Jul 15; 71(14):2871-82.

[95] D. S. Wagner, L. G. Melton, Y. Yan, B. W. Erickson and R. J. Anderegg, Deuterium exchange of {alpha}-helices and {beta}-sheets as monitored by electrospray ionization mass spectrometry, Protein Sci. 1994 3: 1305-1314

[96] Electrospray Ionization Mass Spectrometry Studies on the Hetro-peptide Libraries by Phosphorus Oxychloride Activation Method, published 2004-1-13.

[97] Xavier Daura, Dirk Bakowies, Dieter Seebach Jo¨ rg Fleischhauer, Wilfred F. van Gunsteren Peter Kru¨ ger, *Circular dichroism spectra of b-peptides: sensitivity to*

molecular structure and effects of motional averaging, Eur Biophys J (**2003**) 32: 661–670

[98] Berova N, Nakanishi K, Woody RW (**2000**) *Circular dichroism: principles and application*. Wiley-VCH, New York

[99] F. Albertorio, A.J. Diaz, T.L. Yang, V.A. Chapa, S. Kataoka, E.T. Castellana, P.S. Cremer, *Langmuir* 21 (**2005**) 7476.

[100] Tamm, L.K., *Lateral diffusion and fluorescence microscope studies on a monoclonal antibody specifically bound to supported phospholipid bilayers. Biochemistry*, 1988. **27**(5): p. 1450-1457

[101] Schlessinger, J., et al., *Lateral transport on cell membranes: mobility of concanavalin A receptors on myoblasts*. Proceedings of the National Academy of Sciences of the United States of America, 1976. **73**(7): p. 2409-2413.

[102] Tsuji, A. and S. Ohnishi, *Restriction of the lateral motion of band 3 in the erythrocyte membrane by the cytoskeletal network: dependence on spectrin association state.* Biochemistry, 1986. **25**(20): p. 6133-6139.

[103] Nectarios Klonis, Melanie Rug, Ian Harper, Mark Wickham, Alan Cowman, Leann Tilley, *Eur Biophys J* (**2002**) 31:36-51

[104] Braeckmans, K., et al., Three-dimensional fluorescence recovery after photobleaching with the confocal scanning laser microscope. Biophys J, 2003. 85(4): p. 2240-52.

[105] Denk, W., J.H. Strickler, and W.W. Webb, Two-photon laser scanning fluorescence microscopy. Science, 1990. 248(4951): p. 73-6.

[106] Chen, T.S., et al., High-order photobleaching of green fluorescent protein inside live cells in two-photon excitation microscopy. Biochem Biophys Res Commun, 2002. 291(5): p. 1272-5.

[107] Patterson, G.H. and D.W. Piston, Photobleaching in two-photon excitation microscopy. Biophys J, 2000. 78(4): p. 2159-62.

[108] Carrero, G., et al., Using FRAP and mathematical modeling to determine the in vivo kinetics of nuclear proteins. Methods, 2003. 29(1): p. 14-28.

[109] Sklar LA (Ed): Flow Cytometry for Biotechnology. Oxford University Press; 2005.

[110] Larry A Sklar, Mark B Carter and Bruce S Edwards, Flow cytometry for drug discovery, receptor pharmacology and high-throughput screening, COPHAR-493; NO OF

PAGES 8

[111] Leonore A Herzenberg, James Tung, Wayne A Moore, Leonard A Herzenberg & David R Parks,Interpreting flow cytometry data: a guide for the perplexed, 2006 Nature Publishing Group

[112] Robinson JP: Flow cytometry. In Encyclopedia of Biomaterials and Biomedical Engineering. Edited by Wnek GE, Bowlin GL. Marcel Dekker Inc.; 2004:630-640.

[113] Paul Robinson J (Managing Editor): Current Protocols in Cytometry, Wiley Interscience,

[114] Tung, J.W., Parks, D.R., Moore, W.A., Herzenberg, L.A. & Herzenberg, L.A. *Methods Mol. Biol.* 271, 37–58 (2004).

[115] Burkhard Bechinger, Biophysical Journal Volume 81 October 2001, 2251-2256

[116] Greg T. Hermanson, *Bioconjugate Techniques*, Pierce Chemical Company Rockford, Illinois P 139

[117] Chung, L. A., and T. E. Thompson. 1996. Design of membrane-inserting peptides: spectroscopic characterization with and without lipid bilayers. *Biochemistry.* 35:11343–11354.

[118] Raymond S. Tu. Matthew Tirrell, Bottom-up of biomimetic assemblies, Advanced Drug Delivery Review 56(2004)1537-1563

[119] J.H.Jones, S.J.Harding, Peptides in Immunology, Proceedings of a Symposium under the Auspices of the European Peptide Society April 2-5, 1995, Interlaken, Switzerland, p. 1,

[120] Clauser KR, Baker P, *Role of accurate mass measurement (+/- 10 ppm) in protein identification strategies employing MS or MS/MS and database searching.* Burlingame AL Anal Chem. 1999 Jul 15; **71**(14):2871-82.

[121] Electrospray Ionization Mass Spectrometry Studies on the Hetro-peptide Libraries by Phosphorus Oxychloride Activation Method, published 2004-1-13

[122] Berova N, Nakanishi K, Woody RW (**2000**) *Circular dichroism: principles and application*. Wiley-VCH, New York

[123] Feher, F.J. and D.A. Newman, *Enhanced Silylation Reactivity of a Model for Silica Surfaces.* J. Am. Chem. Soc., 1990. **112**(5): p. 1931.

[124] W.C. Chan, P.D. White, Fmoc Solid Phase Peptide Synthesis, Oxford University Press.

[125] Wirth, M.J., R.W.P. Fairbank, and H.O. Fatunmbi, *Mixed self-assembled monolayers in chemical separations.* Science, 1997. **275**(5296): p. 44-47.

[126] Tripp, C.P. and M.L. Hair, *Reaction of Methylsilanols with Hydrated Silica Surfaces - the Hydrolysis of Trichloromethylsilanes, Dichloromethylsilanes, and Monochloromethylsilanes and the Effects of Curing.* Langmuir, 1995. **11**(1): p. 149-155.

[127] Weston, P.D., *et al.* (1980). Conjugation of enzymes to immunoglobulins using dimaleimides. *Biochem. Biophys. Acta.* **612:**40-9.

[128] King, T.P. and Kochoumian, L. (1979). A comparison of different enzyme-antibody conjugates for enzyme-linked immunosorbent assay. *J. Immunol. Methods.* **28**:201-10.

[129] A. Berquand, P.E. Mazeran, J. Pantigny, V. Proux-Delrouyre, J.M. Laval, C. Bourdillon, *Langmuir* 19 (**2003**) 1700.

[130] Janet R. Kumita‡, Oliver S. Smart§, and G. Andrew Woolley, *PNAS* April 11, **2000** vol. 97 no. 8 3803–3808.

[131] Nadya I.Tarasova, Rishi Seth, Sergey G. Tarasov, Teresa Kosakowska-Cholody, Christine A. Hrycyna, Michael M. Gottesman, and Christopher J. Michejda, *Med. Chem.*, 48 (11), 3768 -3775, **2005**.

[132] Mikhail Merzlyakov, Edwin Li, and Kalina Hristova Directed Assembly of Surface-Supported Bilayers with Transmembrane Helices, *Langmuir* **2006**, *22*, 1247-1253

[133] Gali Steinberg. Etc, *Biopolymer,* Vol. 73, 597-605(**2004**).

[134] Jianjun Pan a, D. Peter Tieleman, et al. *Biochimica et Biophysica Acta* 1788 (**2009**) 1387–1397.

[135] Takeo Iwamoto, Kalina Hristova, et al. *Biochimica et Biophysica Acta* 1668 (**2005**) 240– 247.

[136] Cheng, Y.L., et al., Attenuated total reflection Fourier transform infrared spectroscopic characterization of fluid lipid bilayers tethered to solid supports. *Langmuir*, 1998.14(4): p. 839-844.

[137] Mirzabekov, T., et al., *Paramagnetic proteoliposomes containing a pure, native, and oriented seven-transmembrane segment protein, CCR5.* Nat Biotechnol, 2000. **18**(6): p. 649-54.

[138] N. Bunjes, E. K. Schmidt, A. Jonczyk, F. Rippmann, D. Beyer, H. Ringsdorf, P. Gra¨ber, W. Knoll, and R. Naumann, *Langmuir* **1997,** *13,* 6188-6194.

[139] Giorgio Lenaz , Lipid Fluidity and Membrane Protein Dynamics, *Bioscience Reports, Vol. 7, No. 11, 1987*

[140] "Molecular Biology of THE CELL." Fifth edition- Alberts, Johnson, Lewis, Raff, Roberts, Walter.

[141] N. Kucerka, J.F. Nagle, J.N. Sachs, S.E. Feller, J. Pencer, A. Jackson, J. Katsaras, Lipid bilayer structure determined by the simultaneous analysis of neutron and X-ray scattering data, *Biophys.* J. 95 (**2008**) 2356–2367.

[142] Petrenko VI, Klacsova M, Beskrovnyy AI, Uhrikova D, Balgavy P. *Gen Physiol Biophys*. **2010** Dec; 29(4):355-61.

[143] Arnaldo J. Diaz, Paul S. Cremer et al. *Langmuir,* Vol. 24, No. 13, **2008**, 6820-6826.

[144] Henderson, R., and P. N. T. Unwin. 1975. Three-dimensional model of purple membrane obtained by electron microscopy.Nature (Lond.). 257:28-32.

[145] Mary F. Blackwell, John Whitmarsh, *Biophysical Journal*, volume 58 November **1990** 1259-1271.

[146] Bragg, P.D. and C. Hou, **1975**, *Arch. Biochem. Biophys*. 167, 311.